

# **SEISMIC STABILITY EVALUATIONS OF CHESBRO, LENIHAN, STEVENS CREEK, AND UVAS DAMS (SSE2)**

## **PHASE A: STEVENS CREEK AND LENIHAN DAMS**

### **LENIHAN DAM**

#### **WORK PLAN FOR SITE INVESTIGATIONS AND LABORATORY TESTING (REPORT No. LN-1)**

Prepared for

**SANTA CLARA VALLEY WATER DISTRICT**  
5750 Almaden Expressway  
San Jose, CA 95118

April 2011



**TERRA / GeoPentech**  
a Joint Venture

# TABLE OF CONTENTS

---

SECTION 1	INTRODUCTION .....	1-1
1.1	General .....	1-1
1.2	Organization of Document .....	1-2
SECTION 2	SITE DESCRIPTION AND HISTORY .....	2-1
2.1	General .....	2-1
2.2	Dam and Appurtenant Structures .....	2-1
2.3	Design and Construction History .....	2-2
2.3.1	Initial Design and Construction .....	2-2
2.3.2	Modifications .....	2-5
2.3.3	Instrumentation .....	2-5
2.4	Chronology and Scope of Previous Investigations .....	2-6
2.5	Previous Seismic Performance .....	2-8
SECTION 3	SITE GEOLOGY .....	3-1
3.1	General .....	3-1
3.2	Regional Geologic and Tectonic Setting .....	3-1
3.3	Local Geology, Faulting, and Seismicity .....	3-2
3.3.1	Local Geology .....	3-2
3.3.2	Local Faulting of Consequence to Lenihan Dam (San Andreas, Shannon, Stanford-Monte Vista and Berrocal faults) .....	3-3
3.3.3	Lexington Fault .....	3-4
3.3.4	Seismicity of Local Region .....	3-5
SECTION 4	FOUNDATION CONDITIONS .....	4-1
4.1	General .....	4-1
4.2	Rock Conditions .....	4-1
4.3	Evaluation of Potential for Occurrence of Surficial Soils Remaining In-Place within Dam Foundation .....	4-4
SECTION 5	EMBANKMENT MATERIAL PROPERTIES .....	5-1
5.1	General .....	5-1
5.2	Dam Zoning and Sources of Materials .....	5-1
5.3	Review and Assessment of Previous Testing .....	5-1
5.4	Classification, Index Properties, and "State" of Embankment Materials .....	5-2
5.4.1	Zone 1 – Upstream Shell .....	5-3
5.4.2	Zone 2 – Core .....	5-4
5.4.3	Zone 4 – Downstream Shell .....	5-7
5.5	Engineering Properties of Embankment Materials .....	5-8
5.5.1	Unit Weight .....	5-9
5.5.2	Effective Stress Friction Angle .....	5-9
5.5.3	Undrained Strength .....	5-9
5.5.4	Stress-Strain-Strength Relationship .....	5-10
5.5.5	Dynamic Properties .....	5-11
5.5.6	Permeability .....	5-12

# TABLE OF CONTENTS

---

SECTION 6	PRELIMINARY ENGINEERING ANALYSES .....	6-1
6.1	General.....	6-1
6.2	Purpose and Scope of Preliminary Loma Prieta Evaluation.....	6-1
6.3	Methodology and Approach .....	6-2
6.3.1	General.....	6-2
6.3.2	Loma Prieta Event at the Site .....	6-3
6.3.3	FLAC .....	6-4
6.4	Analysis Section and Input Parameters.....	6-5
6.4.1	Analysis Section .....	6-5
6.4.2	Material Properties.....	6-6
6.4.3	Input Motion .....	6-6
6.5	Results of Analyses.....	6-7
6.5.1	Seismic Response and Input Motion.....	6-7
6.5.2	Seismic Deformation Analyses.....	6-8
6.6	Conclusions and Recommendations .....	6-10
6.6.1	Conclusions.....	6-10
6.6.2	Recommendations.....	6-11
SECTION 7	PROPOSED SITE INVESTIGATIONS AND LABORATORY TESTING.....	7-1
7.1	General.....	7-1
7.2	Objectives and Approach for Field and Laboratory Investigations .....	7-1
7.3	Proposed Scope of Geotechnical Explorations .....	7-3
7.4	Field Personnel and Specialty Contractors .....	7-4
7.5	Procedures for Geotechnical Explorations and Sampling .....	7-5
7.6	Laboratory Testing.....	7-6
7.7	Schedule, Environmental, Safety, and Traffic Considerations .....	7-6
SECTION 8	REFERENCES.....	8-1

## Tables

5-1	Review and Assessment of Available Laboratory and Field Testing Data
5-2	Material Classification Summary
5-3	Summary of Engineering Properties
6-1	Summary of Material Properties Used in Analyses

## Figures

2-1	Regional Site Location Map
2-2A	Footprint and Plan of Previous Explorations
2-2B	Partial Eastern Footprint and Plan of Previous Explorations
2-2C	Partial Western Footprint and Plan of Previous Explorations

## TABLE OF CONTENTS

---

2-2D	Partial Eastern Footprint and Plan of Existing Instrumentation
2-3	Cross-Sections and Measured Piezometric Levels
2-4	As-Built Size of Inclined Drain
2-5	As-Built Fillet of Zone 2 Material
2-6	Review of Piezometer Data along Outlet Pipe
2-7	Effects of Loma Prieta Earthquake
3-1	Regional Fault Map
3-2	Local Region Geologic Map
4-1	Original As-Built Foundation Contours
4-2	Three-Dimensional View of Foundation Surface
4-3	Modified As-Built Foundation Contours
4-4	Cross-Sections with Foundation Surface
4-5	Previous Foundation Exploration Data
5-1	Maximum Cross Section B-B'
5-2	Gradation Ranges
5-3	Fines Content Distribution
5-4	Gradation Summary
5-5	Plasticity Chart
5-6	Plasticity Index Distribution
5-7	Liquidity Index
5-8	Liquidity Index Distribution
5-9	Water Content and Atterberg Limits
5-10	Cross Section B-B' with CPT Data Plots
5-11	Cross Section B-B' with CPT Interpretations
5-12	Soil Behavior Index Distribution
5-13	Soil Behavior Type Chart with Data
5-14	Soil Behavior Type Chart with Statistical Values
5-15	Total Unit Weight Data
5-16	Effective Strength Data
5-17	OCR Relationship from CPT Data
5-18	Undrained Strength from CPT Data



## TABLE OF CONTENTS

---

5-19A	Normalized Stress-Strain Plots – Upstream Shell, Harza Study
519B	Normalized Stress-Strain Plots – Upper Core, Harza Study
5-19C	Normalized Stress-Strain Plots – Lower Core, Harza Study
5-19D	Normalized Stress-Strain Plots – Downstream Shell, Harza Study
5-20	Normalized Stress-Strain Plot
5-21	Shear Wave Velocity Data
5-22	Modulus Reduction and Damping Ratio Curves
6-1	Loma Prieta Performance Map
6-2	Crest Section with Strong Motion Instrument Locations
6-3	Loma Prieta Time Histories
6-4	Loma Prieta Response Spectra
6-5	Idealized Maximum Cross Section
6-6	Idealized Section and FLAC Discretized Mesh
6-7	Input Motion for FLAC Analyses
6-8	Comparison of FLAC and SHAKE Response Spectra
6-9	Response Spectra – Comparison with 2-D Case 3
6-10	Comparison of Computed and Measured Response
6-11	Comparison of Computed Amplification Functions
6-12A	Case 1 Computed Displacement Contours
6-12B	Case 1 Computed Displacement Vectors
6-12C	Case 1 Computed Shear Strain Contours
6-13A	Case 2 Computed Displacement Contours
6-13B	Case 2 Computed Displacement Vectors
6-13C	Case 2 Computed Shear Strain Contours
6-14A	Case 3 Computed Displacement Contours
6-14B	Case 3 Computed Displacement Vectors
6-14C	Case 3 Computed Shear Strain Contours
6-15	Case 3 Deformation Time History at Crest Point
7-1	Existing and Proposed Exploration Plan
7-2	Proposed Exploration Plan – Complete
7-3	Proposed Exploration Plan – Borings and CPTs

## 1.1 GENERAL

In May 2010, the Santa Clara Valley Water District (District) retained Terra / GeoPentech (TGP), a joint venture of Terra Engineers, Inc. and GeoPentech, Inc., to complete seismic stability evaluations of Chesbro, Lenihan, Stevens Creek and Uvas Dams. These evaluations were required by the Division of Safety of Dams (DSOD) in June 2008 as part of their Phase III screening process of the State's dams located in highly seismic environments. The evaluations are also a vital part of the District's Dam Safety Program (DSP). Phase A of the project includes work on Stevens Creek and Lenihan Dams and has a planned completion date of February 2012. Phase B of the project includes work on Chesbro and Uvas Dams and is scheduled to begin in January 2012 and to finish by the end of 2013. The general scope of the project consists of the field, laboratory, and office studies required to evaluate the seismic stability of the four referenced dams.

This document contains the results of our site characterization at James J. Lenihan Dam (Lenihan Dam) based on the data available from the dam construction records and the field investigations and laboratory tests completed to date, presents the results of preliminary engineering analyses aimed at identifying data gaps, and concludes with a work plan for site investigations and laboratory testing focused on filling the data gaps identified by the preliminary analyses.

Our initial review of the large amount of geotechnical data available for Lenihan Dam (Terra / GeoPentech, 2010) led us to conclude that:

- a. there appeared to be sufficient information available to define the geometry of the dam and its foundation; and
- b. a detailed review and thorough evaluation of the available data on the properties of the various zones of the embankment (as indicated by the construction records, field investigations and laboratory tests completed to date) may provide much of the information necessary to support the engineering analyses.

Thus, we recommended to the District (and they concurred) that we proceed with an interim site characterization based on the wealth of existing data, perform preliminary engineering analyses using this site characterization data, identify what supplemental field and laboratory data are necessary to reduce the uncertainties in the results of the seismic stability analyses of the dam, and prepare a work plan for a field and laboratory investigation to obtain these data.

The seismic response of Lenihan Dam was recorded during the Loma Prieta earthquake by three accelerographs (two on the dam crest and one on the abutment), which indicated peak ground acceleration of about 0.4g. This set of recordings and the information on the seismic performance of the dam at that time provide an opportunity to calibrate the FLAC-based seismic deformation model(s) that will be used in the seismic evaluation of the dam under the design earthquake shaking conditions. This calibration of the deformation model(s) was also requested by DSOD. Therefore, the Loma Prieta case history was used in the preliminary engineering analyses documented herein to assess the appropriateness of the material properties developed based on existing information and to make adjustment to these properties, as necessary. These adjustments together with the results of the preliminary engineering analyses were then used to

identify key material parameters and zones that may warrant further refinement. This is a rational approach to develop a plan for additional investigations that is focused on refining critical material properties and characterization and ultimately reduce the epistemic uncertainty. The Loma Prieta recordings will also be used at a later date to evaluate the characteristics of the design earthquake shaking and put the input motions to be used in the seismic evaluation of the dam in perspective.

## **1.2 ORGANIZATION OF DOCUMENT**

This document contains eight sections, including this introduction. Section 2 describes the site and the history of Lenihan Dam including its construction, its documented performance during earthquakes, and the various investigations and studies that were conducted at the dam by a number of investigators. Section 3 discusses the site geology, including regional and local conditions and Section 4 addresses the foundation conditions at the dam. The various zones incorporated into the dam embankment and the characterization of the embankment material properties within these zones are discussed in Section 5. Section 6 documents the preliminary analyses using the Loma Prieta case history and identifies data gaps that should be filled to reduce the uncertainty in the seismic evaluation of the dam. The proposed site investigation as and laboratory testing to fill the data gaps identified by the analyses are presented in Section 7. Section 8 is a list of references.

## 2.1 GENERAL

Lenihan Dam (formerly called Lexington Dam) is located in Santa Clara County, California, about 1 mile south of the City of Los Gatos, as shown on Figure 2-1. The dam is an earthfill structure that was constructed across Los Gatos Creek in 1952. The dam impounds Lexington Reservoir that has a maximum capacity of 19,044 acre-feet at the spillway elevation of 653 feet<sup>1</sup>. DSOD has classified Lenihan Dam as a “High Hazard” dam because of the “extensive urban development in close proximity of the dam” (DSOD, 1981).

Appurtenant structures include a concrete-lined ogee type spillway located in the left abutment and an outlet tunnel through the right abutment connected to an inclined inlet structure in the reservoir, on the upstream side of the right abutment, and to an outlet structure that allows reservoir water to discharge into Los Gatos Creek approximately 150 feet beyond the toe of the dam. The outlet tunnel and inclined inlet structure were completed in 2009 and replaced the original outlet pipe that generally followed the preconstruction thalweg of Los Gatos Creek beneath the dam. The original outlet pipe was filled with grout and abandoned in place in 2009.

## 2.2 DAM AND APPURTENANT STRUCTURES

Figure 2-2A is an aerial photograph of Lenihan Dam that shows the outline of the embankment, the limits of Figures 2-2B and 2-2C, and an overview of the locations of previous explorations that are discussed in Section 2.4. Figures 2-2B and 2-2C provide larger scale location plans that include labels with the identifying name of the exploration (boring, test pit, or cone penetrometer probe). Borings that extended to rock are identified using the larger symbols, as shown in the legend. Figure 2-2D shows the location and labels of instruments (piezometers and inclinometers) that were installed in the borings.

Figure 2-3 contains transverse sections through the current configuration of the dam at Stations 14+10 and 15+95 that are representative of dam zoning and conditions near the center of the valley. The locations of the two sections are shown on Figures 2-2 (A through D). These sections have been heavily instrumented with piezometers, and the piezometer locations are shown on the sections. In some cases (e.g., LVP-19), it was necessary to project the location of piezometers installed at nearby dam stations onto the sections shown and, in the case of LVP-19, this caused a piezometer that was actually installed in the embankment to be shown as located in rock on Section B-B' of Figure 2-3. The location of previous borings are not shown on the cross-sections of Figure 2-3 for clarity but their plan locations are shown on Figures 2-2B and 2-2C, and the information from these borings on depth to rock is presented and discussed in Section 4.0.

As shown on Figure 2-3, Lenihan Dam was constructed as a compacted earth dam with upstream and downstream shells, core and drainage zones. The dam is about 195 feet high as measured from the lowest point in the foundation beneath the axis to the crest, and about 207 feet high as measured from the lowest point of the downstream toe to the crest.

---

<sup>1</sup> Unless otherwise noted in this document, all elevations are referenced to NAVD88 vertical datum.

Following the Loma Prieta Earthquake, it was determined that the crest of the dam had settled about 2.3 feet since construction because of a combination of long-term consolidation and seismically-induced deformation from the earthquake. The crest was subsequently raised by up to 4.5 feet, and the spillway chute walls raised by up to 6 feet, during the 1996-1997 freeboard restoration project. Thus, the crest is currently at nominal Elev. 673 feet and is about 40 feet wide, 830 feet long, and cambered. In general, the upstream face is inclined at 5.25 to 5.5 Horizontal to 1 Vertical (5.25 to 5.5H:1V). The downstream slope is inclined at 2.5 to 3H:1V. The concrete-lined, un-gated ogee crest spillway is located on the left abutment, with a nominal spillway crest elevation of 653 feet.

The original low level outlet pipe was extensively investigated after it experienced several partial collapses of the steel liner. The investigation showed that this occurred because of excess external pressure combined with vacuum pressures, corrosion, and out of roundness, and the outlet was subsequently repaired. The low level outlet was recently replaced by an outlet tunnel through the right abutment. The low level outlet pipe was filled with grout after completion of the outlet tunnel.

## **2.3 DESIGN AND CONSTRUCTION HISTORY**

### **2.3.1 Initial Design and Construction**

A relatively complete summary of the initial design and construction history of the dam and spillway was presented in the Phase 1 Inspection Report prepared by DSOD for the US Army Corps of Engineers (DSOD, 1981). The reader is referred to this document for construction details that are not repeated herein.

The following milestone dates associated with the original design and construction have been selected based on a review of DSOD files by TGP in order to allow discussion of some of the unusual features of the dam construction that may be relevant to understanding subsequent site exploration and dam monitoring data.

February 1948	District submits Application for Approval of Plans and Specifications to DSOD.
December 1951	District begins stripping of abutments and excavation for outlet pipe using District forces, after California Department of Highways completed relocation of Highway 17 adjacent to dam site.
April 1952	District submits amended Application for Approval of Plans and Specifications to DSOD.
May 1952	District awards contract for construction of dam and spillway to Guy F. Atkinson Construction Company.

June 13, 1952	DSOD Consulting Board recommends relocation of dam axis 60 feet upstream at the right abutment and 60 feet downstream at the left abutment. The move on the right abutment would allow avoiding contact of core materials with large rock masses exposed on that abutment. The move on the left abutment would better align the upstream face of the dam and spillway with sound material in that area.
June 1952	Placement of fill in upstream shell (Zone 1) begins.
July 11, 1952	Slide of 250,000 yd <sup>3</sup> occurs at left abutment in vicinity of upstream shell in the vicinity of a smaller slide mapped prior to construction.
August 11, 1952	Construction of outlet conduit is essentially complete.
August 14, 1952	Cleanup of slide is completed and placement of fill in Upstream Shell (Zone 1) and Core (Zone 2) begins again.
October 3, 1952	Upstream shell (Zone 1) and Core (Zone 2) are at elevation 605 feet while Drain (Zone 3) and Downstream Shell (Zone 4) are at elevation 510 feet. Construction of Zone 4 required the use of materials excavated for construction of the spillway and was delayed because the spillway excavation was delayed due to design changes, and did not begin until end of September. Zone 3 is discovered to be misaligned at elevation 510 feet and corrective action is taken as described below.
November 1, 1952	Zones 3 and Zones 4 reach elevation 600 feet where Zone 3 is terminated. DSOD inspection reports indicate quality of materials and control of thickness and continuity of Zone 3 are not always satisfactory.
November 12, 1952	Zone 4 reaches elevation 643 feet.
November 30, 1952	Dam embankment is completed.
December 29, 1952	Construction of spillway is completed.

TGP made the following observations based on our review of the DSOD construction records:

1. DSOD required stripping of the abutments to rock prior to placement of embankment fill and had DSOD inspectors monitor and enforce this requirement. This requirement was also applied to removal of materials that were involved in landslides during construction.
2. The relocation of the dam axis in order to accommodate conditions observed after initial stripping of the abutments; combined with the landslide activity on the left abutment, the proximity of relocated Highway 17, and the geometry of the approach channel to the spillway; delayed completion of the redesign of the spillway location and alignment until November 6, 1952. Excavation in the area of the spillway produced most of the material for Zone 4 and this excavation did not produce substantial amounts of material until early October.
3. The lack of material for construction of Zone 4 until October 1952, and the need to finish the project before the winter rains, required the construction of Zone 1 and Zone 2 fills (without placement of Zone 3 and Zone 4 materials) until Zones 1 and 2 reached elevation 605 feet. The downstream edge of Zone 2 was temporarily terminated at a slope of 1 1/4 H:1V and the portions of Zone 2 immediately adjacent to the temporary downstream slope were not compacted for safety reasons. The width of the zone that was not compacted was approximately 15 feet.
4. The correction of the misalignment of the Zone 3 inclined drain that was discovered in October 1952 is illustrated in the sketch by A. D. Morrison dated October 3, 1952 that is included as Figure 2-4. The corrections included placement of a 5 foot-thick layer of gravel that linked the misaligned portions of the inclined drain that were 25 feet apart. Figure 2-4 shows the width of the Zone 3 inclined drain is 15 feet but the note on this figure and the as-built drawings indicate the minimum width of the drain is 4 feet.
5. Once Zone 4 material became available, construction of the downstream section of the dam required removal of the uncompacted portions of the Zone 2 materials described in Item 3 above, and placement of additional Zone 2 materials in a fillet fill between the temporary downstream slope of Zone 2 and the design slope of Zone 2, as well as placement of Zone 3 drain material and Zone 4 downstream shell material. This is illustrated in the sketch by DSOD inspector D. Dresselhaus dated September 30, 1952 and included as Figure 2-5.
6. A consistent and reliable source of Zone 3 material for the inclined drain was not available. The limited amounts of materials provided from on-site borrow areas varied and were sometimes muddy. Delivery of materials procured from off-site commercial quarries lagged behind the need for the drain material, particularly during the night shift when truck traffic on public roads was not allowed. Although the contractor was cautioned by DSOD to maintain the Zone 3 fill well above the Zone 4 fill and was able to do so through mid October, the inspection report dated October 15, 1952 indicates that the contact of the drain was lost in one place and that placement of drain material was difficult because of the differences in elevation between Zones 2 and 4. The contractor was required to correct this situation. By the end of October, the placement of Zone 3 material lagged behind the placement of Zone 2 and 4 fills and drain material contacts were lost every night. The fill was at approximately elevation 580 feet at the time and the placement of the Zone 3 material was stopped once it reached elevation 600 feet.



7. From the above observations we have concluded that the offset in the inclined Zone 3 drain material at elevation 510 feet may have significantly impacted the hydraulic capacity of the drain and that the continuity and permeability of the Zone 3 inclined drain above this elevation is variable and sometimes severely compromised, particularly near the top of the layer between about elevation 575 feet and 600 feet. In addition, there are no construction records on the gradation of the Zone 3 drain materials.

### **2.3.2 Modifications**

The following modifications were made to the dam and appurtenant structures after the facility was initially completed in December 1952:

1. The spillway was modified to protect the Highway 17 fill in accordance with an agreement reached between the District and the State of California in December 1953. Construction of the spillway modifications was completed in March 1955 and a Certificate of Approval for the dam and reservoir was issued on December 24, 1956.
2. In 1958, gunite reinforcement was placed beneath the downstream end of the spillway as a precaution to prevent undermining of the spillway by Trout Creek that enters Los Gatos Canyon immediately downstream of the end of the spillway.
3. In 1960 the intake structure was raised.
4. In 1961 gunite lining was placed in erosion gullies at the right downstream groin of the dam.
5. In 1966 the County built a bridge across the spillway approach channel.
6. In 1971 gunite lining was again placed in erosion gullies at the right downstream groin of the dam.
7. In 1975 the District did some maintenance work on the intake structure.
8. In 1989 the outlet pipe was extended upstream and a new intake structure was constructed on the right abutment of the dam.
9. In 1997 the crest of the dam was raised by as much as 4.5 feet to restore the original dam freeboard and some modifications were also made to the spillway.
10. In 1998 some partially collapsed sections of the outlet conduit were repaired.
11. In 2009 a new outlet tunnel and inlet structure were completed in the right abutment and the original outlet pipe was abandoned in place by grouting.

### **2.3.3 Instrumentation**

Instrumentation at Lenihan Dam includes the following:

1. Nine survey monuments were originally installed along the dam crest that were replaced by ten survey monuments installed as part of the freeboard restoration project in 1997. In addition, five survey monuments were installed along the bike path to measure settlement and horizontal movement;



2. Five pneumatic piezometers (now abandoned) and three open well piezometers installed in 1975 by Wahler Associates (Wahler) as part of their seismic stability evaluation that are no longer monitored;
3. Twenty-two “permanent” piezometers installed in 1998 to monitor piezometric levels adjacent to the outlet pipe that were abandoned prior to grouting the outlet pipe in 2009;
4. Thirty-two vibrating wire piezometers installed in 1999 and 2001: 23 in the dam embankment, 2 within the bedrock foundation beneath the dam, and 7 within the bedrock at the right abutment;
5. A strong motion accelerometer installed by the District in the control building on the dam crest in 1999 to record crest acceleration in the event of an earthquake and to trigger a change in the reading frequency of the vibrating wire piezometers after a significant earthquake;
6. Three strong motion accelerographs (two on the dam crest and one on the left abutment) installed in 1975 by the California State Division of Mines and Geology; and
7. A weir to measure tunnel seepage discharge at the downstream end of the new outlet tunnel.

Maximum piezometric levels (i.e. measured total head at full reservoir level) from the piezometer data within the dam embankment (Item 4) are shown on Figure 2-3.

The location of piezometers along the outlet pipe and the variation of piezometric level with time for all these piezometers are summarized on Figure 2-6. The maximum piezometric level measured during the period from 2005 to 2007, as reported by the District (SCVWD, 2007), is also shown on the cross section at the top of Figure 2-6. The data from the outlet pipe piezometers show that the piezometric heads along the outlet pipe are very close to the reservoir level until the centerline of the dam crest is reached at which point the total heads drop off rapidly over a distance of about 100 feet.

## **2.4 CHRONOLOGY AND SCOPE OF PREVIOUS INVESTIGATIONS**

There has been a significant number of investigations and studies at Lenihan Dam since the dam was originally built. As discussed in Section 2.2, Figure 2-2A provides an overview of the locations of previous investigations.

The following is a summary of the previous investigations.

1. The first significant field and laboratory investigation at Lenihan Dam was the Seismic Safety Evaluation study by Wahler (1982). This evaluation consisted of three episodes of field investigation in 1975, 1979 and 1981, with the final report prepared in 1982. In all, Wahler completed:
  - 18 rotary borings in the dam, several of which included frequent Pitcher Barrel sampling with some Standard Penetration Tests (SPTs); 12 of these borings were extended into bedrock;
  - two trenches on the downstream slope, with in-place density testing of the embankment;
  - three sets of cross-hole shear wave tests, with seismic refraction and downhole surveys at each cross-hole site;

- installation of 5 pneumatic piezometers in the upstream shell and core (now abandoned), and three open well piezometers in the downstream shell (no longer monitored); and
- a large amount of classification and engineering properties testing including permeability, consolidation, compaction, and triaxial tests (UU, ICU and cyclic).

Wahler concluded that the dam had high seismic resistance and that catastrophic failure due to the maximum credible earthquake (M8.5 on the San Andreas fault) was not likely.

2. The second significant study was performed by Earth Sciences Associates (ESA, 1987) for the Outlet Modification Project. All of the explorations for this study were located outside the limits of the embankment for the purpose of designing a relocated intake structure on the lower upstream right abutment. However, as discussed further in Section 3.3, we used some of the exploration data generated from this work to clarify the likely level of the embankment foundation excavation in this area.
3. Following the Loma Prieta Earthquake in 1989, R. L. Volpe & Associates (RLVA) conducted an investigation of earthquake damage at Lenihan Dam (RLVA, 1990); this investigation included mapping and trenching of earthquake-induced cracking at the dam site.
4. The next significant study was conducted by Geomatrix in 1996 for the Lexington Dam Freeboard Restoration Project (Geomatrix, 1996). Geomatrix completed:
  - 7 shallow hollow-stem auger borings along the dam crest;
  - 14 rotary, core and flight auger borings along the sides of the spillway, ranging from 3 feet to 43 feet in depth;
  - 7 test pits, mostly along the spillway; and
  - laboratory testing including index properties, compaction, and unconfined compression (UC) tests on the shallow embankment materials, and limited UU triaxial tests on weathered rock along the spillway.
5. In 1997, Harza conducted a study to model the Loma Prieta Earthquake deformations at the dam using the GEFDYN program (Harza, 1997). Their work included the drilling of three borings along the maximum section of the dam, with Pitcher Barrel sampling, consolidation testing, and triaxial testing (ICU and cyclic).
6. Another significant study was performed in 1999 and in 2001 by RLVA and the District (RLVA, 1999a and 1999b; SCVWD, 2001), initially for the purpose of evaluating repeated episodes of outlet conduit damage that were first noted following the Loma Prieta Earthquake and that culminated in a Level One emergency at the dam in 1998. Work completed for these studies included a detailed seepage analysis and extensive installation of instrumentation, including most of the piezometers that are now used for monitoring. This work included:
  - 4 Cone Penetrometer Tests (CPTs);
  - 22 rotary borings with installation of 29 vibrating wire (VW) piezometers and two inclinometer casings with 13 in-place inclinometers;
  - installation of 22 piezometers along the outlet conduit (all now abandoned); and

- limited laboratory testing including index properties, consolidation, permeability and triaxial tests (UU and ICU).
7. The most recent significant investigation at Lenihan Dam was performed by Geomatrix in 2006, for the design of the new outlet tunnel (Geomatrix, 2006b). The exploration completed as part of that study was concentrated on the right abutment along the alignment of the new outlet tunnel and included:
- 18 rotary and core borings, some with packer testing and downhole seismic velocity measurements, optical televiewer and acoustic logging, and installation of 5 piezometers;
  - 4 test pits;
  - seismic refraction and electric resistivity lines; and
  - laboratory testing, mostly rock strength properties for tunnel design.

Data from the preceding studies have been consolidated and reviewed by TGP. Other data also reviewed included as-built drawings from the original construction (dated 1956), the intake structure modifications (1989), and the freeboard restoration project (1997), and other reports related to various investigations at Lenihan Dam. These data were obtained from a review of District files and the extensive file on Lenihan Dam maintained at the office of DSOD. In addition, several sets of black and white stereo aerial photographs were reviewed at the District's office, and selected sets were scanned and provided by the District for our later use. We also reviewed the extensive files on Lenihan Dam that are archived at DSOD's offices in Sacramento and scanned memoranda and photos from those files for our project data library. A list of the documents we reviewed is presented in Section 8.0.

## **2.5 PREVIOUS SEISMIC PERFORMANCE**

A major earthquake, the Loma Prieta earthquake, occurred on October 17, 1989 along a branch of the San Andreas fault. The epicenter of this event was located about 13 miles (20 km) from Lenihan Dam.

The effects of the Loma Prieta earthquake on Lenihan Dam were investigated by the District and RLVA in the days following the event as part of an overall investigation of District dams affected by the earthquake. The observed damage at the dam was documented in a report by RLVA (RLVA, 1990).

The dam was found to have sustained about 10 inches of crest settlement along the maximum section and a maximum of about 3 inches of lateral movement downstream, in addition to some localized transverse and longitudinal cracking. Also, about six weeks after the earthquake, a wet area had developed below the footpath near the right abutment, although no flow was reportedly emanating from this area. The mapped locations of the observed cracks and wet area have been highlighted on a copy of the drawing prepared by RLVA (RLVA, 1990) and are presented in Figure 2-7. This figure also includes a summary of the material that was cracked, maximum crack width, and depth of cracking at test trench locations, as reported by RLVA.

### **3.1 GENERAL**

This section describes the geologic and tectonic conditions that characterize the region and local site of Lenihan Dam. Section 3.2 describes the regional geologic and tectonic conditions, and Section 3.3 discusses geology, faulting and seismicity of the local vicinity of the site. The foundation conditions as they are presently understood are addressed in Section 4.0 along with a discussion of our evaluation concluding that the embankment is founded directly on Franciscan bedrock without any surficial soils having been left in-place within the foundation.

### **3.2 REGIONAL GEOLOGIC AND TECTONIC SETTING**

Lenihan Dam is located in the eastern foothills of the southern Santa Cruz Mountains that border the west side of the Santa Clara Valley, within the northwest-trending California Coast Ranges geomorphic province. The Santa Cruz Mountains are divided into two major fault blocks that are composed of different basement rock and separated by the San Andreas fault, approximately 2 km southeast of the dam. The San Andreas fault and associated sub-parallel San Gregorio, Calaveras, and Hayward faults comprise the principal faults of the San Andreas fault system, and accommodate the majority of transverse tectonic motion between the Pacific and North American plates within the region of San Francisco Bay. Principal faults in the region of Lenihan Dam are shown on Figure 3-1.

The fault block basement on the northeast side of the San Andreas fault consists of an assemblage of rocks that originally formed along the convergent Mesozoic continental margin. These rocks include Jurassic and Cretaceous-age volcanic, sedimentary and meta-sedimentary rocks of the Franciscan Complex, Coast Range ophiolite and Great Valley Sequence. This basement has been broken into several discrete fault-bounded wedges, including the Sierra Azul block that is located between the San Andreas fault and a complex line of locally merged segments of the Sargent, Berrocal, Sierra Azul and Aldercroft faults (mostly thrust faults), and the New Almaden block that is situated between this latter line of faults and the Hayward fault on the east side of the Santa Clara Valley. As shown on previous geologic mapping by the United States Geological Survey (USGS) (McLaughlin et al., 2001), Lenihan Dam is located on the New Almaden block near its southwest margin.

The principal fault movement in the region is dominantly right lateral but northeast-vergent (directed) thrusting along a number of reverse faults has resulted in crustal shortening and uplift of the Santa Cruz Mountains and foothills on the northeast side of the San Andreas fault. This crustal shortening is due to a westward restraining bend in the San Andreas fault where it passes through the Santa Cruz Mountains. Most of these faults are oriented sub-parallel to the San Andreas fault and appear to merge with it at depth. These reverse and oblique slip faults include the aforementioned Sargent, Berrocal, Sierra Azul and Aldercroft faults, as well as the Stanford, Monte Vista and Shannon faults that run along the lower foothills/valley margin.

The Mesozoic basement of the New Almaden block is unconformably overlain by Eocene and Miocene marine deposits, and younger unconformably overlying strata of Pliocene and Pleistocene fluvial deposits including the Santa Clara Formation. Since middle Pleistocene, these Miocene and younger rocks of the New Almaden block have been locally deformed and

faulted along the northeast-vergent Sargent, Berrocal and Shannon fault zones (McLaughlin et al, 2001).

Holocene sediments derived from the Santa Cruz Mountains underlie the relatively flat floor of the Santa Clara Valley, and overlap the lowermost foothills along the west side of the valley. Within the mountains, the Holocene deposits are usually limited to floors of the typically narrow stream valleys draining the range.

### 3.3 LOCAL GEOLOGY, FAULTING, AND SEISMICITY

#### 3.3.1 Local Geology

Figure 3-2 is excerpted from McLaughlin et al (2001) and depicts the geology of the local region of Lexington Reservoir. Lenihan Dam was constructed across the narrow canyon of Los Gatos Creek about 1.3 miles upstream from where it emerges from the Santa Cruz Mountains onto the floor of Santa Clara Valley. The upper reach of Los Gatos Creek follows the northwest regional trend defined by the San Andreas fault to the upstream end of Lexington Reservoir, at which point it bends northward, paralleling the Lexington fault and eventually emerging from the mountains at Los Gatos. Lenihan Dam crosses this north-trending downstream reach of the canyon.

The project region is located entirely within the Central Belt of the Franciscan Complex. These Central Belt Franciscan rocks in the area of Lenihan Dam consist mainly of Upper Cretaceous *mélange* and Jurassic-Cretaceous age sandstone of the Marin Headlands terrane. Mapping by the USGS (McLaughlin et al, 2001) shows the immediate area of the dam site as being underlain by the Central Belt *mélange*, with an area of more massive Marin Headlands terrane sandstone occurring at the upper end of the spillway and under the left upstream side of the dam.

The Plio-Pleistocene-age Santa Clara Formation consists of coarse-grained fluvial and, to a lesser extent, fine-grained lacustrine deposits, now exposed as erosional remnants outcropping on the lowermost foothills of the Santa Cruz Mountains and also locally along the margins of Los Gatos Creek and Lexington Reservoir. Some Santa Clara remnants occur as deformed, steeply and tightly folded fault-bound deposits (e.g., as observed along the Lexington fault “Cove exposure” noted below). No deposits of Santa Clara Formation were cited as having been identified within the immediate as-constructed foundation of Lenihan Dam, although a possible Santa Clara remnant was noted along a cut during construction for the relocated highway, just upstream of the foundation on the left abutment and above the elevation of the dam crest (Marliave, 1951).

Numerous landslides occur throughout the Santa Cruz Mountains region and, in the vicinity of the dam site, are concentrated along the west side of Los Gatos Creek and Lexington Reservoir. Several landslides occurred within the dam foundation during construction, mostly along the left abutment, and have also occurred since construction along the left side of the spillway downstream of the crest. These slides were the result of local over-steepening during excavation of the sheared Franciscan shale *mélange*, and of a generally weaker and more sheared condition of the shale along that left side of the dam.



As noted previously, younger Holocene alluvial deposits are usually limited to the floors of creek channels within the typically narrow canyons and ravines of the Santa Cruz Mountains and foothills and, at the dam site, were for the most part limited to the very bottom of Los Gatos Creek. As discussed further below, construction records indicate that all surficial deposits, including stream channel and terrace alluvium, colluvium and landslide deposits, were removed from the dam foundation prior to placement of the embankment.

### 3.3.2 Local Faulting of Consequence to Lenihan Dam (San Andreas, Shannon, Stanford-Monte Vista and Berrocal faults)

As noted above, the significant seismogenic faults affecting seismic hazard at Lenihan Dam are shown on Figure 3-1. The recent Technical Memorandum 3 (TM-3) "Seismotectonic and Ground Motion Study for Seismic Stability Evaluation of DIP Phase 1 Dams" (AMEC, 2009) indicates that the San Andreas, Berrocal, and Stanford-Monte Vista faults are the controlling seismic sources at Lenihan Dam. According to AMEC, the Maximum Credible Earthquake (MCE) on the Stanford-Monte Vista (magnitude  $M_w$  6.9 at 5.5 km map distance northeast of the dam) produces the highest accelerations at short periods whereas the MCE on the San Andreas fault ( $M_w$  7.9 at 2.1 km southwest of the dam) dominates at longer periods.

The Berrocal and Stanford-Monte Vista faults are both west-dipping reverse faults located northeast of the dam, and therefore, they dip directly under Lenihan Dam at fault rupture distances of 2.0 and 4.5 km, respectively. Although the Berrocal fault is situated closer than the Stanford-Monte Vista fault (2.3 vs. 5.5 km map distance), its lesser fault length and attendant MCE ( $M_w$  6.8 vs.  $M_w$  6.9) result in marginally lower median and 84<sup>th</sup> percentile ground motions at the dam (0.69g median and 1.17g 84<sup>th</sup> percentile for the Berrocal vs. 0.71g median and 1.20g 84<sup>th</sup> for the Stanford-Monte Vista). Additionally, TM-3 shows the Berrocal as a conditionally active, low to moderate slip rate fault (< 0.1 to 1.0 mm/yr) whereas the Stanford-Monte Vista is shown as an active, moderate slip rate fault (0.1 to 1.0 mm/yr). The San Andreas fault is a strike-slip fault with a very high slip rate (> 9mm/yr) and was the source of the  $M_w$  7.9 San Francisco earthquake in 1906. A subsidiary oblique-slip fault that is part of the San Andreas system and located on the southwest side of the main trace of the San Andreas fault, in the region south of Lenihan Dam, was the source of the  $M_w$  6.9 Loma Prieta earthquake in 1989. This fault was previously unrecognized prior to the Loma Prieta event.

DSOD has indicated in their recent comments on the SSE-1 Investigations DM-2 and Interim DM-4 for Guadalupe, Almaden, and Calero Dams (DSOD, 2010a) that they have historically considered a combined rupture of the Shannon-Monte Vista fault, in contrast to the Stanford-Monte Vista fault rupture scenario of AMEC. The combined Shannon-Monte Vista scenario is consistent with the interpretation of the fault as defined in Appendix A: California Fault Parameters for the National Seismic Hazard Maps and Working Group on California Earthquake Probabilities (Wills et al, 2008). However, TM-3 provides a basis for the segregation of the Shannon from the Stanford-Monte Vista in the vicinity of Blossom Hill, and we are herein utilizing the delineation of the Stanford-Monte Vista fault as a single fault rupture source separate from the Shannon fault, as is described in TM-3. The maximum moment magnitude of  $M_w$  7 assigned by DSOD to the Shannon-Monte Vista earthquake closely approximates the  $M_w$  6.9 estimate by AMEC for the Stanford-Monte Vista earthquake.

Although the Shannon fault is not shown in TM-3 as one of the primary faults contributing to the greatest seismic hazard at Lenihan Dam, a strong MCE event on the Shannon fault ( $M_w$  6.7 as per TM-3) would undoubtedly result in strong shaking at the dam. As noted below, earthquake-related damage that occurred in the Los Gatos and Blossom Hill areas as a result of the 1989 Loma Prieta earthquake appears to have been indicative of contractional deformation that was triggered along the Monte Vista-Shannon and Berrocal faults (Bryant, 2000).

### 3.3.3 Lexington Fault

The Lexington fault was first named by McLaughlin et al (1992) during geologic mapping studies of the local region by the USGS, following the 1989 Loma Prieta earthquake. However, traces of northward-striking faulting generally paralleling the course of Los Gatos Creek and across or immediately adjacent to the dam site had been previously mapped by several different investigators during earlier studies (e.g., Lewis 1951, Rogers and Armstrong 1971, and Rogers and Williams 1974). As part of our review of existing data, we compiled and reviewed various data related to the Lexington fault, and dam site faulting potential in general. Our initial evaluation of faulting conditions at Lenihan Dam also included some local field mapping, review of site geomorphology, study of pre-construction aerial photos of the area, consideration of local aftershocks of the 1989 Loma Prieta Earthquake, and review of regional and local geodetic data (the latter provided by the District).

In 2006 and 2007, Geomatrix Consultants conducted investigations of the Lexington fault in connection with studies for the new outlet works at Lenihan Dam. During a period of low reservoir level in 2007, Geomatrix and DSOD were able to examine and map an exposure of the fault that had been previously mapped by the USGS (McLaughlin et al, 1992 and 2004) but that is normally submerged beneath Lexington Reservoir. This exposure, located in a “cove” at the northeastern edge of the reservoir (approximately 1,000 feet southeast of the right end of the dam), was found to be a 30-foot wide shear zone with near-vertically tilted beds of Santa Clara Formation (east side) offset against Franciscan Complex rock (west side), along an 80° east-dipping fault contact. Geomatrix produced a detailed log of the fault exposure and then mapped the northward trace of the fault and found that it did not cross the planned outlet tunnel through the right abutment, but rather extended due north and passed about 200 to 300 feet east of the new tunnel alignment and approximately 600 feet east of the right abutment of the dam (Geomatrix, 2007). This “cove” faulting was reviewed by DSOD who concluded it did not cross the outlet tunnel but that it was (at that time) considered conditionally active (DSOD, 2007b).

The relatively recent TM-3 (AMEC, 2009) lists the Lexington fault as low slip rate, conditionally active, oblique-normal fault, consistent with DSOD’s designation of the Lexington fault as a conditionally active fault, at the time TM-3 was prepared. Additionally, TM-3 assigns the Lexington fault a rupture length of 7.5 km based on its intersections with the Berrocal and San Andreas faults to the north and south, respectively, and a corresponding MCE magnitude of  $M_w$  6.0 at a distance of 0.1 km, with peak ground accelerations of 0.46g (median) and 0.72g (84<sup>th</sup> percentile). As such, these calculated parameters would not control site ground motions. Most recently, we have learned that DSOD advised the District in November 2010 that DSOD now considers the Lexington fault to be inactive by their criteria (DSOD, 2010b). Consequently, we

are not considering the Lexington fault as an independent source for either ground motions or foundation fault rupture in our analysis.

### 3.3.4 Seismicity of Local Region

The 1906  $M_w$  7.9 San Francisco and 1989  $M_w$  6.9 Loma Prieta earthquakes dominate the historical seismicity in the region of Lenihan Dam. The 1906 earthquake along the San Andreas fault produced ground rupture along lengths of the fault as close as about 2 km southwest of the dam, where approximately 2 feet of offset was measured at several locations (SCVWD, 1976). Greater surface offset of about 4.5 feet was noted in a rail tunnel at Wrights Station further south, and the USGS has estimated that approximately 10 feet of horizontal slip occurred at depth along the reach of the fault immediately southwest of Lenihan Dam (USGS, 2011). The 1906 earthquake also produced a number of landslides, at least one of which blocked Los Gatos Creek within the present area of the reservoir; this particular slide occurred on the west side of Los Gatos Creek just to the north of Aldercroft Creek (ibid).

The 1989 earthquake occurred with an epicenter 20 km southeast of the dam along a southwest dipping rupture surface that is separate from the main trace of the San Andreas fault. The northernmost reach of fault rupture as was defined by the distribution of aftershocks and extended to a point about 6 km northwest of the dam. The earthquake produced right-oblique movement along the fault at depth, and uplift and shortening of the overlying crust that, in the local epicentral region, resulted in ridge-top spreading, extensional fissuring and other deformational surface features not directly related to surface faulting (Wells, 2004). Also, localized areas of damage indicating contractional deformation were noted in the Los Gatos and Blossom Hill areas along the southwestern margin of Santa Clara Valley, and appear to have resulted from Loma Prieta-triggered slip along the Monte Vista-Shannon and Berrocal faults (Bryant, 2000).



## **4.1 GENERAL**

Foundation conditions at Lenihan Dam have been described to varying degrees in a number of reports on previous geotechnical investigations conducted in association with construction, modifications, and engineering analyses of the dam and outlet works. In particular, an excellent summary and discussion of essentially everything that was known about the local foundation geology at Lenihan Dam through 1999 was written by geologist Phil A. Frame and was included as “Chapter 2 - Geologic and Seismotectonic Setting” in the “Lenihan Dam Outlet Investigation, Vol. 1 – Final Engineering Report” by RLVA (1999a).

Other informative data that was developed subsequent to the 1999 RLVA report and that can be extrapolated to embankment foundation conditions include 2002 field mapping data by Gilpin Geosciences, presented on a detailed geologic compilation map prepared for Treadwell and Rollo’s Geotechnical Feasibility Report for Lenihan Dam New Tunnel Option study (Treadwell and Rollo, 2002). That map presents the most comprehensive compilation of previous subsurface exploration and geologic mapping data that has been produced to date. Other more recent data that can be extrapolated to foundation conditions include selected mapping and rock testing data from the Final Geologic and Geotechnical Data Report, Lenihan Dam Outlet Modification Project, prepared by Geomatrix (2006b).

The rock surface on which the dam is founded was surveyed during construction, after removal of surficial soils. Figure 4-1 shows the original as-built topographic contours from the construction surveys and Figure 4-2 provides a three-dimensional perspective of that bedrock surface. It is unknown how many individual episodes of surveying may have been performed to prepare the as-built topographic surface shown on Figure 4-1; however, as discussed further below, a significant survey error is evident over portions of the right abutment foundation based on our comparison of the as-built rock surface elevations to the original site topographic survey and data on rock elevations from borings. As part of our site characterization work, we have where possible re-drawn the dam foundation contours for the portions of the misrepresented right abutment area under the embankment using available boring information in order to provide a more accurate foundation surface model for our engineering analyses. These revised foundation contours are incorporated into the modified as-built foundation topography presented in the shaded area on Figure 4-3.

Figure 4-4 provides transverse and longitudinal cross-sections through the dam that supplement the primary transverse sections shown on Figure 2-3. It is evident from Figure 2-3 and Figures 4-2 through 4-4 (and particularly the 3-dimensional view of Figure 4-2) that the bedrock surface has a typical, relatively uniform valley slope configuration on the right side of the dam but includes more irregular topography resulting from the presence of massive rock knobs on the upstream left side of the dam.

## **4.2 ROCK CONDITIONS**

Lenihan Dam was constructed on Franciscan Complex bedrock, without a foundation seepage cutoff or grout curtain. As indicated previously and as shown on Figure 3-2, regional geologic mapping by the USGS (McLaughlin et al, 2001) shows the majority of the dam site as being underlain by Franciscan mélange, with an area of more massive sandstone occurring at the upper

end of the spillway and under the left upstream side of the dam. The *mélange* typically consists of intensely fractured to crushed shale that encases blocks of harder sandstone and greenstone, some of which are up to several hundred feet in length, with lesser blocks of serpentinite and chert. The area of more massive sandstone that occurs at the upper end of the spillway on the left abutment includes some interbedded shale.

Much of the dam footprint is presumably directly underlain by the sheared shale matrix of the Franciscan *mélange*, as is indicated on numerous boring logs from studies conducted since construction. Areas of hard rock outcropping that were mapped by Marliave (Marliave, 1948) in the area of the dam foundation, prior to excavation/construction, are depicted on Figure 4-5. Undoubtedly, other areas of hard rock were exposed in the finished foundation excavation after removal of surficial soils; unfortunately, no as-constructed map documenting geologic conditions of the excavated foundation after completion of construction was uncovered in the DSOD project files. Localized areas of hard rock within the foundation can also be very roughly defined based on information presented on several boring logs.

As noted previously, several landslides occurred in the area of the left abutment both prior to and during construction, mainly as a result of the weaker and more sheared condition of the shale that characterizes portions of the left side foundation and spillway excavation downstream of the crest. One of these included a large slide estimated at about 250,000 yd<sup>3</sup> that occurred on the upstream left abutment in July 1952, during stripping activities for construction of Zone 1. This slide was approximately 300 feet wide and 400 feet long, and extended down slope in a southeastern direction from the area of the spillway approach channel; a comparison of the preconstruction and as-built topography indicates that excavations of up to about 65 feet were required in some areas of the slide to remove the debris and attain a suitable foundation. The estimated limits of this slide are shown on Figure 4-5.

Construction records do not provide detailed information on the rock conditions encountered at the base of the outlet pipe, although it is stated that an 800-foot long segment of the outlet conduit from Station 5+70 to Station 13+70 was founded on rock. The outlet pipe foundation was reported to be very hard rock between Station 6+60 and Station 7+30 and blasting of the right abutment rock at streambed level in the vicinity of Station 6+60 was also reported. The inspection report of August 6, 1952 states that 350 feet of outlet pipe remained to be completed at that time: the foundation had not yet been cleaned for the first 100 feet of this remaining segment, from Station 7+74 to Station 8+74; the foundation for the next 100-foot section from Station 8+74 to Station 9+74 had been cleaned and approved and was noted to be soft blue shale through which protruded hard rock outcrops; and, for the last 150 feet, the steel liner was in place and ready for the concrete pour but there is no mention of rock conditions under this portion of the liner in the inspection report. The shale-founded section of the outlet pipe, from Station 8+74 to Station 9+74, corresponds roughly to the area where piezometric levels measured along the outlet pipe dropped significantly, as shown in Figure 2-6. This may indicate a possible correlation between the total heads that were measured along the outlet and the lithology of the pipe foundation (e.g., areas of hard, more open-fractured sandstone, if hydraulically connected to the reservoir, might more readily transmit water pressures from the reservoir than softer, crushed and more impermeable shale).

In-situ permeability (packer) tests were performed in four borings drilled during the 1999 outlet investigation (RLVA, 1999a and 199b) and subsequent Phase B instrumentation project (SCVWD, 2001). Packer tests were also performed in a number of the borings drilled for design of the new outlet tunnel (Geomatrix, 2006b). The four borings drilled by the District in 1999 and 2001 were located along the right abutment, at the crest (LDP-18), on the right side of the upstream embankment slope near the groin (LDP-19), and on the right side of the downstream slope near the groin (LDP-20 and LDP-21). Calculated permeability values for these tests, as presented in the above-referenced data reports, ranged from tight (i.e., no flow) to  $4.7 \times 10^{-4}$  cm/sec. Lower permeability values were commonly in the range of  $10^{-6}$  cm/sec. Our review of these data (including the field test data sheets), led us to conclude that  $10^{-6}$  cm/sec or less probably represents a typical permeability coefficient for the sheared shale mélange matrix comprising significant portions of the foundation (a laboratory permeability test on a sample of sheared shale produced a permeability coefficient of  $10^{-9}$  cm/sec). For the most part, the higher calculated permeability coefficients (up to about  $10^{-4}$  cm/sec) occurred within masses of harder and shallower rock; e.g., above a depth of 62 feet in LDP-20, where total drill fluid losses occurred while drilling through blocks of fractured sandstone, greenstone and serpentinite. Similarly, total drill fluid losses occurred while drilling into sandstone portions of the foundation in Wahler borings LD-4, LD-17 and LD-18, which were located directly under the embankment near the maximum section of the dam. Conversely, none of the 1999 and 2001 borings that were drilled through the deeper channel section of the embankment and into an underlying shale foundation were noted as having experienced drill fluid loss. This suggests that the harder rock blocks within the foundation (e.g., sandstone, greenstone, etc.) are more likely to be open fractured, with an attendant higher hydraulic conductivity, than the sheared mélange matrix (crushed shale) surrounding the blocks.

Numerous shears, localized faults and fractures of various orientations occur throughout the foundation. Many of these are oriented northwest to west-northwest, consistent with the overall local regional trend of the fault- and shear-bounded blocks of rock that comprise this region of the New Almaden block. Mapping by Gilpin Geosciences shows a broad, approximately 100-foot wide zone of west-northwest shearing crossing Los Gatos Creek at the downstream toe of the dam (Treadwell and Rollo, 2002). Several north-south oriented shears, approximately parallel to the course of Los Gatos Creek, have been previously mapped and were also noted during site reconnaissance mapping for this study, mostly along the cut slopes above the spillway walls.

Several slope failures occurred during foundation excavation, particularly along the left side, and the dam axis was shifted downstream on the left side and upstream on the right side to take advantage of better rock conditions. Much of this construction slope instability was probably the result of local over-steepening of the weak sheared shale that characterizes the Franciscan mélange matrix.

Several shear wave velocity surveys were conducted during previous studies. These include cross-hole surveys that were extended through the embankment and into the foundation by Wahler in 1975 (3 sets) and later in 1981 (one set), and two downhole surveys in the right abutment ridge by Geomatrix along the new outlet tunnel alignment in 2006 (in Borings B-6 and B-11, at the upstream and downstream ends of the new tunnel, respectively). The shear wave velocities recorded in the

rock foundation are discussed hereinafter while the measurements made in the embankment materials are addressed in Section 5.5.5.

The 1975 Wahler surveys, which apparently penetrated a mixture of sandstone and shale to depths of up to 19 feet into the foundation beneath the embankment, produced shear wave velocities ranging from 1,600 to 2,200 feet per second (fps). However, the 1975 results were questioned and later re-evaluated based on data from the 1981 survey (Wahler, 1982). The 1981 survey, which may have penetrated mostly sandstone foundation and extended up to only 4 feet into the foundation beneath the embankment, produced results ranging from 2,680 to 3,110 fps. The downhole Geomatrix surveys resulted in shear wave velocities ranging from 1,700 to 3,250 fps at depths ranging from 11 to 150 feet, for the Franciscan rocks (sandstone, greenstone, serpentinite and mélange) comprising the right abutment ridge (Geomatrix, 2006b).

### **4.3 EVALUATION OF POTENTIAL FOR OCCURRENCE OF SURFICIAL SOILS REMAINING IN-PLACE WITHIN DAM FOUNDATION**

We closely examined a number of maps and reports that document the conditions in the foundation area that existed prior to, during, and after construction of the dam, for the purpose of determining whether potentially liquefaction-prone soil deposits were left in-place overlying the bedrock in the dam foundation. The data sources reviewed for this analysis included:

1. the pre-construction and as-constructed topographic maps of the foundation area;
2. the pre-construction geologic mapping and report of the dam site area (Marliave, 1948), along with subsequent memoranda describing foundation conditions as encountered during construction by Marliave and others;
3. pertinent exploration data from the various subsequent investigations of the dam, particularly explorations that penetrated the foundation under the dam including the 1975-1981 borings by Wahler (Wahler, 1982), the ESA exploration for design of the new intake structure (ESA, 1987), and later Phase A and B instrumentation borings drilled in 1999 and 2001 (RLVA, 1999a and 1999b; SCVWD, 2001); and
4. detailed geologic mapping of the dam site area by Treadwell and Rollo (2002).

We also reviewed the District's Foundation Analysis Report of SSE-2 Dams (SCVWD, 2010a). That report includes figures that depict the District's estimate of pre-construction soil thickness (colluvium, alluvium and landslide deposits) at Lenihan Dam (SCVWD 2010a, Figure 2), their estimated depths of foundation excavation (ibid, Figure 6), and their estimated distribution and thickness of in-place surficial soils remaining within the dam foundation (SCVWD 2010a, Figure 10). In our comparison of the pre-construction and as-built topographic surfaces (using digitized maps provided by the District), we found that the District's estimated depths of excavation as shown on Figure 6 of their report are in good agreement with the amount of excavation indicated by those maps. As noted on Figure 6 of the District's 2010 Foundation Analysis Report, the pre-construction and as-built maps indicate areas of anomalously positive excavation values (i.e. fill, not excavation), where the as-built surface is shown to be higher than the pre-construction surface over areas of the upstream and downstream right abutment slopes. Based on their estimated depths of excavation, subtracted from their assumed thicknesses of pre-

construction soils, the District identified several discrete areas of the upstream foundation area that might contain significant thicknesses of in-place soils remaining in the foundation.

Figure 4-5, presented herein, shows a compilation of pertinent data that we used to make our assessment of the foundation conditions under the dam. Borings that encountered bedrock are depicted along with the elevation of top of rock as encountered at each boring. Additionally, Figure 4-5 shows surface exposures of bedrock within, and adjacent to, the dam foundation as mapped by Marliave in 1948 and by Treadwell and Rollo in 2002, and includes notes that relate local geologic data to the District's estimated in-place soils for those areas. Our independent interpretation of foundation conditions at each of these areas found the following:

1. The areas of anomalously positive excavation values (and attendant estimated thicknesses of in-place soils of up to 18 feet) on the right abutment are most likely the result of a localized but pervasive as-constructed survey error over the upstream and downstream right abutment slopes. This is indicated by exploration data at borings LDP-19 and LDP-20 (Figure 4-5), which show the rock foundation directly under the embankment, but at elevations 18 feet to 27 feet higher than indicated on the as-built contour map. Similarly, geologic sections A-A and C-C from ESA's 1987 report indicate that their borings LO-1, LO-2 and LO-3, located on the upstream right abutment just above the original intake and the lowermost upstream embankment, were drilled into a rock slope without the overlying surficial soils that are suggested in that area on Figure 10 of the District's report (SCVWD, 2010a).
2. The central area of estimated 10-foot-thick in-place soils, approximately 250 feet upstream of the axis, shown on the District's Figure 10 are within an area mapped by Marliave as containing several outcrops of massive sandstone. Consequently, we conclude that this area was probably overlain by minimal thicknesses of soil rather than the approximately 20 feet of pre-construction soils estimated for this area on the District's Figure 2 (see note on Figure 4-5 herein).
3. The upstream left abutment areas shown on the District's Figure 10 as being underlain by 14 to 20 feet of in-place soils along the upstream toe are within an area where the embankment abuts an upstream bedrock ridge spur that is shown to be underlain by areas with surface exposures of Franciscan Complex sandstone as mapped by Treadwell and Rollo in 2002 (see Figure 4-5). Given the mapped rock surface exposures in this area, we conclude that this foundation area was probably blanketed by only thin colluvial soils rather than the 35 feet of pre-construction colluvium estimated for that area on the District's Figure 2.
4. A portion of the mid-left abutment area, on the left end of the upstream embankment, is shown on the District's Figure 10 as being underlain by up to 18 feet of possible in-place landslide material (the District's Figure 2 shows an estimated thickness of 45 feet of pre-construction landslide material within this area). In the various construction inspection memoranda reviewed by TGP, we did not note any reports of slide debris being left in-place within the foundation and believe it is appropriate to think that most, if not all, slide materials were removed from the foundation area.

The results of our analysis indicate it is unlikely that there are any significant areas of thicker, in-place soils remaining in the foundation between the embankment and the underlying Franciscan Complex bedrock. This is consistent with Marliave's concluding statement, from his 1948

geologic report, that bedrock is at, or within a few feet of, the surface within the narrow, V-shaped canyon underlying the dam site (Marliave, 1948). In summary:

1. Most of the previous exploration borings that have extended into the foundation indicate that the as-built elevation contours accurately depict the embankment foundation surface, except for areas of the right abutment where we believe a survey error mis-characterized the level of the foundation.
2. All of the borings drilled into the foundation under the dam show Franciscan Complex bedrock in direct contact with the overlying embankment.
3. DSOD construction memoranda indicate close inspection of the foundation preparation, and describe a common sequence of foundation excavation, clean-up and approval that immediately preceded fill placement. These records also document adherence to the design criteria of founding the entire embankment on Franciscan Complex.
4. The areas of estimated in-place soils depicted under the upstream portion of the embankment on the District's Figure 10 (SCVWD, 2010a) are likely the result of the above-mentioned survey error for portions of the right abutment, and an over-estimation of the pre-construction soil thickness in the central and left side areas of the upstream foundation.

Given the information described above, it is our opinion that, for all practical purposes, the compacted dam embankment is founded directly on bedrock and that no alluvium or colluvium soils are present beneath the dam.



## **5.1 GENERAL**

Using the data available from previous investigations, the material property characterization divides the dam embankment into zones of similar materials, describes the general nature and variation of the materials within each zone, and provide information on the state of each material that is relevant to the engineering analyses of seismic deformations. The following subsections address the zoning of the dam and the general sources of the embankment materials, document the result of our review and assessment of previous testing performed on the embankment materials, and summarize the index properties and engineering properties of the embankment materials that are relevant to the engineering analyses.

## **5.2 DAM ZONING AND SOURCES OF MATERIALS**

As noted in Section 2.2, Lenihan Dam was constructed as an earthfill embankment consisting of various zones. Figure 5-1 shows a generalized configuration of the dam through the maximum section (section B-B' on Figure 2-2A) including the idealized limits of each zone based on construction records. These zones consist of the following: Zone 1 – Upstream Shell, Zone 2U – Upper Core, Zone 2L – Lower Core, Zone 3 – Drain, and Zone 4 – Downstream Shell. The predominant soil classification in each of the zones is also listed on Figure 5-1. The fillet of Zone 2 fill material shown on Figure 2-5 and discussed in Section 2.3.1 was placed to achieve the design geometry of the embankment zones while accommodating the delayed construction of Zone 3 and Zone 4 and is not shown on the generalized cross section.

The upstream shell and upper core materials are generally classified as gravely clayey sand to sandy clays (for the upstream shell) and gravelly clayey sands to clayey gravel (for the upper core). The materials forming the lower core are generally classified as sandy highly plastic clays to sandy highly plastic silts. Materials for the core and upstream shell of the dam were obtained from borrow sources upstream of the dam. Materials for the upstream shell and the upper core were derived from excavation of Franciscan Complex just upstream of the upstream toe. The lower core was derived from clayey alluvial/colluvial fan deposits that occurred at the mouth of Limekiln Canyon just south of the boat ramp on the upstream right abutment.

The downstream shell consists mainly of gravely clayey sands to clayey gravels. The downstream shell was primarily derived from the spillway excavation. There is no classification information available on the drain materials. However, construction records indicate that limited amounts of materials for the drain were obtained from on-site borrow areas but that most of the materials were procured from off-site commercial quarries.

## **5.3 REVIEW AND ASSESSMENT OF PREVIOUS TESTING**

All existing data considered appropriate for material characterization, including field and laboratory test results, were reviewed. In particular, previous investigations performed by Wahler (1982), Geomatrix (1996), Harza (1997), RLVA (1999a and 1999b), and SCVWD (2001) all contained information regarding the properties of the embankment materials; we examined the pertinent aspects of these investigations and evaluated whether or not the data from these investigations could be reliably used for deriving the material properties for the preliminary engineering analyses.

Table 5-1 is a summary of our review of the existing information regarding material properties. The types of tests and/or material properties available from each of the five investigations listed above have been divided among the following categories: classification properties, in-situ properties (properties based on in-situ test results), effective stress strength (effective stress strength parameters), undrained strength (undrained stress-strain-strength parameters), cyclic properties, shear wave velocity, and other properties. For each investigation and each category, we indicate whether or not the data was used in the material property characterization and the reasons why, under the headings "Application" and "Reasoning", respectively.

The material properties described in the following sections are based on the data and information from the previous investigations listed above that were judged to be adequately complete, appropriate, and reliable. The term "complete" refers to studies where testing encompassed all key zones of the dam and all pertinent data were reported. The term "appropriate" refers to testing methods and details considered to be adequately consistent with the current preferred approach. The term "reliable" refers to data and results judged to be reliable after careful review of the data and the discussions contained in reports.

As shown on Table 5-1, the results of cyclic property tests reported by Wahler (1982) and Harza (1997) were considered but not used in our material property characterization for the following reasons. The modulus degradation with cycles derived from these tests may be of interest. However, the tests were for triaxial loading conditions rather than direct simple shear loading conditions. In addition, the tests by Wahler were stress-controlled, making interpretation difficult. The other set of tests by Harza was strain-controlled but the specimens were consolidated to pre-testing effective confining pressures that were considerably greater than the in-situ stresses and there is a lack of information on the depth and in-situ effective stresses for the samples, again making interpretation difficult.

#### **5.4 CLASSIFICATION, INDEX PROPERTIES, AND "STATE" OF EMBANKMENT MATERIALS**

The following sections provide a summary and discussion of the embankment material classification, index properties, and "state" obtained from previous investigations performed by Whaler (1982), Geomatrix (1996), Harza (1997), RLVA (1999a and 1999b) and SCVWD (2001). Each zone of the embankment is addressed except Zone 3 – Drain because no samples were collected or tested for that zone.

Soil is classified using the Unified Soil Classification System (USCS) based on the gradation of particles that make up the soil (i.e., the amount by weight of gravel-, sand-, and silt- or clay-size particles) and the plasticity characteristics (Liquid Limit and Plasticity Index) of the material passing the No. 40 sieve. The "state" of the soil is estimated by comparing the density and strength of the soil under the in-situ state of stress to the density and strength of a normally consolidated soil under the same in-situ stress. The Overconsolidation Ratio (OCR) is a commonly used indicator of the "state" of a soil. OCR is defined as the ratio of the maximum vertical effective stress the soil has experienced in the past to the current vertical effective stress. For a normally consolidated soil the OCR is 1.

The "state" of compacted soils is controlled by the density the soil achieved when the material was placed and compacted, and by the current state of stress. The density of the soil achieved



when the material was placed and compacted is analogous to the density of a sedimentary soil at the maximum past pressure. Consequently, the OCR for a compacted soil is based on the equivalent maximum past pressure associated with the in-place density of the soil. As a result, the OCR for a compacted clay is expected to decrease with depth and be minimum at the contact between the embankment and its foundation.

The classification and index properties of each zone are summarized in Table 5-2 in terms of generalized USCS classification, in-situ conditions (i.e., dry unit weight, moisture content, and compaction), gradation characteristics (i.e., percent each by weight of gravel-, sand-, silt-, and clay-size particles), and Atterberg limits (i.e., Liquid limit and Plasticity Index). Average index properties are listed as well as minimum and maximum values.

#### 5.4.1 Zone 1 – Upstream Shell

The upstream shell of the dam is founded on bedrock and has an upstream slope between 5.25 and 5.5H:1V. Samples obtained from Zone 1 have been classified as gravely clayey sands (SC per USCS) to sandy clays (CL per USCS). In previous studies, the conditions of the upstream shell material were determined by unit weight and moisture content testing on intact samples. A total of 19 unit weight tests were performed on intact samples of Zone 1 material and produced an average dry unit weight of 119 pcf. Similarly, a total of 21 moisture content tests were performed on Zone 1 samples and showed an average moisture content of 15.0%. To date, maximum density has not been determined in the laboratory for Zone 1 materials. Previous studies, including RLVA 1999, have reported an estimated maximum dry unit weight of 125 pcf for the upstream shell (based on ASTM D-1557 modified to 20,000 ft-lb/ft<sup>3</sup> of compactive energy), which would correspond to an average relative compaction of 95%.

As shown on Figure 5-2, a wide range of gradations have been recorded on samples tested by others. A total of 14 gradation tests were performed on samples from Zone 1 with average gravel, sand, and fines contents of 27%, 34%, and 39%, respectively. Additionally, hydrometer tests were performed on 8 samples of Zone 1 material showing an average clay content of 21%. It was noted in reviewing the gradation information that several samples had over 40% gravel content, including one with 43% gravel. Several other samples had less than 20% gravel, including one with no gravel. Similarly, the fines content observed ranged from a high of 97% to a low of 19% by weight. The cumulative distribution of fines content is plotted on Figure 5-3; it is noted that, despite the wide range of fines contents observed for all samples, the 20<sup>th</sup> and 80<sup>th</sup> percentile values form a much narrower range, approximately 20% to 45% by weight. Simplified results of the 14 gradation tests performed have been plotted vs. elevation on the left side of Figure 5-4 for the Zone 1 material. As shown in this plot, changes in gradation occur gradually with depth with the exception of one sample at elevation 520 feet, which has 97% fines content and 44% clay content and closely resembles the classification of the Zone 2L – Lower Core material.

A total of 8 Atterberg limits tests were performed on Zone 1 samples collected during previous investigations. The results of these tests are grouped closely together as shown on the plasticity chart on Figure 5-5. Upstream shell materials had a liquid limit range of 30 to 39 with an average value of 33, and a plasticity index (PI) range of 6 to 24 with an average value of 15. The cumulative distribution of PI is shown on Figure 5-6; it is noted that the 50<sup>th</sup> percentile PI is

also 15. Moisture content and Atterberg limits information was combined to calculate liquidity index (LI) for all eight samples tested. The results are presented on the Liquidity Chart on Figure 5-7. It is observed that the LI values for upstream shell samples ranged from -1.87 to 0.23 with an average value of -0.57. The cumulative distribution of LI values is plotted on Figure 5-8; it is noted that the 50<sup>th</sup> percentile LI is -0.47. These low values suggest that the upstream shell materials are very over-consolidated to somewhat over-consolidated, depending on the confining pressure, as one would expect for soils compacted to 95% relative compaction. All index test and moisture content data are plotted vs. elevation on Figure 5-9 to show where the in-situ water content falls with respect to the plastic limit and liquid limit of the upstream shell. Review of this figure indicates that the in-situ moisture content consistently falls near or below the plastic limit of the materials, again indicative of an over-consolidated material.

Four Cone Penetration Tests (CPTs) were performed by RLVA to collect in-situ data on the embankment materials (RLVA, 1999b). The data from these CPTs are plotted on Figure 5-10; in this figure the data from all four CPTs has been projected to the maximum section B-B' at Station 15+95. As shown on Figure 5-10, CPT-1 and CPT-3 recorded continuous profiles of the Zone 1 material.

The data presented on Figure 5-10 consists of tip resistance to the right and friction ratio to the left, both of which have been normalized for confining pressure in accordance with the guidelines developed by Robertson (2009). Similarly, following the procedure developed by Robertson (2009), these normalized values are used to determine the Soil Behavior Type Index,  $I_c$ , and to estimate over-consolidation ratio (OCR) through a correlation. The  $I_c$  and inferred OCR data for all four CPTs are plotted on Figure 5-11. Generally stated, the higher the  $I_c$  value, the finer, and more clay-like in behavior, the material: an  $I_c$  value of 2.6 is used to divide soils that will exhibit clay-like behavior and those that will exhibit sand-like behavior.

Figure 5-12 presents the cumulative distribution of the  $I_c$  values for each material. The median  $I_c$  value for the upstream shell materials is 2.52. As can be seen on Figures 5-11 and 5-12, many of the samples from the upstream shell fall at or above the 2.6 threshold suggesting that clay-like behavior will likely control. The inferred OCR values shown on Figure 5-11 (computed only for those points where the  $I_c$  value is greater than 2.6) indicate that the clayey materials in the upstream shell are likely over-consolidated. Figure 5-13 reinforces this, showing a soil behavior type chart (Robertson and Wride, 1998) with a majority of the upstream shell points falling in the upper right portion of the plot, in the area representing materials that are interpreted as being more over-consolidated or aged.

## 5.4.2 Zone 2 – Core

The core of Lenihan Dam has been divided into two zones based on source material and classification information reviewed; the Zone 2U - Upper Core exists from the dam crest to elevation 590 feet, and the Zone 2L – Lower Core exists from elevation 590 feet to the bedrock foundation. The material characterization for both zones is addressed in the following sections.

### *5.4.2.1 Zone 2U – Upper Core*

Samples obtained from Zone 2U have been predominantly classified as gravely clayey sands (SC per USCS) and clayey gravels (GC per USCS). Additionally, several samples have been classified as silty sands (SM per USCS) and sandy clays (CL per USCS). As noted in Section 5.2, Zone 1 and Zone 2U were derived from the same source material and therefore, the two zones have been shown to have similar in-situ gradation and index properties.

In-situ property testing from previous studies included determination of unit weight and moisture content on intact samples. A total of 60 unit weight tests were performed on intact samples of Zone 2U material and produced an average dry unit weight of 119.1 pcf. Similarly, a total of 61 in-situ moisture content tests were performed on Zone 2U samples and showed an average moisture content of 11.4%. To date, maximum density has not been determined in the laboratory for Zone 2U materials. Previous studies, including RLVA in 1999, have reported an estimated maximum dry unit weight of 125 pcf for the upstream shell which is similar to the upper core and would correspond to an average relative compaction of 95% for the upper core (based on ASTM D-1557 modified to 20,000 ft-lb/ft<sup>3</sup> of compactive energy).

The middle plot on Figure 5-2 shows the full range of gradations for Zone 2U and Zone 2L materials on samples tested by others. A total of 25 gradation tests were performed on samples from Zone 2U with average gravel, sand, and fines contents of 33%, 35%, and 31%, respectively. Additionally, hydrometer tests were performed on 11 samples of Zone 2U material showing an average clay content of 17%. It was noted in reviewing the gradation information that seven samples had over 50% gravel content, including one with 58% gravel. Conversely, six samples had less than 20% gravel, including one with 3% gravel. The values of fines content observed ranged from a high of 53% to a low of 16% by weight. The cumulative distribution of fines content is plotted on Figure 5-3; it is noted that despite the wide range of fines contents observed for all samples, the 20<sup>th</sup> and 80<sup>th</sup> percentile values form a much narrower range, approximately 20% to 40% by weight. Simplified results of the 25 gradation tests performed have been plotted vs. elevation on the top half of the middle plot of Figure 5-4 for the Zone 2U materials. As shown in this plot, changes in gradation are rather abrupt; significantly higher gravel content is observed in the top 30 feet (above elevation 643 feet), and higher fines content is observed in the lower 20 feet (between elevations 590 feet and 610 feet).

A total of 13 Atterberg limits tests were performed on Zone 2U samples collected during previous investigations. The results of these tests are grouped closely together as shown on the plasticity chart on Figure 5-5. Upper core materials have a liquid limit range of 31 to 43 with an average value of 38, and a plasticity index (PI) range from 14 to 29 with an average value of 17. The cumulative distribution of PI is shown on Figure 5-6; it is noted that the 50<sup>th</sup> percentile PI is also 17. Moisture content and Atterberg limits information was combined to calculate liquidity index (LI) for 13 samples tested; these results are presented on the Liquidity Chart on Figure 5-7. It can be seen that the LI values for the upper core samples range from -0.53 to 0.23 with an average value of -0.34. The cumulative distribution of LI values is plotted on Figure 5-8; it is noted that the 50<sup>th</sup> percentile LI is -0.43. These low values suggest that the upper core materials are very over-consolidated. All index test and moisture content data are plotted on Figure 5-9 vs. elevation to show where the in-situ water content falls with respect to the plastic limit and liquid

limit of the upper core. This figure shows that the in-situ moisture content consistently falls near or below the plastic limit of the materials, again indicative of an over-consolidated material.

As shown on Figure 5-10, CPT-1 and CPT-2 provide continuous profiles of the upper core material. The  $I_c$  and inferred OCR data are plotted on Figure 5-11. The cumulative distribution of the  $I_c$  values is shown on Figure 5-12 and indicates that the median value of  $I_c$  for the upper core materials is 2.58. As can be seen in Figures 5-11 and 5-12, many of the samples from the upper core fall at or above the 2.6 threshold suggesting that clay-like behavior will control. The inferred OCR values shown on Figure 5-11 (computed only for those points where  $I_c$  value is greater than 2.6) indicate that the clayey materials in the upper core are likely over-consolidated. Figure 5-13 shows a similar trend on a soil behavior type chart with all of the upper core points, except for two, falling in the upper right portion of the plot, in the area representing materials that are interpreted to be more over-consolidated or aged.

#### 5.4.2.2 Zone 2L – Lower Core

Samples obtained from Zone 2L have been predominantly classified as sandy highly plastic clays (CH per USCS) and silty sands-sandy highly plastic silts (SM/MH per USCS). Additionally, several samples have been classified as clayey sands (SC per USCS) and sandy clays (CL per USCS). In-situ property testing from previous studies included determination of unit weight and moisture content on intact samples. A total of 24 unit weight tests were performed on Zone 2L material and produced an average dry unit weight of 99.8 pcf. Similarly, a total of 24 in-situ moisture content tests were performed on Zone 2L samples and yielded an average moisture content of 24.0%. Maximum density was determined in the laboratory for Zone 2L materials during the RLVA 1999 study, showing a maximum dry unit weight of 98.2 pcf, which would correspond to an average relative compaction of 101% (based on ASTM D-1557 modified to 20,000 ft-lb/ft<sup>3</sup> of compactive energy).

The middle plot on Figure 5-2 shows the full range of gradations for Zone 2U and 2L materials on samples tested by others. A total of 18 gradation tests were performed on samples from Zone 2L with average gravel, sand, and fines contents of 6%, 15%, and 79%, respectively. In addition, hydrometer tests were performed on 18 samples of Zone 2L material and yielded an average clay content of 42%. The fines content observed ranged from a high of 97% to a low of 29% by weight. The cumulative distribution of fines content is plotted on Figure 5-3; it is noted that only 20% of the samples tested had less than 50% fines. Simplified results of the 18 gradation tests performed have been plotted vs. elevation on the bottom half of the middle plot on Figure 5-4 for the Zone 2L material. As shown in this plot, gradation characteristics for the lower core are fairly uniform with the exception of two samples near elevation 550 feet that more closely resemble upstream shell material.

A total of 14 Atterberg limits tests were performed on Zone 2L samples collected during previous investigations. The results of these tests predominantly fall to the right of the B-line as shown on the plasticity chart on Figure 5-5 and are consequently classified as clays of high plasticity. Lower core materials had a liquid limit that ranged from 43 to 68 with an average value of 62, and a plasticity index (PI) that ranged from 15 to 44 with an average value of 34. The cumulative distribution of PI is shown on Figure 5-6; it is noted that the 50<sup>th</sup> percentile PI is also 34. Moisture content and Atterberg limits information was combined to calculate liquidity

index (LI) for 14 samples tested; these results are presented on the Liquidity Chart on Figure 5-7. It was observed that the LI values for lower core samples ranged from -0.79 to 0.12 with an average value of -0.17. The cumulative distribution of LI values is plotted on Figure 5-8; it is noted that the 50<sup>th</sup> percentile LI is -0.11. These low values indicate that the lower core materials are over-consolidated. The same characteristic is indicated by the distribution of in-situ water contents and plastic and liquid limits vs. depth plotted on Figure 5-9. The in-situ moisture content of the lower core materials consistently falls near or below the plastic limit of the materials, indicative of an over-consolidated material.

As shown on Figure 5-10, CPT-1, CPT-2, and CPT-4 provide continuous profiles of the lower core material. The  $I_c$  and inferred OCR data are plotted on Figure 5-11. The cumulative distribution of the  $I_c$  values is shown on Figure 5-12 and indicates that the median value of  $I_c$  for the lower core material is 2.95, and is well above the  $I_c$  value of 2.6 used to differentiate sand-like behavior from clay-like behavior. As can be seen in Figures 5-11 and 5-12, almost every sample from the lower core falls at or above the 2.6 threshold indicating that clay-like behavior will control. The inferred OCR values shown on Figure 5-11 (computed only for those points where  $I_c$  value is greater than 2.6) indicate that the clayey materials in the lower core are likely over-consolidated; note on Figure 5-11 that the inferred OCR values tend to become lower with depth, indicating a trend that is consistent with compacted (and therefore, over-consolidated) clay becoming less over-consolidated with increasing overburden pressure, as discussed in Section 5.5.3. Figure 5-13 shows a soil behavior type chart with all of the lower core points falling in the upper right portion of the plot, in the area representing materials that are interpreted to be over-consolidated.

### 5.4.3 Zone 4 – Downstream Shell

The downstream shell of the dam is founded on bedrock and is inclined between 2.5 and 3:1H:1V. Samples obtained from Zone 4 have been predominantly classified as gravely clayey sands (SC per USCS) to clayey gravels (GC per USCS). Additionally, several samples have been classified as poorly-graded sands (SP per USCS) sandy clays (CL per USCS) and silty gravels (GM per USCS). In-situ property testing from previous studies included determination of unit weight and moisture content on intact samples and samples tested in test pits. A total of 45 unit weight tests were performed on samples of Zone 4 material and produced an average dry unit weight of 124.3 pcf. A total of 46 in-situ moisture content tests were performed on Zone 4 samples and showed an average moisture content of 12.0%. Maximum density was determined in the laboratory for Zone 4 materials during the RLVA 1999 study, showing a maximum dry unit weight of 140 pcf, which would correspond to an average relative compaction of 89% (based on ASTM D-1557 modified to 20,000 ft-lb/ft<sup>3</sup> of compactive energy).

The lower plot on Figure 5-2 shows the range of gradations for Zone 4 materials on samples tested by others. It is noted that the 70<sup>th</sup> percentile of samples tested represents a narrower range than the entire set of samples tested. A total of 30 gradation tests were performed on samples from Zone 4 with average gravel, sand and fines contents of 32%, 38% and 30%, respectively. Additionally, hydrometer tests were performed on 10 samples of Zone 4 material showing an average clay content of 11%. The cumulative distribution of fines content is plotted on Figure 5-3; it is noted that the distribution is very similar to those of the upper core and upstream shell



materials. Simplified results of the 30 gradation tests performed have been plotted vs. elevation on the right of Figure 5-4 for the Zone 4 materials. As shown in this plot, changes in gradation are small and gradual with elevation.

A total of 17 Atterberg limits tests were performed on Zone 4 samples collected during previous investigations. The results of these tests are grouped closely together as shown on the plasticity chart on Figure 5-5. Downstream shell materials had a liquid limit that ranged from 22 to 41 with an average value of 32, and a plasticity index (PI) that ranged from 6 to 23 with an average value of 14. The cumulative distribution of PI is shown on Figure 5-6; it is noted that the distribution is nearly identical to that of the upstream shell. Moisture content and Atterberg limits information was combined to calculate liquidity index (LI) for 17 samples tested; these results are presented on the Liquidity Chart on Figure 5-7. The LI values for the downstream shell samples ranged from -1.09 to -0.01 with an average value of -0.45. The cumulative distribution of LI values is plotted on Figure 5-8; it is noted that the 50<sup>th</sup> percentile is -0.41 and that the distribution is very similar to that of the upper core materials and suggests that the downstream shell materials are also very over-consolidated. All index test and moisture content data are plotted vs. elevation on Figure 5-9; the in-situ moisture content consistently falls near or below the plastic limit of the materials, again indicative of an over-consolidated material.

CPT-4 provides a continuous profile of the downstream shell material, as shown on Figure 5-10. The  $I_c$  and inferred OCR data are plotted on Figure 5-11. The cumulative distribution of the  $I_c$  values is shown on Figure 5-12 and indicates that the median value of  $I_c$  for the downstream shell material is 2.50. As can be seen in Figures 5-11 and 5-12, many of the samples from the downstream shell fall at or above the 2.6 threshold suggesting that clay-like behavior will control. The inferred OCR values shown on Figure 5-11 (computed only for those points where  $I_c$  value is greater than 2.6) indicate that the clayey materials in the downstream shell are likely over-consolidated. Figure 5-13 shows a similar trend on a soil behavior type chart with all of the downstream shell points, except for one, falling in the upper right portion of the plot, in the area representing materials that are interpreted to be more over-consolidated or aged.

## 5.5 ENGINEERING PROPERTIES OF EMBANKMENT MATERIALS

The preliminary engineering analyses discussed in Section 6 require the following material properties for the various zones shown on Figure 5-1: unit weight, effective stress friction angle, undrained strength, undrained stress-strain-strength relationship, and dynamic properties (i.e., shear-wave velocity, shear modulus reduction, and damping ratio curves). In addition, the permeability of the various materials is required as initial input to the seepage analyses that will support the engineering analyses of seismic deformations. The following sub-sections describe how material properties were derived from the existing data for all zones except Zone 3. The Zone 3 drain materials should be predominantly sand or sand and gravel mixes but no classification or engineering information is available from previous studies for these materials. For our preliminary engineering analyses of seismic response and permanent displacements, we have assigned the Zone 3 materials the same stiffness and strength as the Zone 4 materials.

Table 5-3 provides a summary of the properties selected for each of the zones in terms of actual values and/or numbers of figures where the appropriate relationships are displayed. It should be noted that, in some cases, the same properties were chosen for more than one zone. This was

supported by trends observed in the available data. There is strong evidence, as discussed in Section 5.4, that all four zones of the embankment are both clayey and over-consolidated. In addition, Zones 1, 2U, and 4 were observed to have very similar PI and  $I_c$  characteristics with Zone 2L being somewhat different as shown by the cumulative distributions of PI and  $I_c$  presented on Figures 5-6 and 5-12, respectively. The CPT data points plotted on the soil behavior type chart in Figure 5-13 have been summarized on another soil behavior type chart (Figure 5-14) by plotting the average normalized cone data for each zone with a range representing one standard deviation of the full body of data. This figure reinforces the observation that the material types of Zones 1, 2U, and 4 can be considered similar with that of Zone 2L being somewhat different.

### 5.5.1 Unit Weight

The unit weight selected for each material corresponds to moist (or total) unit weight,  $\gamma_t$ , based on testing performed during previous studies. Figure 5-15 shows the cumulative distribution of unit weight for all samples tested. Based on the results shown on this figure, the 50<sup>th</sup> percentile moist unit weight value was adopted for each material. Moist unit weights of 138 pcf, 132 pcf, 124 pcf, and 140 pcf were selected for Zone 1, Zone 2U, Zone 2L, and Zone 4, respectively. In selecting the moist unit weight, no attempt was made to correct for small potential differences in the degree of saturation of the materials.

### 5.5.2 Effective Stress Friction Angle

An effective stress friction angle for each zone is needed for long term slope stability analyses. As shown in Table 5-1, thirty-four (34) isotropically consolidated undrained triaxial compression test (ICU'C) were performed on Pitcher samples during previous studies. A secant effective stress friction angle was calculated at maximum obliquity for each test; i.e., the friction angle was determined as the angle of the line tangent to the failure envelope with zero cohesion intercept. The calculated values are plotted vs. effective normal stress on Figure 5-16. The parameters for each zone that were adopted by Harza (1997) are also plotted on Figure 5-16. As shown on this figure, the Harza parameters appear to adequately capture an average of all test results; thus, they were adopted in this characterization. Several ICU'C tests were performed on re-compacted samples of Zone 4 material by Wahler (1982); these results were considered in the evaluation, but were not used directly on the plot shown on Figure 5-16.

### 5.5.3 Undrained Strength

Undrained shear strength is necessary for all materials in the seismic deformation analyses. The undrained strength under direct simple shear loading would be most appropriate in the preliminary analyses of the Loma Prieta Earthquake discussed in Section 6 (Ladd, 1971; Robertson, 2009). As noted in Section 5.4, all zones of the dam (except for Zone 3) are both clayey in nature and over-consolidated to various extents. On the other hand, all the laboratory shear strength tests conducted previously were under triaxial testing conditions as inferable from Table 5-1; in addition, little is known about the past stress history of triaxial specimens tested in previous studies, and, as discussed in Section 5.3, significant variations were observed between

the in-situ effective confining pressure of samples and the pre-testing effective confining pressures of test specimens, making the interpretation of the test results difficult to evaluate the undrained strength expected in situ.

Given these considerations, it was decided to use in situ undrained shear strength and over-consolidation ratio (OCR) inferable from the CPT data provided by RLVA (1999a and 199b) as the main guide in developing undrained strength. The SHANSEP approach (Ladd, 1971; Ladd and DeGroot, 2003) was also used as a framework in interpreting the CPT data.

Based on Robertson (2009), the CPT data was normalized for confining pressure effects using estimates of phreatic conditions during CPT soundings. The normalized tip resistance,  $Q_{tn}$ , was then used to estimate undrained strength ratio for all samples with  $I_c$  greater than 2.6 using the following relationship from Robertson (2009):

$$S_u / \sigma'_{vc} = Q_m / N_{kt} \quad \text{Eq. 5-1}$$

In this relationship  $N_{kt}$  is a cone factor that has a range of 10 to 20; a value of 14 was selected for this evaluation. This strength ratio was used to back calculate the OCR for each CPT data point using the SHANSEP equation:

$$S_u / \sigma'_{vc} = S_d \cdot (OCR)^m \quad \text{Eq. 5-2}$$

In this equation,  $S_d$  represents the undrained shear strength ratio of material with OCR = 1 under direct simple shear loading conditions, which was assumed to be 0.22, and  $m$  is an OCR exponent assumed to be 0.8, both of these values are based on Ladd and DeGroot (2003). The back calculated OCR values are plotted versus estimated effective in-situ confining pressure on Figure 5-17. From this plot, a relationship between OCR and  $\sigma'_{vc}$  was developed that approximates the trend of the CPT inferred data, capped at an OCR of 20. This OCR relationship will be used with equation 5-2 to estimate the undrained strength ratio in various material zones in the preliminary analyses of the Loma Prieta earthquake. To show how this parameter compares to the CPT inferred undrained strength data, the estimated undrained strength for all CPT data has been plotted over a large range of effective pressures on Figure 5-18. As expected, the trend line for inferred undrained shear strength derived from the OCR data is consistent with the undrained strength inferred from CPT data.

#### 5.5.4 Stress-Strain-Strength Relationship

In addition to the undrained shear strength discussed in Section 5.5.3, undrained stress-strain relationships for the materials are required for the development of full undrained stress-strain-strength relationships needed in the engineering analyses. The undrained laboratory test results (ICU'C data) by Harza (1997) were chosen to develop the stress-strain-strength relationships because of the uniform way in which the samples were collected and tested for all four zones (Zones 1, 2U, 2L, and 4). For each of the four zones, intact Pitcher barrel samples were obtained, index properties were determined, and four ICU'C tests were performed at four confining pressures.

Deviator stress versus axial strain data and excess pore pressure versus axial strain data were digitized from the plots presented by Harza (1997). The values obtained by dividing half the



deviator stress by the initial effective confining pressure are plotted versus axial strain on Figures 5-19A through 5-19D. The values of in-situ confining pressure were estimated for each of the samples (based on available information) to estimate the ratio of the effective confining pressure prior to shearing to the effective confining pressure in-situ. As noted in the legend of each figure, some samples were consolidated to pressure less than their in-situ values, thus inducing additional over-consolidated conditions, and some samples were consolidated to pressures much higher than their in-situ values, thus reducing the over-consolidation effects. In general, it was observed that the peak shear stress ratio decreases with higher tested confining pressure to in-situ confining pressure ratio, as expected.

The shear stress data from each test was normalized by dividing it by the maximum undrained strength. The range in this normalized data is plotted on Figure 5-20; a stress-strain relationship was selected that falls within this range as shown on this figure. The normalized stress-strain relationship shown on Figure 5-20 combined with undrained shear strength information discussed in Section 5.5.3 will be used to develop an initial estimate of the full undrained shear stress-strain-strength relationship for the embankment materials within each of the four zones for use in the preliminary engineering analyses described in Section 6. We believe the relationship shown in Figure 5-20 may underestimate the stiffness of the material because it is based on laboratory tests on intact samples that have undoubtedly been disturbed during sampling because of the presence of gravel in the clay matrix and other factors. Nevertheless, it provides a reasonable starting point for the analyses and will be adjusted as necessary based on the initial results of the FLAC analyses.

### 5.5.5 Dynamic Properties

Dynamic properties adopted for the preliminary engineering analyses consist of shear wave velocity, shear modulus reduction curves, and damping ratio curves. As noted in Table 5-1, Wahler (1982) was the only investigator to collect shear wave velocity data at the site. They conducted cross-hole, downhole, and surface refraction surveys at three locations at the dam site. The data collected from the cross-hole surveys is plotted versus effective confining pressure on Figure 5-21. As noted above the similarities in PI and cone data for Zones 1, 2U, and 4 materials led to the adoption of one parameter which fit the shear wave velocity for all three zones. The shear wave velocity for Zone 2L has been plotted separately for two reasons: (1) the material was consistently observed to have higher PI and fines content than the other zones and (2) two surveys (one in 1975 and one in 1981, both performed by Wahler) resulted in very different shear wave velocities. For this study, a trend line was developed that best fits both sets of data.

The small strain shear modulus for each material type can be obtained from shear wave velocity and the known mass density of the material using the following relationship:

$$G_{\max} = \rho \cdot V_s^2 \quad \text{Eq. 5-3}$$

In this relationship,  $G_{\max}$  is the small strain shear modulus,  $\rho$  is the mass density of the material, and  $V_s$  is the shear wave velocity.

Based on the observed clayey nature of the material for all zones of the dam, the shear modulus reduction and damping ratio curves were selected based on the work by Vucetic and Dobry

(1991), corresponding to median plasticity index (PI) values of 15, 17, 34, and 14 for Zone 1, Zone 2U, Zone 2L, and Zone 4, respectively, as shown on Figure 5-22. These parameters will be utilized in the preliminary engineering analyses and adjusted as necessary to provide an appropriate fit of the predicted deformations to the measured performance during the Loma Prieta earthquake.

## 5.5.6 Permeability

The "Lenihan Dam Outlet Investigation, Vol. 1 – Final Engineering Report" (RLVA, 1999a) summarized all the data available on soil permeability of embankment materials that were available at the time; no permeability data have been added since then. Whaler (1982) conducted one triaxial permeability test on intact samples of the upstream shell, upper core, and lower core. They also measured permeability on a reconstituted sample of the downstream shell. RLVA (1999a) conducted triaxial permeability tests on samples of all zones of the embankment and also calculated values of permeability from the results of one-dimensional consolidation tests where measurements of coefficient of consolidation and soil stiffness were made. In addition, RLVA estimated soil permeability based on pore pressure dissipation tests in CPTs. The permeability values from these various tests are summarized in the following table.

Material	Measured Permeability, cm/sec			Estimated Permeability, cm/sec (RLVA, 1999)	
	Triaxial Test	1-Dimensional Consolidation	Field CPT	Horizontal	Vertical
Upstream Shell	1.7 x 10 <sup>-8</sup> 3.3 x 10 <sup>-8</sup> 2.9 x 10 <sup>-9</sup>	2.0 x 10 <sup>-9</sup>	3.7 x 10 <sup>-8</sup> 7.3 x 10 <sup>-7</sup> 7.2 x 10 <sup>-7</sup> 7.9 x 10 <sup>-8</sup> 7.3 x 10 <sup>-9</sup>	5 x 10 <sup>-8</sup>	5 x 10 <sup>-9</sup>
Upper Core	1.7 x 10 <sup>-8</sup>	2.5 x 10 <sup>-8</sup>	2.4 x 10 <sup>-8</sup> 1.0 x 10 <sup>-8</sup> 1.1 x 10 <sup>-8</sup> 1.0 x 10 <sup>-8</sup>	1 x 10 <sup>-8</sup>	1.0 x 10 <sup>-9</sup>
Lower Core	6.6 x 10 <sup>-9</sup> 4.5 x 10 <sup>-9</sup> 5.3 x 10 <sup>-9</sup> 8.1 x 10 <sup>-9</sup> 4.4 x 10 <sup>-9</sup> 1.1 x 10 <sup>-9</sup>	5.0 x 10 <sup>-8</sup> 2.5 x 10 <sup>-9</sup>	1.2 x 10 <sup>-8</sup> 5.7 x 10 <sup>-9</sup> 2.4 x 10 <sup>-8</sup>	1 x 10 <sup>-8</sup>	5 x 10 <sup>-9</sup>
Downstream Shell	3.1 x 10 <sup>-6</sup>			1 x 10 <sup>-7</sup>	1 x 10 <sup>-7</sup>
Foundation	3.3 x 10 <sup>-9</sup>				

We noted that the data for the downstream shell and foundation are very limited and that the ratios of horizontal to vertical permeability were biased by the judgment of RLVA. Nevertheless, these values provide a starting point for the seepage analyses and will be adjusted, as appropriate, based on the results of the analyses.

The permeability of the foundation is indicated to be very low based on the one available test. However, as discussed in Section 4.2, data from borehole packer tests and from observed water loss in borings indicate that the very low permeabilities are representative of the sheared shale mélangé within the Franciscan complex but that the harder sandstone blocks contained within the mélangé can have permeabilities on the order of  $1 \times 10^{-4}$  cm/sec.

No data are available on the permeability of the Zone 3 drain materials but, from an engineering perspective, they are essentially free draining compared to the very low permeabilities of the other embankment zones provided they are continuous.

The continuity and effectiveness of the inclined drain is of concern. As discussed in Section 2.3.1, the inclined Zone 3 drain material was interrupted at elevation 510 feet because of misalignment of the zone below elevation 510 feet that was corrected by adding a horizontal gravel layer as shown in Figure 2-4. We believe that this correction may significantly limit the effectiveness of the drain material above elevation 510 feet because of the potential for the gravel layer to be "choked" by fines from Zone 2 materials washing into the layer since Zone 2 and the gravel layer are not filter-compatible and there are significant downward vertical gradients at this location. Moreover, the construction records indicate that the quality and continuity of the Zone 3 drain materials may have been compromised because the placement of Zone 3 materials sometimes lagged behind the placement of Zones 2 and 4 materials and the Zone 3 layer had to be dug out after being covered by Zone 2 and/or Zone 4 material. In addition, the measured piezometric levels in the downstream shell shown on Figure 2-3 indicate that the downstream shell piezometers are not always dry as they should be if the inclined drain were functioning properly. Consequently, we believe that the Zone 3 inclined drain may not function as intended and will consider evaluating this further in our seepage analyses.

## 6.1 GENERAL

The seismic response of Lenihan Dam was recorded during the Loma Prieta earthquake by three accelerographs (two on the dam crest and one on the abutment), which indicated peak ground acceleration of about 0.4g. In addition, some quantitative and observational seismic performance data were collected at the dam during and after the Loma Prieta event. Seismic performance evaluations of Lenihan Dam during the Loma Prieta event have been made a number of times in the past for various purposes (DSOD, 2006; Geomatrix, 1992; Harza, 1997; Woodward-Clyde, 1993). The data and observations related to the Loma Prieta event provide an opportunity for us to not only calibrate the FLAC-based seismic deformation model(s) to be used in the seismic evaluation of the dam under the design earthquake shaking conditions but also to evaluate the usefulness of the preliminary material properties developed from the existing data and to identify data gaps and key material parameters and zones that may warrant further refinement.

The engineering analyses documented in this section consist of a preliminary evaluation of the response of the dam to the Loma Prieta earthquake for the primary purpose of identifying data gaps and supporting the work plan for additional site investigations and laboratory testing. The performance of the dam during this event will be revisited, after the additional information has been obtained and interpreted, as part of the seismic stability evaluation of the dam.

## 6.2 PURPOSE AND SCOPE OF PRELIMINARY LOMA PRIETA EVALUATION

A preliminary seismic evaluation of the dam using the Loma Prieta case history provides a strong basis for identifying general material properties that may require adjustments from those provided in the interim site characterization report. These adjustments together with the results of the preliminary engineering analyses will then be used to identify key parameters that may warrant further refinement. This rational approach to develop a plan for additional site investigations and laboratory testing focuses on refining critical material properties and characterization, based in part on the field performance, and should improve the reliability of the seismic evaluation.

The purposes of the preliminary Loma Prieta evaluation then are:

1. to develop an overall understanding of the seismic behavior of the dam in terms of major contributing factors using this important case history; and
2. to evaluate whether the material properties documented in the interim site characterization report based on existing data are appropriate for the future seismic design evaluation and, if they are not adequate, to help focus the plan for additional material characterization (field investigations, laboratory testing, and data interpretation) in order to reduce the uncertainty in the material properties.

The scope of the preliminary Loma Prieta evaluation includes:

1. Seismic performance evaluation of the dam using the computer program FLAC (Itasca, 2008) using an abutment recording from the Loma Prieta event as the input motion and the preliminary material properties from the interim site characterization report as the initial input properties;

2. Limited parametric analyses as appropriate; and
3. Evaluation of the results of the analyses, identification of data gaps, and recommendations for additional field investigations and laboratory testing, as appropriate.

Section 6.3 describes the methodology and approach used in the preliminary Loma Prieta evaluation including a further description of the Loma Prieta event at Lenihan Dam and a brief description of the computer program FLAC. Section 6.4 presents the analysis section, initial material properties, and input motion used in the preliminary Loma Prieta evaluation. Section 6.5 presents the results of the analyses by focusing on input motion, seismic response, and seismic deformations. Conclusions and recommendations are presented in Section 6.6.

## **6.3 METHODOLOGY AND APPROACH**

### **6.3.1 General**

The maximum section of the dam – Section B-B' shown on Figure 2-2A – was used in the preliminary Loma Prieta evaluation. The input horizontal motion was derived from the abutment ground motions recorded during the 1989 Loma Prieta earthquake. The zoning and material properties described in Section 5.0 were used as the initial input properties.

The preliminary Loma Prieta evaluation included a one-dimensional equivalent linear analysis using the computer program SHAKE and a limited number of parametric analyses with the computer program FLAC. The seismic response computed by SHAKE was compared to the results obtained from FLAC as well as to the seismic response of the dam that was recorded during the Loma Prieta event. The seismic deformations calculated by FLAC were compared to the observed patterns and values of seismic deformations recorded during the event.

The uncertainties involved in the characterization of the dam and in the selection of the input ground motions, as well as the uncertainty inherent to the two-dimensional FLAC model analysis, were considered in evaluating and interpreting the results of the analyses and the sensitivity of these results to the input parameters. The results of the preliminary evaluation were used to identify data gaps and key parameters that require refinement, and to focus the program of field investigations and laboratory testing to fill these data gaps and refine the material characterization.

The seismic performance of dams results from the interaction of many factors (including some unknown factors and some factors that may appear relatively minor) that all contribute to uncertainty. However, for this preliminary evaluation, the following first-order effects have been identified as the major components of epistemic uncertainties:

1. Input Motion
  - a. The incoming seismic energy into a dam can be quite variable along the contact surface between the embankment and the bedrock foundation; this may be particularly true when the bedrock materials covered by the dam consist of both "soft" rock and "hard" rock as may be the case for Lenihan Dam (Terra/GeoPentech, 2011a). Therefore, an appropriate "single-point" input motion for use in the seismic analysis of a two-dimensional section for a past event ideally should reflect the combined effects of all these uncertainties.

- b. Ground motions were recorded at two locations on the dam and one location on the left abutment during the Loma Prieta earthquake. The only candidate input motions recorded at the site are the three-component time histories at the left abutment and it is unclear whether these input motions are truly appropriate for the analysis section. The applicability of these input motions to the section being analyzed is the main source of uncertainty associated with the input ground motions.

## 2. Seismic Response

- a. Given an appropriate input motion, the first-order seismic behavior of the dam is controlled by the seismic response of the structure. The seismic response of the dam can be represented using, for example, the response spectra resulting from the seismic event at various points on the dam.
- b. The main source of uncertainty regarding the seismic response of the dam is associated with the dynamic properties of the dam materials (shear wave velocity and associated small-strain shear modulus, shear modulus reduction curves, and damping ratio curves) and how the values of these properties are distributed throughout the dam.

## 3. Seismic Deformation

- a. Given appropriate input motion and seismic response, the first-order seismic deformation behavior of the dam is controlled by how the materials yield at various points within the dam, and therefore, how permanent strains accumulate during the seismic event.
- b. The main source of uncertainty in the seismic deformation is the shear strength of the materials in the dam and how the shear strength values are distributed throughout the dam.

The evaluation of a case history to refine material properties (or to improve the seismic design of a dam) should focus on the major issues discussed above and assess how comfortable one feels about these issues and about one's ability to control, in a practical way, the epistemic uncertainties of the evaluation. In this regard, too much focus on "matching" the recorded data by "manipulating" some details of the analyses (which could lead to getting the right answers for the wrong reasons) without gaining an overall appreciation of the key lessons a given case history has to offer would not be fruitful. Thus, the preliminary Loma Prieta evaluation documented herein is aimed at developing an overall understanding of the seismic behavior of the dam and identifying key issues/parameters that need refinement for the seismic deformation analyses rather than providing a close match of calculated to recorded deformations.

The following sections provide a summary of the effects of the Loma Prieta event at the site and a description of the computer program FLAC and of its application in the preliminary Loma Prieta evaluation.

### 6.3.2 Loma Prieta Event at the Site

The Loma Prieta earthquake occurred on October 17, 1989, along a branch of the San Andreas fault. The epicenter of this event was located about 13 miles (20 km) from Lenihan Dam, as shown on Figure 3-1. The effects of the Loma Prieta earthquake on Lenihan Dam were investigated by the District and R.L. Volpe & Associates (RLVA) in the days following the



event as part of an overall investigation of District dams affected by the earthquake. The observed damage at the dam was documented in a report by RLVA (RLVA, 1990).

Following the Loma Prieta earthquake, the dam was found to have sustained about 10 inches of crest settlement at the maximum section and a maximum of about 3 inches of lateral movement downstream, in addition to some localized transverse and longitudinal cracking. Also, about six weeks after the earthquake, a wet area was observed below the footpath near the right abutment although no flow was reportedly emanating from this area. The general observed seismic displacements and the locations of the observed cracks and wet area are summarized on Figure 6-1. This figure also shows the locations of the three strong-motion instruments at the site and the section selected for the preliminary analyses (Section B-B').

Three sets of three-component ground motions were recorded during the earthquake at two locations on the crest and one at the left abutment, as shown on Figure 6-1. Figure 6-2 is a longitudinal cross section of the dam used to illustrate the location of the abutment recording station relative to the embankment and the surrounding topography.

The dam parallel, dam transverse, and vertical acceleration time histories for the three recording locations are shown on Figures 6-3; the response spectra at 5 percent damping corresponding to these acceleration time histories are shown on Figure 6-4. As shown on Figure 6-3, the peak horizontal ground accelerations at all locations are similar and in the range of 0.34g to 0.45g. However, as shown on Figure 6-4, the spectral accelerations at the crest, when compared to those at the abutment, show a significant amplification at about one-second period. This is especially the case at the right crest location, which is close to the maximum section of the dam used in the analyses. Also, the peak vertical accelerations and spectra values are in general much lower than the corresponding horizontal values.

### 6.3.3 FLAC

The computer program FLAC (Fast Lagrangian Analysis of Continua) is a two-dimensional explicit finite difference program for geotechnical and mining applications that was developed by Itasca (2008). An analysis section is divided into elements and nodal points in a way analogous to the finite element method. FLAC uses the Lagrangian formulation of momentum equations (Newton's second law of motion) and, thereby, inherently accounts for the mass conservation law and allows elements with fixed masses to translate, rotate, or deform in space. The analysis input motion is specified at the base of the analysis section, incorporating the effects of a compliant boundary representing the bedrock in the evaluation.

The calculation loop in FLAC has two main alternating components: element calculations and nodal point calculations. In the element calculations, the current velocities and displacements of nodal points are used to compute the strain increments in the element formed by these nodes; these strain increments, in turn, are used to compute the stress increments of the element. With the new state of stress, the out-of-balance force can be computed and then used to calculate the incremental displacements of the nodes.

Various stress-strain models are available in FLAC. However, for the evaluation documented herein only the Mohr-Coulomb model and the elastic model were used in the analyses. Details of these models are provided in Itasca (2008), and a PDF file of the FLAC user's manual



containing the descriptions of these models can be accessed at [www.itascacg.com](http://www.itascacg.com). The elastic model was used for the bedrock and the Mohr-Coulomb model was used for all the other materials.

The Mohr-Coulomb model consists of elastic-perfectly-plastic stress-strain relationships. Therefore, the materials are elastic before yielding. To make the elastic portion of the analysis reasonable, we perform an equivalent-linear analysis using the computer program SHAKE (Idriss and Sun, 1992) on a one-dimensional soil column through the crest to obtain the strain-compatible modulus and damping values for the postulated shaking conditions. The analysis results from SHAKE provide the basis for the strain-compatible shear modulus and damping values to be used in the elastic portion of the Mohr-Coulomb model in the FLAC analyses. The equivalent-linear portion of the seismic deformation analyses is usually done using the computer program QUAD4MU (Idriss, 2003). However, for this preliminary evaluation the results of the SHAKE analysis were considered adequate, primarily because the emphasis of the analyses was on evaluating the adequacy of the material properties and because the uncertainty associated with the input motion was considered large.

The key material parameters and areas within the dam that warrant further investigation and refinement were identified through limited parametric FLAC analyses. The main criterion used to judge the need for further investigation and refinement was how well the adopted material properties allowed the FLAC model to predict the seismic response and deformation patterns of the dam observed during the Loma Prieta earthquake, while keeping in mind that the ultimate purpose of the material property selection is the seismic stability evaluation of the dam under design earthquake conditions.

## **6.4 ANALYSIS SECTION AND INPUT PARAMETERS**

### **6.4.1 Analysis Section**

Figure 6-5 shows the section of the dam selected for the analyses. The plan location of this section is shown on Figure 2-2A as well as on the insert in Figure 6-5. The generalized embankment zones and material types established in the interim site characterization report are also tabulated on Figure 6-5.

Section B-B' was chosen for the analyses because it is the maximum section and also because the bedrock surface along the section is irregular with a significant bedrock "knob" at the upstream side of the core as shown on Figure 6-5; the shape of the bedrock surface may affect the seismic response of the dam. Only one section was analyzed in the preliminary Loma Prieta evaluation because the focus of the evaluation was the first-order material properties, as discussed in Section 6.3.1. At least one other section will be considered in the analyses of the seismic stability of the dam under design earthquake shaking.

Figure 6-5 also shows the phreatic surface within the dam prior to the Loma Prieta earthquake that was assumed in the analyses. This surface is the same as that used by DSOD in their analyses (DSOD, 2006). The results of our seepage analyses suggest that this phreatic surface may be too high but that there is considerable uncertainty regarding its location. Given this uncertainty, we decided to use the DSOD estimated phreatic surface for preliminary evaluation.

The detailed results of the seepage analyses will be used when the Loma Prieta earthquake is revisited as part of the seismic evaluation of the dam and for the evaluation of seismic performance during the design earthquake.

Figure 6-6 illustrates how the idealized analysis section was discretized into a finite difference mesh for use in the FLAC analyses. The mesh shown on Figure 6-6 was generated based on the need to: (1) ensure appropriate dynamic wave propagation in the system; (2) control kinematic constraints provided by the linear elements used in FLAC; and (3) minimize numerical problems introduced by element shapes.

Although not shown on Figure 6-6, the bedrock was also discretized for the sole purpose of providing a compliant base that would appropriately and adequately allow the incoming seismic waves and absorb the outgoing seismic waves. The numbers shown in various zones of the dam on Figure 6-6 correspond to the zone numbers identified on Figure 6-5.

### 6.4.2 Material Properties

The material properties used in the analyses are documented in Section 5.5 and summarized in Table 6-1. They include: unit weight; small-strain shear modulus (shear wave velocity,  $V_s$ ; or maximum shear modulus,  $G_{max}$ ); shear modulus reduction and damping ratio curves; and shear strength. The shear wave velocity of the bedrock is also listed in Table 6-1. The shear modulus reduction and damping ratio curves are shown on Figure 5-22.

The material properties used in the evaluation were the same for all cases analyzed except for the shear strength which was divided into drained (or effective stress) shear strength and undrained shear strength and treated differently above and below the phreatic surface, as discussed in Section 6.5.2.

### 6.4.3 Input Motion

The input motion representing the 1989 Loma Prieta earthquake ground motions at the site that was used in the analyses is the transverse component of the three-component ground motions recorded at the left abutment (Figures 6-1 and 6-2). The selected acceleration time history and response spectrum for this input motion are identified by a dashed rectangle on Figures 6-3 and 6-4. The same input motion is presented on Figure 6-7 in terms of acceleration, velocity, displacement time histories, and associated response spectrum at 5 percent damping. The input motion was applied at the rock knob on the upstream side of the core (Figure 6-5).

As discussed in Section 6.3.1, the use of the abutment time history as an input motion at the base of the dam necessarily results in potentially significant uncertainty. One previous study (Harza, 1997) indicated that the response of the dam might have affected the abutment recording. As can be inferred from Figures 6-1 and 6-2, the topographic high at the left abutment could also have affected the recorded ground motions at that location and the variability of the rock conditions beneath the embankment could be even more important than the geometric effects. Nevertheless, it was decided to use the as recorded transverse motion shown on Figure 6-7 for this preliminary evaluation because it was measured on rock some distance from the dam and the

transverse direction of shaking is appropriate for the section chosen for the analyses. Additional comments on this issue are contained in Section 6.5.1.

## **6.5 RESULTS OF ANALYSES**

The following sections present the results of the analyses performed for the preliminary Loma Prieta evaluation. The seismic response of the dam as calculated by SHAKE and FLAC is discussed first and then the results of three FLAC seismic deformation analyses are presented and discussed. The results of these analyses and the discussions presented hereinafter lead to the conclusions and recommendations provided in Section 6.6.

### **6.5.1 Seismic Response and Input Motion**

One-dimensional "equivalent-linear" response analyses of a vertical soil column under the crest of the dam were performed using SHAKE and FLAC. The resulting response spectra (at 5 percent damping) at the crest and at the top of the Lower Core zone are plotted on Figure 6-8. The response spectra at the ground surface (Point A on the crest) and at the top of the Lower Core (Point B) are shown on the left and right sides of the figure, respectively. Also shown on the left side of Figure 6-8 is the 5 percent damping response spectrum of the transverse component of the recording from the Loma Prieta earthquake at the crest station close to the analysis section; i.e., the "Right Crest" station identified on Figure 6-2.

The response spectra predicted by SHAKE and FLAC are very similar at Points A and B indicating that the shear modulus and damping values used in the FLAC model are reasonable when compared to the SHAKE results in terms of seismic response.

Figure 6-8 shows that the response spectra from the one-dimensional SHAKE and FLAC analyses at Point A are quite similar in general shape to that from the recording; however, the recorded motion shows significantly less amplification than the calculated results up to a period of about 1 second and significantly higher amplification at the peak acceleration around a period of 1 second. These differences may be caused by the fact that the "actual" input motion at the base of the dam may be somewhat different from that recorded at the left abutment and used in the analyses, or because the dynamic properties selected for the various materials are not the most appropriate. They may also be a result of the one-dimensional nature of the SHAKE and FLAC analyses and their inherent limitations.

Figure 6-9 contains the same information as plotted on the left side of Figure 6-8 with the addition of the 5 percent damping response spectrum at Point A from the two-dimensional Case 3 FLAC analysis discussed in Section 6.5.2. Review of Figure 6-9 indicates that the two-dimensional analysis results are similar to those of the one-dimensional analyses, but have somewhat higher amplifications in a period range from about 0.05 to 0.5 second. Similar results can be obtained from the other two two-dimensional analyses discussed in Section 6.5.2.

Figure 6-10 compares the 5 percent damping response spectra corresponding to the input motion (i.e., the transverse abutment record from the Loma Prieta earthquake) to (a) the computed response spectrum at Point A from the two-dimensional Case 3 FLAC analysis and (b) the transverse motion recorded at the crest near the analysis section. Figure 6-11 shows the same information as Figure 6-10 except that the values plotted are the ratios of the crest surface

response spectral values (computed or measured) divided by the input response spectral value at the same period. These plots can be viewed as "response spectral amplification functions."

The amplification function in the left portion on Figure 6-11 reflects primarily the uncertainties in the input motion and the dynamic properties used in the analysis, as well as the uncertainty inherent to the FLAC model. The amplification function in the right portion of the figure reflects mainly the uncertainty in the input motion. These amplification functions probably are not reliable beyond a period of a few seconds.

There is no easy way of discerning in any quantitative manner what is contributing to what in these amplification functions. However, the values and shape of the "recorded" amplification function in the right portion on Figure 6-11 (no amplification to negative amplification up to about 0.4 second and a high peak slightly above a period of 1 second) indicate some uncertainty in the input motion is likely present throughout the period range; i.e., not just at the peak near a period of 1 second (Figure 6-7). In reviewing the proximity of the abutment recording location relative to the dam (Figure 6-2) it appears unlikely that the presence of the dam had any measureable impact on the abutment ground motions. However, trying to reduce the uncertainty in the input motion from the Loma Prieta event for the purpose of the seismic deformation analyses would not be fruitful because additional data on input motions are not available and because of issues related to variable bedrock and incoming seismic energy. Nevertheless, one could speculate that the appropriate amplification function for the two-dimensional analyses discussed herein would likely exhibit attributes of the two amplification functions shown on Figure 6-11.

Assuming that the uncertainty in the input motion cannot be quantified, the analysis amplification function in the left portion on Figure 6-11 may be open for refinement. The main parameters that contribute to the analysis amplification functions for a given shaking level are shear wave velocity (values and distribution) and shear modulus reduction and damping ratio curves. The shear modulus reduction and damping ratio curves presented in Figure 5-22 are considered reasonably robust (with respect to shear wave velocity) and may require extensive efforts to refine. On the other hand, shear wave velocity values and distribution are considered less robust (with respect to reduction and damping ratio curves) and are amenable to refinement at a more manageable level of effort.

### 6.5.2 Seismic Deformation Analyses

Three two-dimensional FLAC analyses were performed for the preliminary Loma Prieta evaluation. In the analysis section shown on Figure 6-6, the embankment can be divided into two portions: one above the phreatic surface and the other below it. The first FLAC analysis (Case 1) used undrained shear strength below the phreatic surface and effective stress shear strength above the phreatic surface (see Table 6-1); a minimum cutoff of 1 kip/ft<sup>2</sup> (ksf) was used for the effective stress shear strength to avoid having very weak material near the surface. This combination of undrained shear strength below the water table and effective shear strength above the water table is often used in the seismic analysis of dams. The second FLAC analysis (Case 2) used undrained shear strength both below and above the phreatic surface; this may be more appropriate for the clayey materials present in Lenihan Dam. Case 3 is similar to Case 2 except that the shear strength has been uniformly reduced by 30 percent from that used in Case 2.

The 30% reduction was chosen to evaluate the sensitivity of the seismic deformations to reasonable reductions in shear strength.

Figures 6-12A, 6-12B, and 6-12C document the results of the FLAC analysis for Case 1. Figure 6-12A shows the seismic displacement contours in the embankment at the end of shaking. The computed vertical and horizontal seismic displacement values and directions at the crest of the dam are shown as vector components near the crest. Figure 6-12B shows the end-of-shaking seismic displacement vectors, describing the general pattern of seismic deformations. Figure 6-12B should be considered for seismic deformation patterns only; an exaggerated scale is used to plot the displacement vectors for clarity of presentation and that exaggerated scale provides a somewhat unrealistic sense of the calculated overall seismic deformations which are very small. Figure 6-12C shows color-coded contour intervals of computed shear strains at the end of shaking. Most of the embankment has shear strains between 0.00 and 0.01 and this contour interval is "colored" white. The areas where the shear strains are greater than 0.01 are shown in blue.

Even considering the uncertainties discussed in Section 6.5.1, the deformation values computed for Case 1 appear low. It should be noted that, if a minimum cutoff shear strength of 1ksf had not been used, greater deformations would have been computed at the surface, but such near-surface seismic deformations for clayey materials would not have been credible.

Figures 6-13A, 6-13B, and 6-13C document the results of Case 2. Although the shear strength used in Case 2 is considered more appropriate than that of Case 1 because of the clayey nature of the embankment materials, the results from Case 2 do not appear that different from those of Case 1.

Figures 6-14A, 6-14B, and 6-14C present the results of Case 3, where the shear strength used in Case 2 has been reduced by 30 percent. As can be seen on Figure 6-14A, the calculated seismic displacements are much greater than for the other two cases analyzed. The calculated lateral displacement at the crest is of the same order of magnitude as the displacement observed after the Loma Prieta earthquake, but the calculated vertical displacement remains significantly less than that observed. Unlike the observed seismic displacement values, the computed values show higher horizontal movement than vertical settlement; this may be caused in part by the undrained strength values and distribution reported in the interim site characterization report and used for this evaluation.

It is interesting to note that the pattern of deformations shown on Figure 6-14B suggests that the upstream shell of the dam in the general area above the bedrock knob is in a tensile state relative to the pre-earthquake conditions; this is the same general area where ground cracks were observed after the Loma Prieta earthquake (Figure 6-1). Figure 6-14C indicates that much of the shearing is taking place at depth. The same patterns, but to a lesser extent, can be seen on Figures 6-12B and 6-12C and on Figures 6-13B and 6-13C for Cases 1 and 2, respectively.

Figure 6-15 documents the calculated horizontal and vertical time histories of displacements at the crest for Case 3. The input motion in terms of acceleration, velocity, and displacement time histories is also shown on Figure 6-15. This figure indicates that the seismic displacements take place during the strong shaking portion of the input motion and stabilize after that.



## 6.6 CONCLUSIONS AND RECOMMENDATIONS

### 6.6.1 Conclusions

The following conclusions can be drawn from the results of the preliminary Loma Prieta evaluation presented herein:

1. The use of the undrained shear strengths presented in the interim site characterization report for the embankment materials, with some adjustment, lead to calculated seismic deformations that appear to approximate the general trends of seismic deformations observed at the dam after the Loma Prieta event in a way that is considered adequate for this preliminary evaluation. However, refining the undrained shear strength of the embankment materials to try and obtain better agreement between calculated and observed deformations is considered worthwhile before completing the seismic stability evaluation of the dam.
2. The amplification (defined as the ratio of response spectra of surface motion to input motion) values associated with the analyses appear to be significantly different from the values that can be inferred from the recording, as discussed under Item 3 below. This difference may be caused in part by an inappropriate input motion assumed in the analyses; i.e., the transverse motion at the left abutment may not represent the appropriate "effective" input motion for the two-dimensional analyses. This would mean the amplification values shown in the right portion on Figure 6-11 may not be appropriate. However, the difference may also be caused in part by the dynamic properties used in the analyses which would mean that the amplification values shown in the left portion on Figure 6-11 may be wrong. The appropriateness of the input motion is further addressed in Item 3 below. As far as the dynamic properties are concerned, it is unlikely that the shear modulus reduction and damping ratio curves are off by significant amounts; thus, it is considered worthwhile to verify and/or refine the shear wave velocity values in the embankment materials and the distribution of these values throughout the embankment.
3. One very significant uncertainty in the preliminary Loma Prieta evaluation is the input motion used in the analyses. A comparison of the transverse motion at the left abutment with the transverse motions at the crest indicates that the amplification of the input motion for periods less than about 0.4 second is very small but that the amplification of the input motion around a period of about 1 second is quite high.
4. The bedrock knob beneath the upstream portion of Lower Core and the downstream portion of the Upstream Shell (see Figure 6-5) appears to have a significant impact on the localized calculated seismic response of the analysis section, and this is consistent with the observations of cracks made after the Loma Prieta earthquake. In addition, a significant part of this rock knob may be hard rock instead of the softer rock that is predominant in the foundation bedrock. As shown in Section 4.2, it is common within the Franciscan complex to have hard resistant "knockers" of one rock type embedded in a softer sheared rock matrix. Incorporating an appropriate bedrock geometry in the seismic deformation analyses of the dam (through the use of several two-dimensional analysis sections, as appropriate) appears to be important.



5. Among other parameters, the design input ground motions to be developed for the seismic evaluation of the dam will depend on the shear wave velocity in the upper 30 m (100 feet) of the bedrock. This, along with the discussion in Item 4 above, would indicate that shear wave velocity information in both "soft" rock and "hard" rock could be important.
6. The contours of seismically induced shear strains such as those shown on Figure 6-14C for Case 3 provide guidance on zones that may require refinement in terms of undrained shear strength and other related properties.

### 6.6.2 Recommendations

The results of the preliminary Loma Prieta evaluation discussed herein have allowed us to identify data gaps that should be filled and key parameters that should be refined to reduce the overall uncertainty of the seismic stability evaluation of Lenihan Dam. The following recommendations can be made based on the conclusions stated in Section 6.6.1:

1. It is considered worthwhile to refine the values and distribution of undrained shear strength in the embankment materials. The values of undrained shear strength in the embankment materials should be based on sampling and laboratory testing of intact samples collected from borings. Specimens should be selected for consolidation tests and determination of undrained shear strength under direct simple shear conditions. These tests should be accompanied by appropriate classification tests. The relative values and spatial distribution of undrained shear strength in the embankment materials should be refined by performing a number of additional Cone Penetrometer Tests (CPTs) distributed through the dam.
2. The values and distribution of shear wave velocity in the embankment materials should be refined using OYO P-S suspension logging and seismic CPTs. Shear wave velocity information should also be obtained in both "soft" and "hard" bedrock using OYO P-S suspension logging and surface seismic surveys to adequate depths to estimate  $V_{s30}$  (shear wave velocity in the upper 30 m) for the development of appropriate design ground motions.
3. The input ground motions to be developed for the seismic stability evaluation will depend on the shear wave velocity in the upper 30 m (100 feet) of the bedrock; thus, the potential effects of the presence of "soft" rock and "hard" rock on the design ground motions should be considered in some manner.
4. The effect of bedrock variation may be important to the seismic stability evaluation of the dam; thus, the variability of the bedrock beneath the embankment should be considered when selecting analysis sections for the evaluation.
5. The contours of seismically induced shear strains such as those shown on Figure 6-14C should be used for guidance in identifying zones that may require refinement in terms of undrained shear strength and other related properties.

## **7.1 GENERAL**

This section contains a work plan for site investigations and laboratory testing at Lenihan Dam that has been developed based on the results of our review of the existing field and laboratory geotechnical data and our preliminary engineering analyses documented in the foregoing sections. The following topics are addressed hereinafter:

1. Objectives and Approach for Field and Laboratory Investigations
2. Proposed Scope of Geotechnical Explorations
3. Field Personnel and Specialty Contractors
4. Procedures for Geotechnical Explorations and Sampling
5. Laboratory Testing
6. Schedule and Environmental Considerations

## **7.2 OBJECTIVES AND APPROACH FOR FIELD AND LABORATORY INVESTIGATIONS**

Our review of the existing field and laboratory geotechnical data, and the use of these data for the preliminary engineering analyses of the performance of Lenihan Dam during the Loma Prieta earthquake indicate the following:

1. The dam is founded on bedrock; i.e. for practical purposes, all of the alluvial and colluvial soils were removed prior to placement and compaction of the dam embankment materials.
2. The undrained shear strength and stress-strain behavior of the various embankment zones of the dam for direct simple shear loading, and the variation of shear strengths within each of the zones, are required for the dynamic deformation analyses and are not well defined.
3. The small stain stiffness of the embankment materials, as indicated by the shear wave velocity of the embankment materials, is required for the dynamic deformation analyses and the available data are inconsistent.
4. The Franciscan Complex bedrock includes both soft and hard rock and the difference in shear wave velocities between the soft and hard rock is not well defined and may influence the input ground motions.

Item 1 above is a very significant finding because it eliminates the potential for liquefaction of foundation soils. However, the absence of poor foundation soils makes the detailed characterization of the compacted clayey embankment soils more critical than would be the case if liquefaction of foundation soils were a concern.

Our approach for obtaining the data required for Item 2 (shear strength and stress-strain behavior of the various embankment materials for direct simple shear loading) is to collect intact samples of embankment materials with a 4-inch diameter Pitcher Barrel Sampler and to test these samples in the laboratory using undrained shear strength tests with pore pressure measurements. We plan to conduct laboratory engineering property tests on nine to twelve intact samples of embankment materials. These tests will be distributed in the Upper Core, Lower Core and Downstream Shell based on a close look at the results of the preliminary deformation analyses and the

measurements made in Cone Penetrometer Test (CPT) soundings adjacent to the mud rotary borings, as discussed below. All the samples will be tested to determine undrained stress-strain behavior and undrained shear strength using direct simple shear tests and/or consolidated undrained triaxial compression tests (hereinafter referred to as undrained shear tests). Duplicate specimens will be selected from approximately six of the samples and one-dimensional consolidation tests will be completed on these specimens. The samples used for undrained shear strength testing will be consolidated to near the estimated maximum in-situ effective stress prior to shearing.

The laboratory engineering property tests will be complemented by measurements of grain size, water content, and Atterberg Limits on all the samples tested. In addition to these tests, physical and index property tests will also be completed on a relatively large number of samples obtained using the modified California Sampler or the split spoon sampler. These additional physical and index property tests will be used to evaluate how representative the samples used for strength testing are of the average conditions within each of the embankment zones.

The data from the laboratory undrained shear tests will be utilized together with the results of the CPT soundings (made adjacent to the mud rotary borings that are used to obtain the Pitcher Barrel samples) in order to develop site specific factors for correlating the undrained shear strength with the CPT data. This will facilitate using the CPT data at other locations in the dam to develop an aerial distribution of undrained shear strength and stress-strain behavior of materials within the dam embankment. The measured cone data will be filtered to remove localized spikes in the data due to gravel or very thin layers of softer soils within the predominately clay soils, before the CPT data are used to develop the distribution of undrained shear strength in the dam. Once calibrated using the laboratory tests, additional CPT soundings can be economically made at a relatively large number of locations on the dam to evaluate the variability of material properties between embankment zones and within each of the embankment zones.

The CPT soundings at potential locations of mud rotary boreholes will be completed before the mud rotary boreholes are drilled and the data from these initial CPT soundings will be used to finalize the boring locations and identify depths within the mud rotary borings where the presence of gravel in the embankment appears to be less likely. These depths will be targeted for obtaining good quality Pitcher Barrel samples. This is a very important role for the use of the CPT data because the experience from past geotechnical investigations is that the gravel content of the embankment materials made obtaining good quality Pitcher Barrel samples very difficult.

Our approach for obtaining the data required for Items 3 and 4 (shear wave velocity measurements within the embankment soils and underlying bedrock) includes the use of the following three different field geophysical methods:

1. OYO P-S Borehole Suspension Logging;
2. Downhole geophysical logging using the “seismic cone” as part of the CPT sounding work; and
3. Multisource Spectral Analysis of Surface Wave (MSASW) geophysical survey lines.

The OYO Suspension Logging provides detailed downhole measurements of shear wave velocities and is performed upon completion of the mud rotary borings. The mud rotary borings will be extended into the Franciscan Complex to obtain shear wave velocity measurements within the upper 25 feet of the bedrock. The data from the OYO Suspension Logging is considered to provide the most accurate measurements of the variation of shear wave velocity with depth. These data will be compared to shear wave velocities measured using downhole geophysical logging as part of the CPT probes that will be completed adjacent to the mud-rotary borings used for the OYO logging. If this comparison shows that the shear wave velocities measured using the “seismic cone” are consistent with the measurements from the OYO logging, measurements of shear wave velocity will be made at the location of other CPT probes to provide data on the variability of shear wave velocity within the dam.

The MSASW geophysical surveys will be used to evaluate the variation of shear wave velocity along survey lines that cross boundaries between soft and hard rock within the Franciscan Complex. This is a relatively new technology for conducting surface geophysical surveys and has been shown to provide good estimates of the overall shear wave velocity of relatively large masses of materials. In addition, the method is non-intrusive and relatively economical.

### **7.3 PROPOSED SCOPE OF GEOTECHNICAL EXPLORATIONS**

The proposed locations of the geotechnical explorations are shown on three figures. Figure 7-1 shows the proposed explorations as well as the locations of previous site investigations superimposed on a site plan that includes elevation contours of the bedrock surface beneath the dam, ground surface elevation contours outside the footprint of the dam, and elevation contours for the surface of the dam. Figure 7-2 shows the proposed exploration locations superimposed on an aerial photograph of the dam and illustrates that the exploration locations have been aligned with the crest of the dam and the paved bicycle pathway on the downstream slope, in order to facilitate access by truck-mounted drilling equipment and minimize disturbance to adjacent vegetated areas. Figure 7-3 is a larger scale plan of the proposed explorations on the dam only.

The proposed program will begin by completing four Phase 1 CPT probes, one each adjacent to the potential locations of the two mud rotary borings. These CPT probes will include the standard continuous measurements of tip resistance, side friction and pore pressure as well as measurements of shear wave velocities based on downhole geophysical measurements at 10-foot intervals using the seismic cone. The tip resistance from the CPT probes will be used to select the final locations of the two borings and target depths within the mud rotary borings for obtaining Pitcher Barrel samples that will provide specimens for undrained strength and consolidation tests.

Two mud rotary borings will then be made at the locations shown on Figures 7-1 to 7-3 and driven samples or intact Pitcher Barrel samples will be obtained at 5-foot intervals. The mud rotary borings will extend into rock. Upon completion of each boring, OYO P-S Geophysical Suspension Logging will be completed to measure shear wave velocity within the dam and to a depth of 25 feet below the top of the rock foundation.

A Phase 2 program of six additional CPT probes will be implemented concurrently with the mud rotary borings. The Phase 2 CPT probes will include measurements of shear wave velocity using

the “seismic cone” as well as the standard tip resistance, side friction and pore pressure measurements. The CPT probes will also include pore pressure dissipation tests at selected locations to measure the permeability of the embankment materials.

MSASW geophysical survey lines will be completed while the drilling or CPT soundings are underway along two lines the locations of which have been selected to cross over the boundaries between hard and soft rock. The approximate locations of these lines are shown on Figure 7-2.

## **7.4 FIELD PERSONNEL AND SPECIALTY CONTRACTORS**

Richard Harlan, PG, CEG, the Geology Task Leader for the project, has over 25 years of experience related to dam investigations and studies. He has had a lead role in:

1. assembling and reviewing the information on Lenihan Dam that was available in District files and in the files of DSOD;
2. reviewing air photos,
3. geologic mapping of materials in the vicinity of the dam site;
4. reviewing and preparing geologic base maps showing the distribution of foundation materials beneath the dam, and
5. preparing this work plan.

Mr. Harlan will be in the field full time during the field investigation program and will be responsible for the field supervision and logging of all the field explorations and field testing. We have planned the work to be accomplished using one drill rig at a time so that Mr. Harlan can personally observe all the drilling, sampling, and field testing work; log all the borings; and observe the field geophysical survey work. We believe this approach will ensure the quality and consistency of the work and avoid many of the problems associated with field investigations that require the use of multiple rigs and multiple field personnel.

The mud rotary drilling and sampling will be done by Pitcher Drilling. Pitcher Drilling invented the Pitcher Barrel Sampler and is widely recognized as one of the most qualified and experienced geotechnical drilling contractors in California. Pitcher Drilling completed the geotechnical drilling for TGP on Stevens Creek Dam and has worked on a number of other dam site investigations including San Pablo Dam, Turner Dam, Chabot Dam, Calaveras Dam, and Folsom Dam.

The CPT probes will be completed by Gregg Drilling and Testing, Inc. Gregg is well-known in California as having excellent CPT equipment and we have found that the technical support provide by Dr. Peter Robertson of Gregg Drilling is very timely and valuable. Gregg Drilling completed the CPT probes that were made previously at Lenihan Dam and recently completed an initial round of CPT probes for TGP at Stevens Creek Dam.

The downhole geophysical OYO logging and MSASW surface seismic surveys will be completed by GeoVision. GeoVision has completed geophysical logging at 30 dams over the past decade, including geophysical logging at four of the District’s dams. They recently completed geophysical logging at Stevens Creek Dam for TGP.

ENGEO is responsible for the geotechnical laboratory testing. ENGEO is a full-service earth science consulting firm that maintains three Northern California soil and materials testing laboratories managed by registered civil engineers: in San Ramon, Rocklin, and Manteca. ENGEO's laboratories are Caltrans-certified, hold current verification status with the US Army Corps of Engineers, and are accredited through the National Institute of Standards and Technology (NIST) by participating in the Cement and Concrete Reference Laboratory (CCRL) and in the AASHTO Materials Reference Laboratories (AMRL) proficiency sample and laboratory inspection programs. Because of the special equipment required for the undrained direct simple shear tests, ENGEO will arrange for the Fugro Geotechnical Laboratory in Houston to conduct these tests. Richard Ladd directs this laboratory and is a recognized expert in direct simple shear testing.

## **7.5 PROCEDURES FOR GEOTECHNICAL EXPLORATIONS AND SAMPLING**

The mud-rotary borings will be drilled using a Fraste Model MD/XL drill rig that has dimensions of 30 feet x 8 feet x 11 feet (length x width x height) for highway travel and weighs 28,660 lbs. The boreholes will be approximately 6 inches in diameter and will be advanced using a tri-cone bit. In general, a driven modified California Sampler (3-in OD) will be alternated with a driven split barrel sampler using the Standard Penetration Test to obtain samples every 5 feet in the embankment sections. A 4-inch diameter Pitcher Barrel Sampler will be used to obtain approximately 15 intact samples of embankment materials.

The drilling fluid pressure will be constantly monitored to minimize the risk of hydro fracturing in the dam. We will monitor the fluid pressure with an approved gauge to ensure that the drilling fluid pressure does not exceed 0.45 psi per foot of boring depth. We will also minimize the drilling fluid pressure by keeping the fluid relatively clean and by maintaining appropriate drilling rates. All fluid losses will be monitored and recorded. If we suspect that hydro fracturing may be occurring, we will suspend drilling and notify the District immediately. The borings will be advanced approximately 40 feet into rock to allow the sensors on the down-hole geophysical logging tool to measure shear wave velocity at the top of rock. The rock sections of the borings will be logged based on cuttings, drill action, drill fluid return, rate of drilling, and any other pertinent fugitive data which will be noted accordingly on the boring logs; coring of the bedrock is not necessary and will not be performed.

The CPT soundings will be completed using a 20-ton capacity truck-mounted cone rig. In addition to measuring tip resistance and side friction, we will conduct 10 pore pressure dissipation tests at various depths within the embankment in order to obtain field data on soil permeability. We will also measure shear wave velocity using the seismic cone at 10-foot intervals in the CPT probes.

Upon completion, the borings and CPT probes will be grouted with cement bentonite grout. We propose to use the grout mix used on Stevens Creek Dam and the SSE1 projects that consists of the following quantities mixed in order:

1. 30 gallons of water
2. 25 pounds of bentonite powder
3. 94 pounds of cement



The minimum mixing time for the grout mix is 5 to 7 minutes. If needed, the proportions of the grout mix may be modified.

Cuttings and drilling fluid will be collected and placed in drums or in a central tank at the site. We will coordinate the disposal of the cuttings and drilling fluid; however, it is noted that the District will be required to sign the disposal manifests and provide justification for assuming that the materials do not contain constituents of concern.

## **7.6 LABORATORY TESTING**

Samples will be transported to the laboratory within three days of sampling along with preliminary laboratory testing assignments. The type and approximate number of laboratory tests planned for the samples obtained from the borings are summarized below.

40	Moisture Content
25	Sieve Analyses
25	Liquid Limit, Plastic Limit and Plasticity Index
9 to 12	Undrained Shear Strength Tests with Pore Pressure Measurements
6	One-Dimensional Consolidation Tests

The final number of tests of each type will be adjusted to reflect the soil conditions actually encountered. Consequently, variations from the planned number of tests should be expected.

## **7.7 SCHEDULE, ENVIRONMENTAL, SAFETY, AND TRAFFIC CONSIDERATIONS**

The project schedule shows field investigations at Lenihan Dam being completed in June 2011. Drilling will generally take place Monday through Friday between 7:00 am and 6:00 pm, with the option to drill on Saturday if the schedule requires it. The amount of time in the field to complete the proposed investigation program is expected to be about 15 days. The work will be performed on the crest of the dam and along the paved bike path that cuts across the downstream slope of the dam. None of the exploration locations are in environmentally sensitive areas. Consequently, there are no special environmental considerations for this project. However, restrictions will be required on the use the bike path and traffic control will be needed when working on the dam crest.

The field crews will receive a briefing by environmental specialists from the District at the start of the field work to make field personnel aware of general environmental requirements and to delineate and discuss environmentally sensitive areas and species in the vicinity of the work area. In addition, a safety briefing will be conducted by the TGP site geologist covering traffic control; management, handling, and on-site storage of materials and equipment; and hazards associated with poison oak.

The borings and CPT probes on the dam crest will require closing one lane of the public crest road in the vicinity of the work. Traffic control will be provided by dedicated flag person(s) specially trained for traffic control and equipped with radios, signs, cones, and other traffic control, equipment, as appropriate. If only one rig is operating on the road, traffic control will be

## SECTION 7.0

## PROPOSED SITE INVESTIGATIONS AND LABORATORY TESTING

---

provided by a single flag person. Two flag persons will be provided when two rigs (mud rotary and CPT) are working on the road at the same time.

- AMEC, 2009 (January), Technical Memorandum No. 3, Seismotectonic and Ground Motion Study, Seismic Stability Evaluation of DIP Phase 1 Dams.
- Bryant, W.A., compiler, 2000, Fault no. 56, Monte Vista-Shannon fault zone, in Quaternary fault and fold database of the United States: U.S. Geological Survey website, <http://earthquakes.usgs.gov/regional/qfaults>.
- California Department of Water Resources, 1948-1954, Geological and Engineering Construction Inspection Memoranda to Mr. H.W. Holmes, Lexington Dam, by E.C. Marliave, D.F. Dresselhaus, et al (on file at DSOD).
- California Department of Water Resources, Division of Safety of Dams (DSOD), 1981 (July), Phase 1 Inspection Report for Lexington Dam.
- California Department of Water Resources, Division of Safety of Dams (DSOD), 2006a (May), Memorandum of Geologic Review of Seismic Hazard, James J. Lenihan Dam, dated May 25, 2006.
- California Department of Water Resources, Division of Safety of Dams (DSOD), 2006b (October), Geologic Review of Geotechnical Data Report and Lexington Fault Evaluation Memo, dated October 23, 2006.
- California Department of Water Resources, Division of Safety of Dams (DSOD), 2006c (October), Memorandum of Design Review – Review of Performance During the Loma Prieta Earthquake, James J. Lenihan Dam, dated October 23, 2006.
- California Department of Water Resources, Division of Safety of Dams (DSOD), 2007a (June), Memorandum of Design Review, James J. Lenihan Dam, dated June 29, 2007.
- California Department of Water Resources, Division of Safety of Dams, 2007b (November), Geologic Inspection of Lexington Fault Exposure and Review of Lexington Fault Cove Exposure Memo, dated November 26, 2007.
- California Department of Water Resources, Division of Safety of Dams (DSOD), 2009 (October), Updated Ground Motion Estimates, J. Lenihan Dam, dated October 15, 2009.
- California Department of Water Resources, Division of Safety of Dams (DSOD), 2010a (June), DSOD Comments on DM-2 and Interim DM-4, Guadalupe, Almaden, and Calero Dams, dated June 10, 2010.
- California Department of Water Resources, Division of Safety of Dams (DSOD), 2010b (November), Email message from Jeffrey D. Kuhl of DSOD to Steven Wu of Santa Clara Valley Water District, dated November 8, 2010.
- Cotton and Associates, 1993, Pre-Design Investigation, Lexington Dam Freeboard Restoration Project, Santa Clara Valley Water District.
- Earth Science Associates (ESA), 1987 (December), Lexington Reservoir Outlet Modifications, Final Geotechnical Investigation, prepared for Santa Clara Valley Water District.
- Geomatrix Consultants, 1992, Analysis of the Recorded Response of Lexington Dam During the Loma Prieta Earthquake.

- Geomatrix Consultants, 1996 (April), Geologic/Geotechnical Study and Basis of Design report, Lexington Dam Freeboard Restoration Project.
- Geomatrix Consultants, 2006a (July), Evaluation of Lexington Fault near Lenihan Dam, Memorandum to Mr. Nolting - Jacobs Associates, Lenihan Dam Outlet Modification Project, Memorandum, dated July 14, 2006.
- Geomatrix Consultants, 2006b, Final Geologic and Geotechnical Data Report, Lenihan Dam Outlet Modification Project.
- Geomatrix Consultants, 2007 (October), Field Review of Lexington Fault Exposure in “The Cove”, Memorandum to Mr. Nolting, Jacobs Associates, in support of Lenihan Dam Outlet Modification Project, dated October 12, 2007.
- Harza Engineering Company, 1997 (January), GEFDYN Verification of Lexington Dam, Draft Report, prepared for Tennessee Valley Authority.
- Idriss, I. M., and Joseph I. Sun, J. I., 1992 (November), User’s Manual for SHAKE-91. University of California, Davis, Center for Geotechnical Modeling, Department of Civil & Environmental Engineering.
- Idriss, I. M., 2003, Personal communication.
- Itasca, 2008, FLAC, version 6.0, Itasca Consulting Group Inc., Minneapolis.
- Ladd, C.C., 1971, Strength Parameters and Stress-Strain Behavior of Saturated Clays, Research Report R71-23, Department of Civil Engineering, Massachusetts Institute of Technology, Chapter 9.
- Ladd, C.C. and DeGroot, D.J., 2003, Recommended Practice for Soft Ground Site Characterization, the Arthur Casagrande Lecture, Proceedings of the 12<sup>th</sup> Panamerican Conference on Soil Mechanics and Geotechnical Engineering, Boston MA, Vol.1, pp. 3-57.
- William Lettis & Associates, Inc. (Lettis), 2008 (December), Final Technical Memorandum, Seismic Source Identification and Development of Earthquake Parameters for Deterministic Seismic Hazard Analysis, Eleven Santa Clara Valley Water District Dams, Santa Clara County, California.
- Lewis, R.W. Jr., 1951, The Lexington Dam Site: unpublished report to Col. Van Court Warren, dated June 15, 1951.
- Marliave, E.C., 1948, Geological Report on the Lexington Dam Site.
- Marliave, E.C., 1951, Memorandum to Mr. H. W. Holmes, Lexington Dam No. 72-8, Inspected January 3 and 4, 1951.
- McLaughlin, R.J., Oppenheimer, D., Helley, E.J., and Sebrier, M., 1992, The Lexington fault zone: a north-south link between the San Andreas fault and range front fault system, Los Gatos, California: Geologic Society of America Abstracts with Programs, v. 24, no. 5, p. 69.

- McLaughlin, R.J., Clark, J.C., Brabb, E.E., and Helley, E.J., 2001, Geologic Maps and Structure Sections of the Southwestern Santa Clara Valley and Southern Santa Cruz Mountains, Santa Clara and Santa Cruz Counties, California, Sheet 1: Los Gatos Quadrangle.
- McLaughlin et al, 2004, Geologic Map of the Loma Prieta Region, California, USGS Professional Paper 1550E.
- Robertson, P.K. and Campanella, R.G., 1990, Guidelines for Use, Interpretation and Application of CPT and CPTU, University of British Columbia, Soil Mechanics Series 105, Civil Engineering Department, Vancouver, B.C., V6T 1W5, Canada.
- Robertson, P.K. and Wride, C.E., 1998, Evaluating Cyclic Liquefaction Potential Using the Cone Penetrometer Test, Canadian Geotechnical Journal, Vol. 35, No. 3, pp. 442-459.
- Robertson, P.K., 2009, Interpretation of Cone Penetrometer Tests – a unified approach, Canadian Geotechnical Journal, Volume 46, Number 11, 1 November 2009, pp. 1337-1355.
- Rogers, T.H., and Armstrong, C.F., 1971, Environmental geologic analysis of the Santa Cruz Mountains study area, Santa Clara County, California: California Division of Mines Open File Report 72-21, 75p.
- Rogers, T.H. and Williams, J.W., 1974, Potential seismic hazards in Santa Clara County, California: California Division of Mines and Geology Special Report 107, 39 p., map scale 1:62,500.
- William Lettis & Associates (WLA), 2008, Seismic Source Identification and Development of Earthquake Parameters for Deterministic Seismic Hazard Analysis, Letter to Geomatrix Consultants, December 17, 2008.
- Santa Clara Valley Water District (SCVWD), 1976, Reconnaissance of Landslide Conditions at Lexington Reservoir.
- Santa Clara Valley Water District (SCVWD), 1996, Specifications and Contract Documents for the Construction of Lexington Dam Freeboard Restoration Project.
- Santa Clara Valley Water District (SCVWD), 2001 (October), Phase B Instrumentation Project Basic Data Report.
- Santa Clara Valley Water District (SCVWD), 2007 (July), Second Summary Surveillance Report, December 2003 through July 2007, Lenihan Dam No.72-8.
- Santa Clara Valley Water District (SCVWD), 2010a (January), Foundation Analysis Report on Chesbro No.72-11, Lenihan No.72-8, Stevens Creek No. 72-7, and Uvas No. 72-12 Dams (SSE-2 Dams), prepared by James L. Nelson.
- Santa Clara Valley Water District (SCVWD), 2010b (June), 2010 Surveillance Report, March 2009 through April 2010, Lenihan Dam No.72-8.
- Terra / GeoPentech, 2010 (November 24), Technical Memorandum SSE2-TM-1LN, Initial Review of Available Data for Lenihan Dam.
- Treadwell and Rollo, 2002, Geotechnical Feasibility Report for Lenihan Dam New Tunnel Option.

- URS Corporation, 2010 (October), Design Memorandum No.4, Task 3 – Site Specific Design Earthquake Motions, Seismic Stability Evaluation of Almaden, Calero, and Guadalupe Dams.
- U.S. Geological Survey website, 2011, Rupture Length and Slip – The Northern California Earthquake April 18, 1906: <http://quake.wr.usgs.gov/info/1906/offset.htm>.
- Volpe, R.L. and Associates (RLVA), 1990, Investigation of SCVWD Dams Affected by Loma Prieta Earthquake of October 17, 1989, Report to Santa Clara Valley Water District.
- Volpe, R.L. and Associates (RLVA), 1997, Evaluation of Partial Collapse of Low Level Outlet Pipeline, James J. Lenihan Dam.
- Volpe, R.L. and Associates (RLVA), 1998, Instrumentation Design and Review, Lenihan Dam.
- Volpe, R.L. and Associates (RLVA), 1999a, Lenihan Dam Outlet Investigation, Vol. 1 – Final Engineering Report.
- Volpe, R.L. and Associates (RLVA), 1999b, Lenihan Dam Outlet Investigation, Vol. 2 – Basic Data Report.
- Vucetic, M. and Dobry, R., 1991, Effect of Soil Plasticity on Cyclic Response, Journal of Geotechnical Engineering Division, ASCE, Vol. 117, No. 1, pp.89-107.
- Wahler Associates, 1982, Final Report on Seismic Safety Evaluation of Lexington Dam.
- Wahler Associates, 1993, Investigation of Seepage on the Downstream Face of Lexington Dam.
- Wells, R., editor, 2004, The Loma Prieta, California, Earthquake of October 17, 1989 - Geologic Setting and Crustal Structure, USGS Professional Paper 1550E.
- Wills, C., Weldon, R., and Bryant, W., 2008, Appendix A: California Fault Parameters for the National Seismic Hazard Maps and Working Group on California Earthquake Probabilities 2007, USGS Open File Report 2007-1437A.
- Woodward-Clyde Consultants, 1993, Nonlinear Dynamic Response Analysis of Lexington Dam.



## TABLES

TABLE 5-1  
REVIEW AND ASSESSMENT OF AVAILABLE LABORATORY AND FIELD TESTING DATA

Study	Classification Properties	In-situ Properties	Effective Stress Strength	Undrained Strength	Cyclic Properties	Shear Wave Velocity	Other Properties
<b>Wahler, 1982</b>  Study conducted between 1975 and 1981, data compiled in 1982 report	Moisture content, density, specific gravity, sieve analysis, hydrometer and Atterberg limits	In-place density tests and limited SPTs	9 ICU'C tests on pitcher samples for Zone 1, 2U and 2L, 3 ICU'C tests on re-compacted samples for Zone 4	9 ICU'C tests on pitcher samples for Zone 1, 2U and 2L, 3 ICU'C tests on re-compacted samples for Zone 4	Stress controlled cyclic testing on pitcher samples and re-compacted samples	Cross-hole, downhole and surface refraction surveys for all zones	Resonant column, consolidation, permeability and maximum density
	<u>Application</u> : Much of data used, see Section 5.4	<u>Application</u> : Density data used	<u>Application</u> : Data used, except re-compacted samples of Zone 4	<u>Application</u> : Data considered for comparison	<u>Application</u> : Data considered but not used	<u>Application</u> : Much of data used, see Section 5.5	<u>Application</u> : Density and permeability data used
	<u>Reasoning</u> : Data was complete and considered reliable	<u>Reasoning</u> : SPT data not used because materials were clayey and hammer energy was not calibrated	<u>Reasoning</u> : Zone 4 samples were not appropriate for comparison	<u>Reasoning</u> : Sampling and testing was inconsistent between zones	<u>Reasoning</u> : See Section 5.5 for discussion	<u>Reasoning</u> : Data was complete and considered	<u>Reasoning</u> : Shear wave data used in lieu of resonant column data for shear modulus
<b>Geomatrix, 1996</b>  Study conducted between 1995 and 1996	Moisture content, density, specific gravity, sieve analysis, and limits for Zone 2U	SPTs using modified California sampler	Unconfined compression (UC) tests on soil and rock samples	UU testing on disturbed rock samples obtained by modified California sampler	No testing performed	No data collected	Maximum density on Zone 2U material
	<u>Application</u> : Much of data used, see Section 5.4	<u>Application</u> : Data not used	<u>Application</u> : Data not used	<u>Application</u> : Data not used			<u>Application</u> : Density data used
	<u>Reasoning</u> : Data was considered reliable but limited to Zone 2U	<u>Reasoning</u> : SPT data not used because a non-standard sampler was used, materials were clayey and energy was not calibrated	<u>Reasoning</u> : UC testing is not applicable for determining effective stress strength parameters	<u>Reasoning</u> : Sampling and testing considered inappropriate for assigning shear strength			<u>Reasoning</u> : Data was considered reliable
<b>Harza, 1997</b>  Study conducted between 1996 and 1997	Moisture content, density, specific gravity and Atterberg limits	No testing performed	16 ICU'C tests on four samples from each zone, moisture and limits tested for each sample	16 ICU'C tests on four samples from each zone	Strain controlled cyclic testing on all zones	No data collected	Consolidation tests on all zones
	<u>Application</u> : Much of data used, see Section 5.4		<u>Application</u> : Much of data used, see Section 5.5	<u>Application</u> : Data used for basis of stress-strain relationship	<u>Application</u> : Data considered but not used		<u>Application</u> : Data not used
	<u>Reasoning</u> : Data was complete and considered reliable		<u>Reasoning</u> : Data was complete and considered reliable	<u>Reasoning</u> : Effective confining pressure used in testing was inconsistent with in-situ conditions of samples	<u>Reasoning</u> : Effective confining pressure used in testing was inconsistent with in-situ conditions of samples		<u>Reasoning</u> : Testing was performed in non-standard way for determining maximum past pressure
<b>RLVA, 1999</b>  Study conducted between 1998 and 1999	Moisture content, density, specific gravity, sieve analysis, hydrometer and Atterberg limits	CPT data on all four zones	No testing performed	Inferred data from CPT	No testing performed	No data collected	Consolidation, permeability and pore pressure dissipation testing performed
	<u>Application</u> : Much of data used, see Section 5.4	<u>Application</u> : Much of data used, see Sections 4 and 5		<u>Application</u> : Data used as a basis for developing relationship between CPT inferred Su (DSS) conditions and in-situ effective confining pressure.			<u>Application</u> : Much of data used, see Section 5.5
	<u>Reasoning</u> : Data was considered reliable but excluded Zone 4	<u>Reasoning</u> : Data was complete and considered reliable		<u>Reasoning</u> : See Section 5.5 for discussion.			<u>Reasoning</u> : Permeability data was complete and reliable
<b>SCVWD, 2001</b>  Study conducted in 2001	Moisture content, density, specific gravity, sieve analysis, hydrometer and Atterberg limits for Zone 4	No testing performed	9 ICU'C tests on Zone 4 samples	9 ICU'C tests on Zone 4 samples	No testing performed	No data collected	Permeability testing performed on Zone 4 Samples
	<u>Application</u> : Much of data used, see Section 5.4		<u>Application</u> : Much of data used, see Section 5.5	<u>Application</u> : Data considered for comparison			<u>Application</u> : Much of data used, see Section 5.5
	<u>Reasoning</u> : Data was considered reliable but limited to Zone 4		<u>Reasoning</u> : Limited because testing was only performed on Zone 4	<u>Reasoning</u> : Limited because testing was only performed on Zone 4			<u>Reasoning</u> : Data was complete reliable

Notes: 1. A solid red box around the "Application" section indicates that the data were used in the material property characterization; a dashed red box indicates the data were considered but not used.  
2. In the "Reasoning" sections, "complete" is used to characterize studies where testing encompassed all zones and all pertinent data was reported; "considered reliable" is based on judgment.

**TABLE 5-2**  
**MATERIAL CLASSIFICATION SUMMARY<sup>1</sup>**

Zone <sup>2</sup>	Idealized Material Description	Generalized USCS Classification	In-Situ Conditions <sup>3</sup>			Gradation <sup>3</sup>				Atterberg Limits <sup>3</sup>	
			Dry Unit Weight, $\gamma_d$ (pcf)	Moisture Content, $W_c$ (%)	Compaction (%) <sup>4</sup>	Gravel (%)	Sand (%)	Fines (%)	Clay Fraction, $-2\mu$ (%)	Liquid Limit LL	Plasticity Index PI
1	Upstream Shell	SC-CL	119.3 (95.2 - 132.3)	15.0 (10.3 - 26.5)	95 (76 - 106)	27 (0 - 43)	34 (3 - 44)	39 (19 - 97)	21 (12 - 44)	33 (30 - 39)	15 (6 - 24)
2U	Upper Core (Above El. 590 ft)	SC-GC-SM-CL	119.1 (108.0 - 131.5)	11.4 (6.0 - 17.7)	95 (81 - 112)	33 (3 - 58)	35 (23 - 48)	31 (16 - 53)	17 (13 - 30)	38 (31 - 43)	17 (14 - 29)
2L	Lower Core (Below El. 590 ft)	CH-CL-MH-SM-CL	99.8 (89.7 - 111.2)	24.0 (17.8 - 32.3)	101 (91 - 113)	6 (0 - 29)	15 (3 - 43)	79 (29 - 97)	42 (16 - 53)	62 (43 - 68)	34 (15 - 44)
4	Downstream Shell	SC-GC-SP-CL-GM	124.3 (100.6 - 143.3)	12.0 (6.2 - 19.9)	89 (72 - 102)	32 (13 - 50)	38 (24 - 60)	30 (15 - 63)	17 (11 - 26)	32 (22 - 41)	14 (6 - 23)

Notes:

1. Data in this table are averages with minimum and maximum values in parentheses. No data is available for Drain Material (Zone 3).
2. See Figure 5-1.
3. In-situ conditions, gradation and Atterberg limits are summarized based on laboratory testing performed by Wahler (1981), Geomatrix (1996), Harza (1997), RLVA (1999), and SCVWD (2001).
4. Per D1557 modified, 20,000 ft-lbs.

**TABLE 5-3**  
**SUMMARY OF ENGINEERING PROPERTIES**

Zone	Moist Unit Weight (pcf) $\gamma_t$	Effective Friction Angle <sup>(1)</sup> $\phi'$	Undrained Strength Parameter <sup>(2)</sup> $S_u/\sigma_{vc}'$	Stress-Strain Strength Relationship <sup>(3)</sup> $S_u/\sigma_{vc}'$	Dynamic Properties <sup>(4)</sup>	
					$V_s$	$G/G_{max}$ and Damping
1	138	36 °	(2-1), (2-2)	(3-1)	(4-1)	Figure 5-22
2U	132	34 °	(2-1), (2-2)	(3-1)	(4-1)	Figure 5-22
2L	124	26 °	(2-1), (2-2)	(3-1)	(4-2)	Figure 5-22
4	140	34 °	(2-1), (2-2)	(3-1)	(4-1)	Figure 5-22

Notes:

<sup>(1)</sup> Effective Friction Angle,  $\phi'$  (with no cohesion)

<sup>(2)</sup> Undrained Strength Parameter,  $S_u/\sigma_{vc}'$  (undrained shear strength ratio)

$$^{(2-1)} S_u/\sigma_{vc}' = 0.22 \cdot OCR^{0.8}$$

$$^{(2-2)} OCR = \exp(-1.41 \cdot \ln(\sigma_{vc}') + 14.44), \sigma_{vc}' > 3300 \text{ psf}, OCR = 20, \sigma_{vc}' < 3300 \text{ psf}$$

<sup>(3)</sup> Stress-Strain Strength Relationship,  $\tau = \text{fn}(\gamma, S_u)$

$$^{(3-1)} \tau = S_u \cdot \exp(0.17 \cdot \ln(\gamma) - 0.52)$$

<sup>(4)</sup> Dynamic Properties,  $V_s$  (shear wave velocity),  $G/G_{max}$  (shear modulus) and Damping Ratio

$$^{(4-1)} V_s = \exp(0.23 \cdot \ln(\sigma_{vc}') + 5.4)$$

$$^{(4-2)} V_s = \exp(0.79 \cdot \ln(\sigma_{vc}'))$$

**TABLE 6-1**  
**SUMMARY OF MATERIAL PROPERTIES USED IN ANALYSES**

<b>Zone</b>	<b>Moist Unit Weight (pcf)</b> $\gamma_t$	<b>Effective Friction Angle<sup>(1)</sup></b> $\phi'$	<b>Undrained Strength Parameter<sup>(2)</sup></b> $S_u/\sigma_{vc}'$	<b>Stress-Strain Strength Relationship<sup>(3)</sup></b> $\tau = fn(\gamma, S_u)$	<b>Dynamic Properties<sup>(4) (5)</sup></b> $G_{max}$ or $V_s$
1	138	36 °	(2-1), (2-2)	(3-1)	(4-1)
2U	132	34 °	(2-1), (2-2)	(3-1)	(4-1)
2L	124	26 °	(2-1), (2-2)	(3-1)	(4-2)
4	140	34 °	(2-1), (2-2)	(3-1)	(4-1)

**Notes:**

<sup>(1)</sup> Effective Friction Angle,  $\phi'$  (with no cohesion)

<sup>(2)</sup> Undrained Strength Parameter,  $S_u/\sigma_{vc}'$  (undrained shear strength ratio)

$$^{(2-1)} S_u/\sigma_{vc}' = 0.22 \cdot OCR^{0.8}$$

$$^{(2-2)} OCR = \exp(-1.41 \cdot \ln(\sigma_{vc}')) + 14.44, \sigma_{vc}' > 3300 \text{ psf}, OCR = 20, \sigma_{vc}' < 3300 \text{ psf}$$

<sup>(3)</sup> Stress-Strain Strength Relationship,  $\tau = fn(\gamma, S_u)$

$$^{(3-1)} \tau = S_u \cdot \exp(0.17 \cdot \ln(\gamma) - 0.52)$$

<sup>(4)</sup> Dynamic Properties,  $V_s$  (shear wave velocity),  $G/G_{max}$  (shear modulus) and Damping Ratio

$$^{(4-1)} V_s = \exp(0.23 \cdot \ln(\sigma_{vc}')) + 5.4$$

$$^{(4-2)} V_s = \exp(0.79 \cdot \ln(\sigma_{vc}'))$$

$$^{(4-3)} \text{Bedrock } V_s = 3,000 \text{ fps}$$

<sup>(5)</sup>  $G/G_{max}$  Reduction and Damping Ratio Curves are shown on Figure 5-22.

## FIGURES





Note: Base map printed from USGS 1:24,000 scale  
topographic maps by TOPO! © 2003 National Geographic.

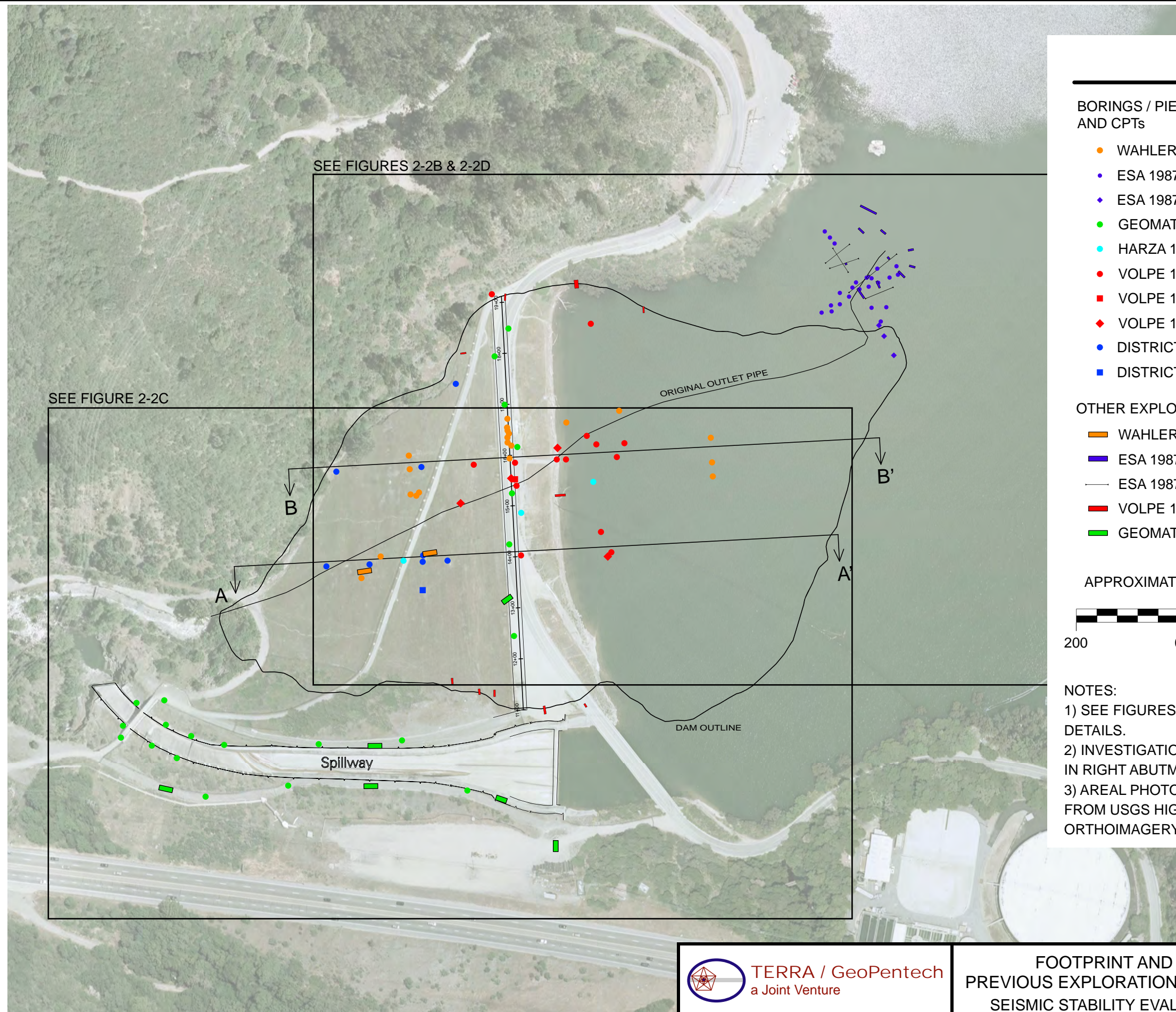
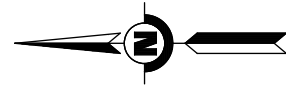


**TERRA / GeoPentech**  
a Joint Venture

**REGIONAL SITE LOCATION MAP**  
**LENIHAN DAM**  
**SEISMIC STABILITY EVALUATIONS (SSE2)**

**Figure**  
**2-1**





## LEGEND

### BORINGS / PIEZOMETERS / INCLINOMETERS AND CPTs

- WAHLER 1982 BORING
- ESA 1987 BORING
- ◆ ESA 1987 CPT
- GEOMATRIX 1996 BORING
- HARZA 1997 BORINGS
- VOLPE 1999 PIEZOMETER
- VOLPE 1999 INCLINOMETER
- ◆ VOLPE 1999 CPT
- DISTRICT 2001 PIEZOMETER
- DISTRICT 2001 INCLINOMETER

### OTHER EXPLORATIONS

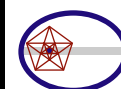
- WAHLER 1982 TEST PIT
- ESA 1987 TEST PIT
- ESA 1987 SEISMIC REFRACTION LINE
- VOLPE 1990 TRENCH
- GEOMATRIX 1996 TEST PIT

APPROXIMATE SCALE, FEET



### NOTES:

- 1) SEE FIGURES 1B AND 1C FOR ADDITIONAL DETAILS.
- 2) INVESTIGATIONS FOR NEW OUTLET TUNNEL IN RIGHT ABUTMENT NOT SHOWN.
- 3) AREAL PHOTOGRAPH DATED APRIL 2006 FROM USGS HIGH RESOLUTION STATE ORTHOIMAGERY

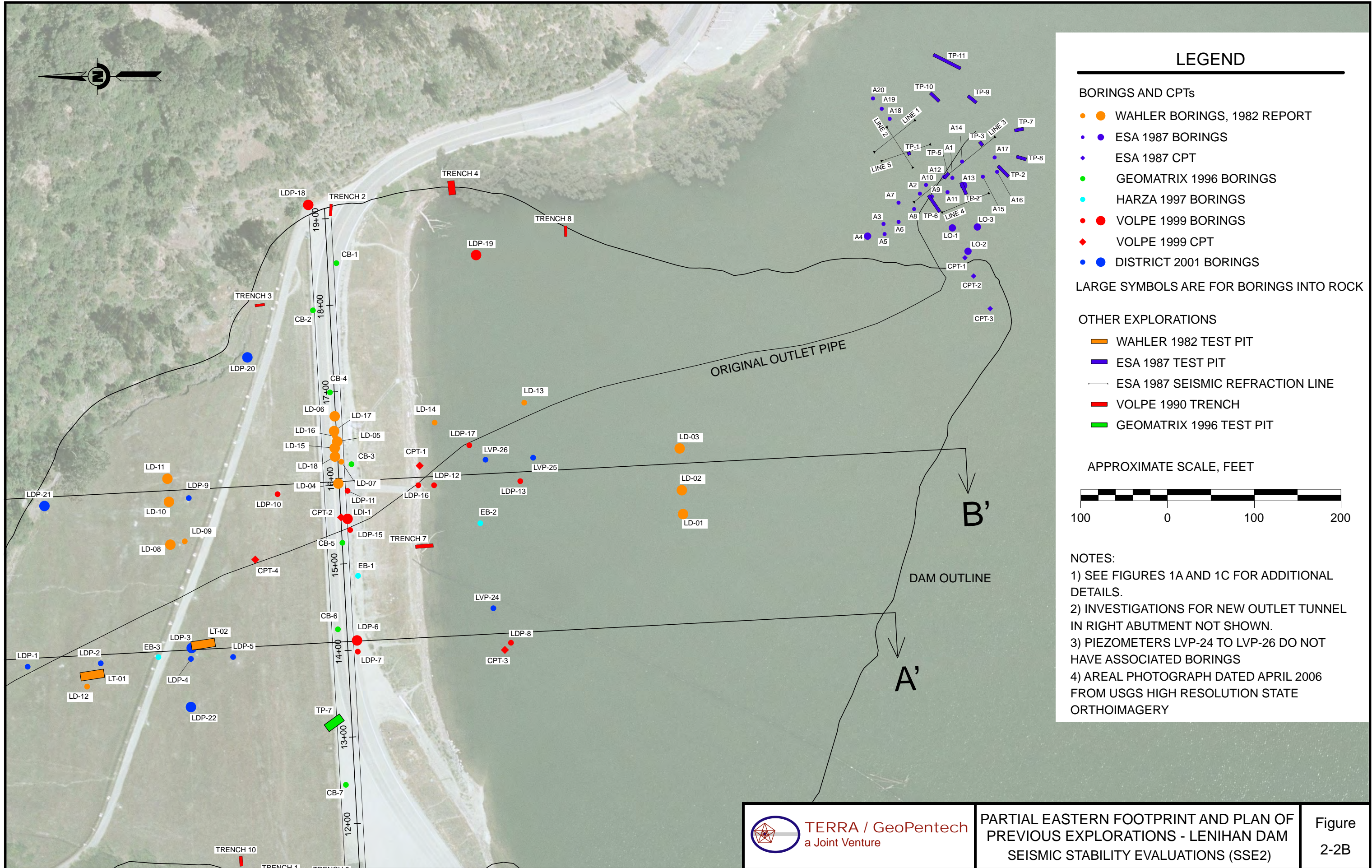


**TERRA / GeoPentech**  
a Joint Venture

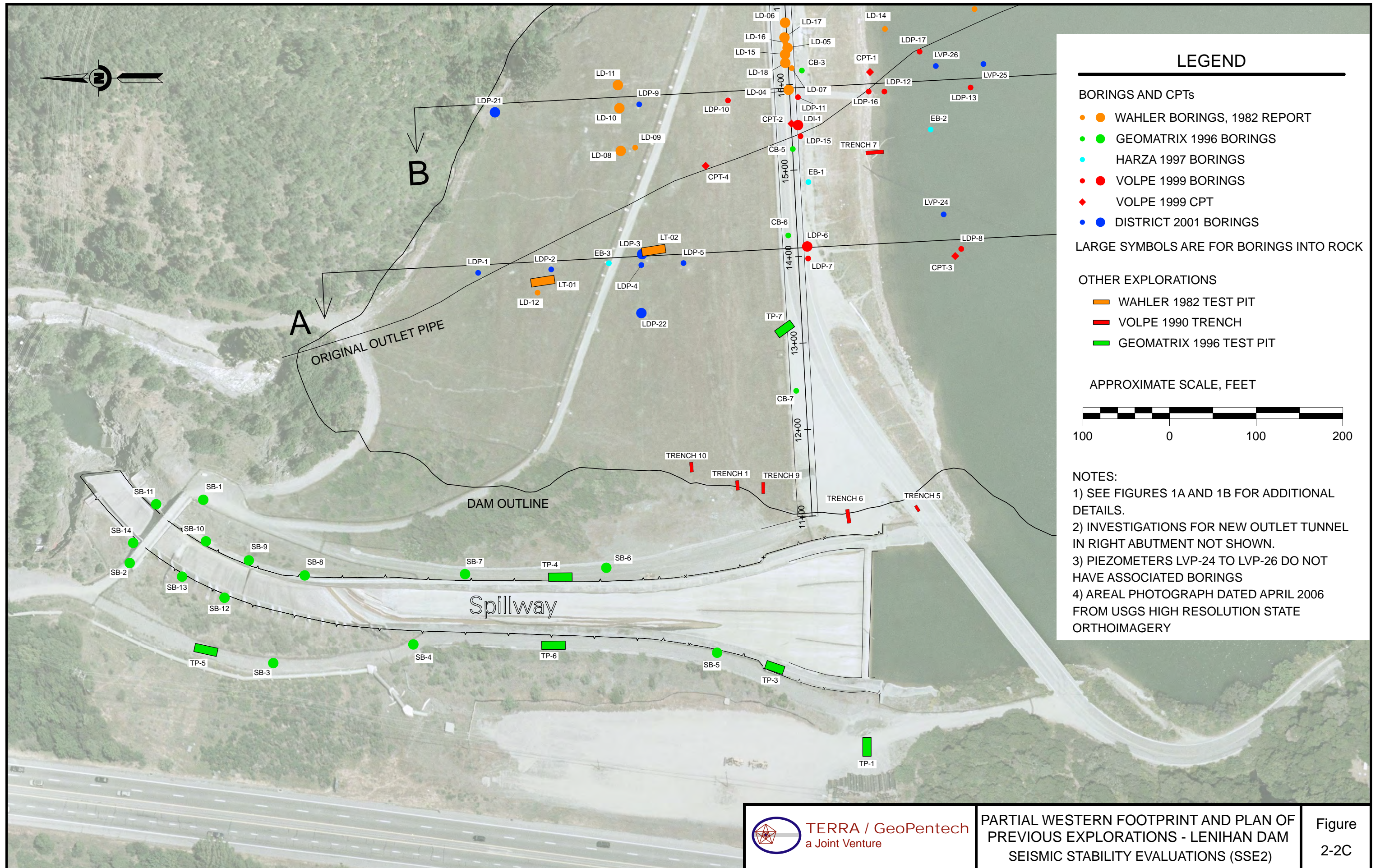
FOOTPRINT AND PLAN OF  
PREVIOUS EXPLORATIONS - LENIHAN DAM  
SEISMIC STABILITY EVALUATIONS (SSE2)

Figure  
2-2A



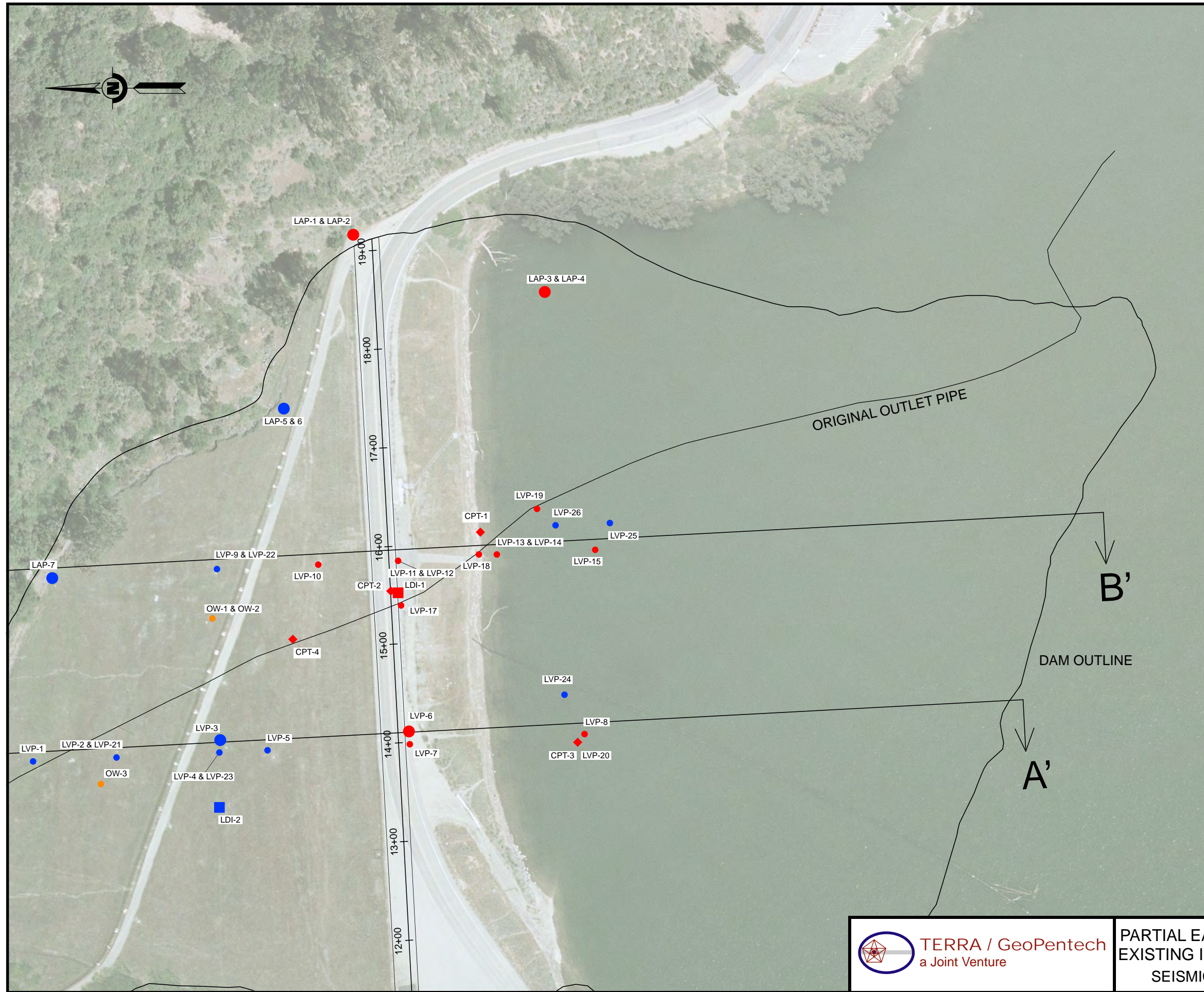








Rev. 3 03/28/2011 SSE2-WP-1LN



## LEGEND

### PIEZOMETERS / INCLINOMETERS AND CPTs

- WAHLER BORINGS, 1982 REPORT
- VOLPE 1999 PIEZOMETERS
- VOLPE 1999 INCLINOMETER
- VOLPE 1999 CPT
- DISTRICT 2001 PIEZOMETERS
- DISTRICT 2001 INCLINOMETER

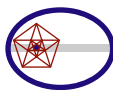
LARGE SYMBOLS ARE FOR BORINGS INTO ROCK

APPROXIMATE SCALE, FEET



### NOTES:

- 1) SEE FIGURES 1A AND 1C FOR ADDITIONAL DETAILS.
- 2) INVESTIGATIONS FOR NEW OUTLET TUNNEL IN RIGHT ABUTMENT NOT SHOWN.
- 3) AREAL PHOTOGRAPH DATED APRIL 2006 FROM USGS HIGH RESOLUTION STATE ORTHOIMAGERY

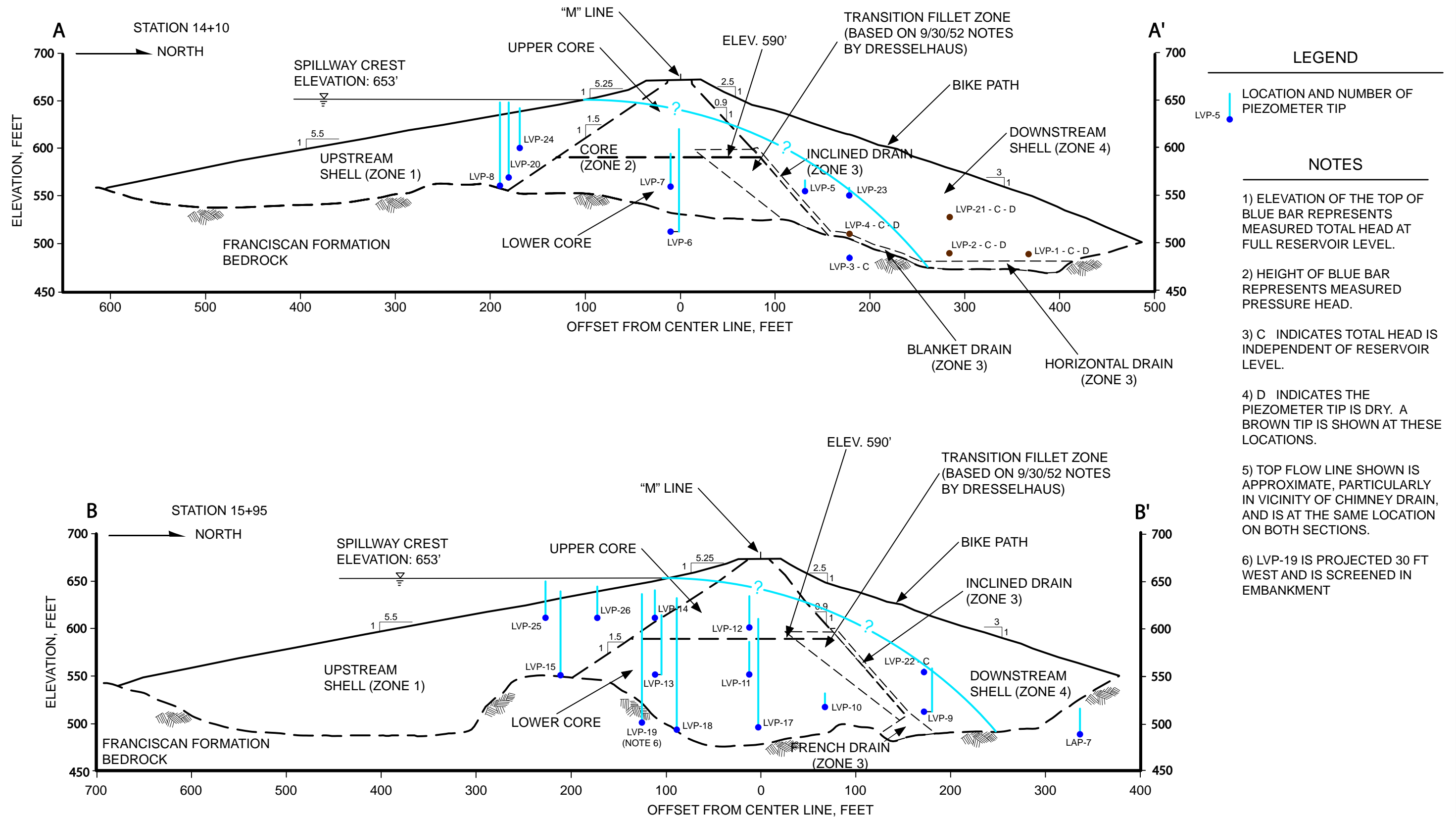


**TERRA / GeoPentech**  
a Joint Venture

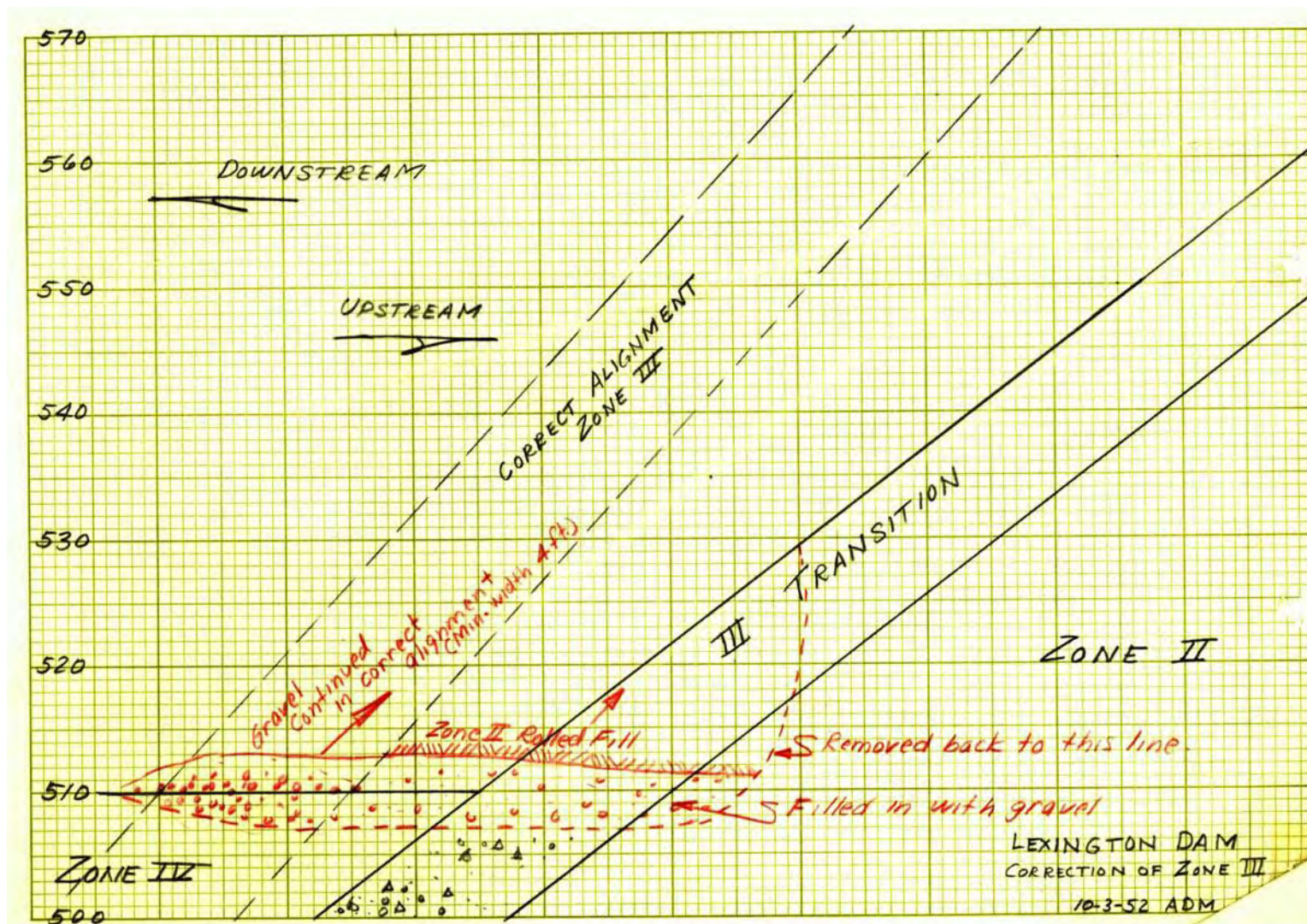
PARTIAL EASTERN FOOTPRINT AND PLAN OF  
EXISTING INSTRUMENTATION - LENIHAN DAM  
SEISMIC STABILITY EVALUATIONS (SSE2)

Figure  
2-2D

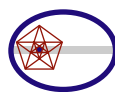








Note: Sketch by A.D. Morrison (DSOD) dated October 3, 1952, excerpted from DSOD Files.

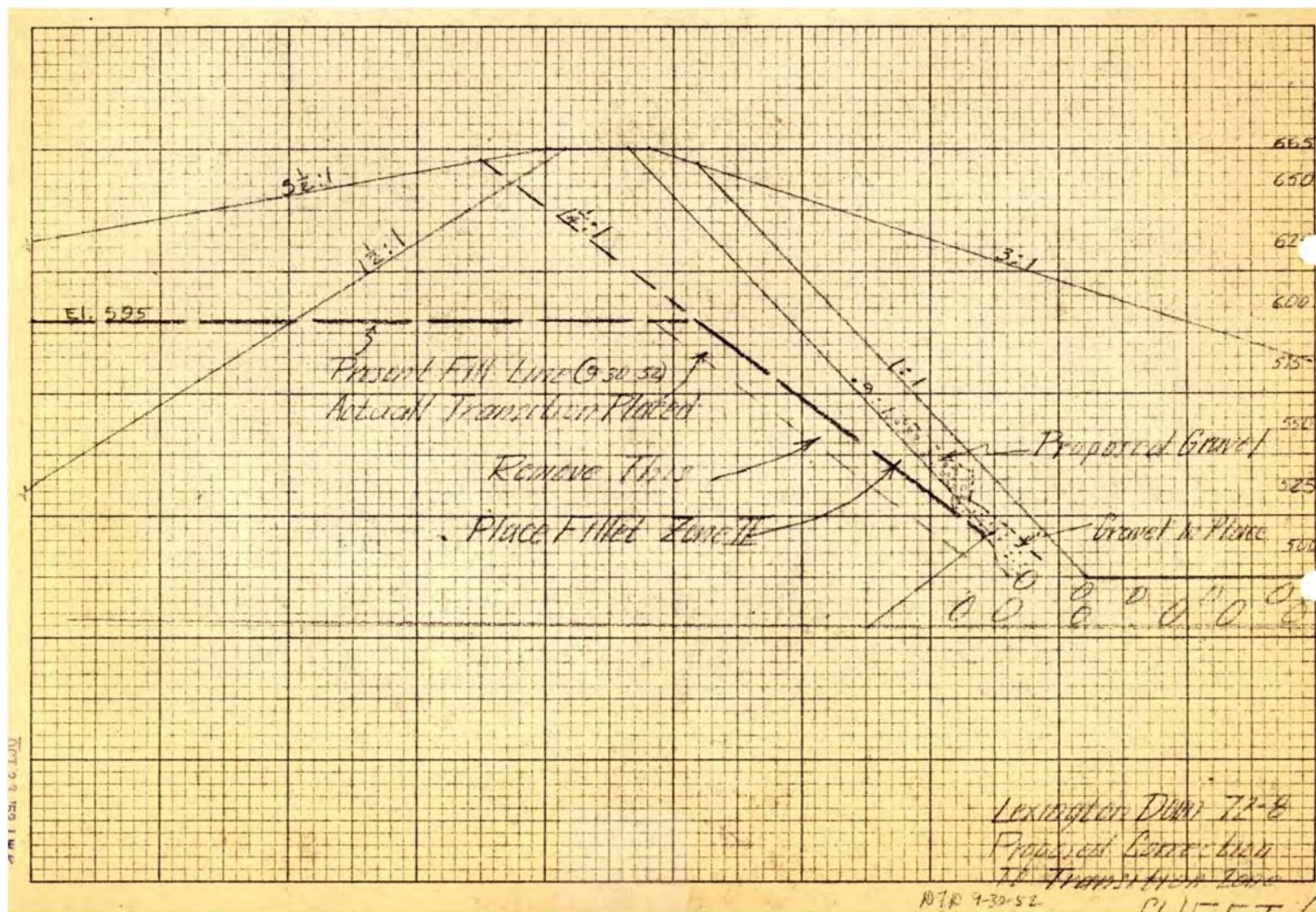


TERRA / GeoPentech  
a Joint Venture

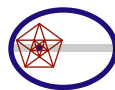
AS-BUILT SIZE OF INCLINED DRAIN  
LENIHAN DAM  
SEISMIC STABILITY EVALUATIONS (SSE2)

Figure  
2-4





Note: Sketch by DSOD inspector D. Dresselhaus dated September 30, 1952, excerpted from DSOD Files.

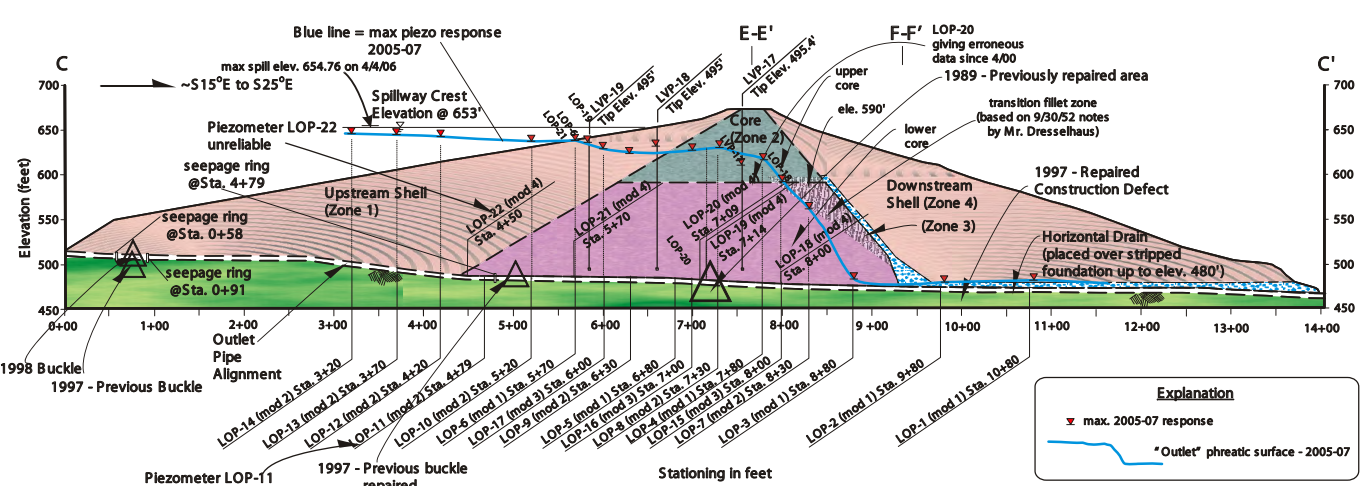


**TERRA / GeoPentech**  
a Joint Venture

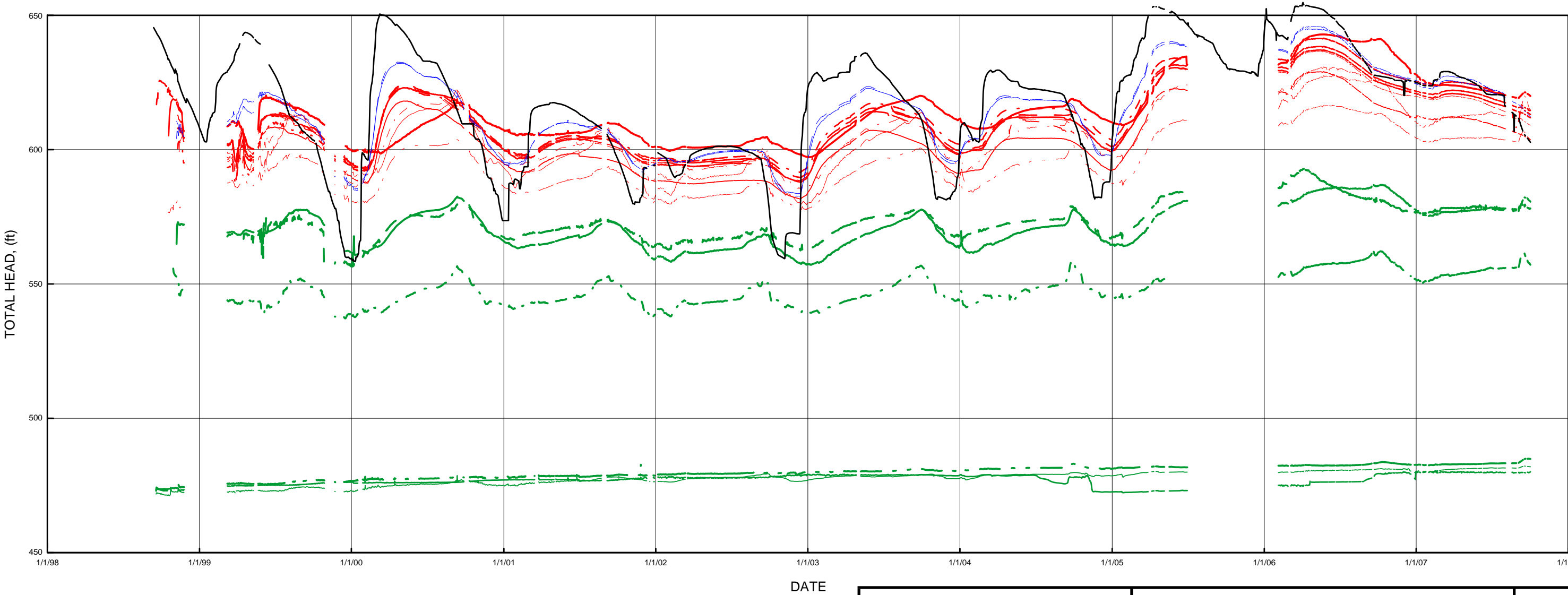
**AS-BUILT FILLET OF ZONE 2 MATERIAL  
LENIHAN DAM**  
SEISMIC STABILITY EVALUATIONS (SSE2)

Figure  
2-5

LINE	PIEZOMETER NUMBER	STATION	EMBANKMENT ZONE
—	Reservoir		
—	LOP-14	3+20	UPSTREAM SHELL
—	LOP-13	3+70	
—	LOP-12	4+20	
—	LOP-10	5+20	
—	LOP-06	5+70	
—	LOP-21	5+70	CORE
—	LOP-17	6+00	
—	LOP-09	6+30	
—	LOP-16	7+00	
—	LOP-19	7+14	
—	LOP-08	7+30	
—	LOP-04	7+80	
—	LOP-15	8+00	
—	LOP-18	8+00	
—	LOP-07	8+30	
—	LOP-03	8+80	DRAIN
—	LOP-02	9+80	
—	LOP-01	10+80	

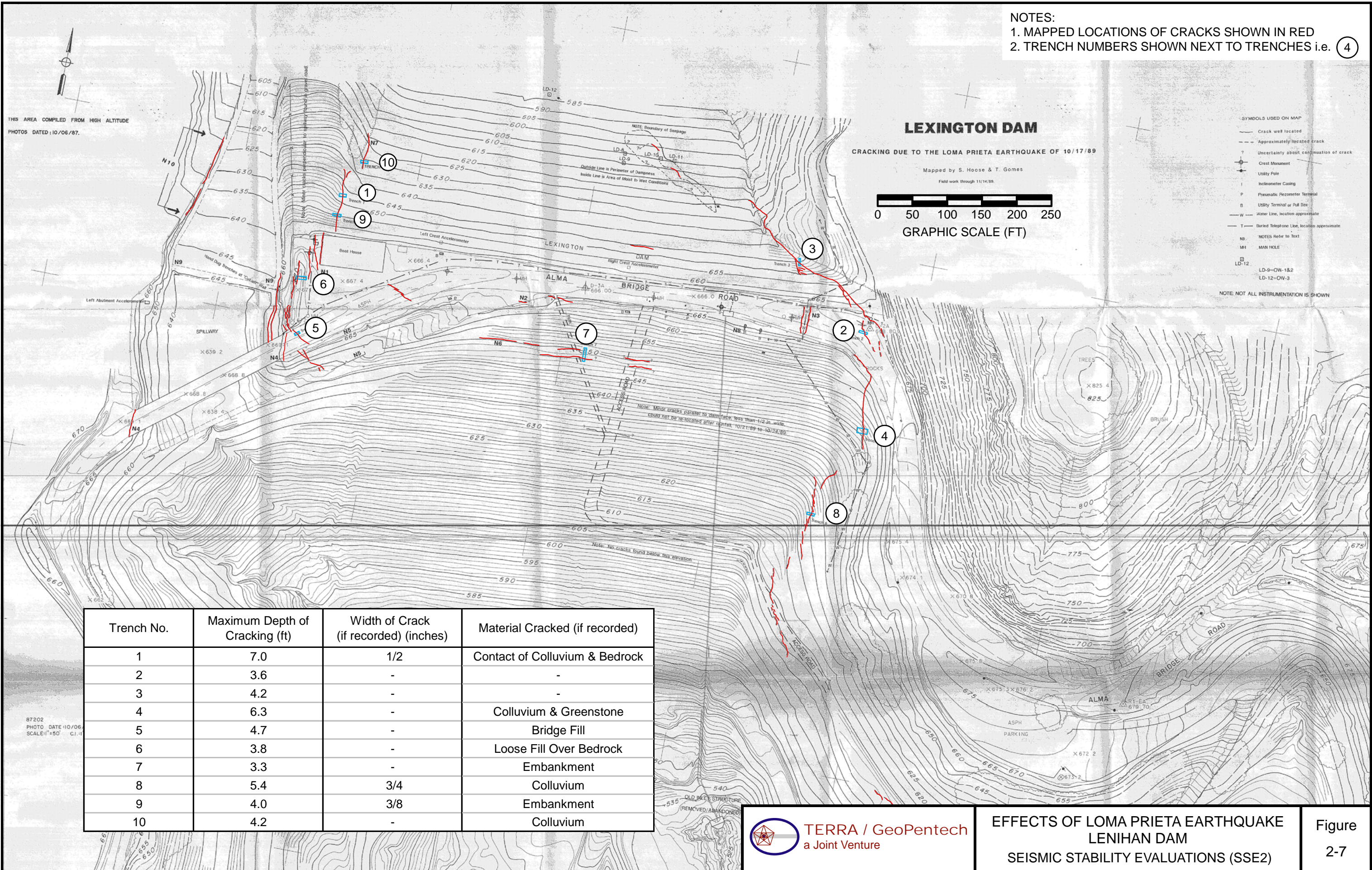


SECTION ALONG OUTLET PIPE  
(EXCERPTED FROM SECOND SUMMARY SURVEILLANCE REPORT, SCVWD (2007) )

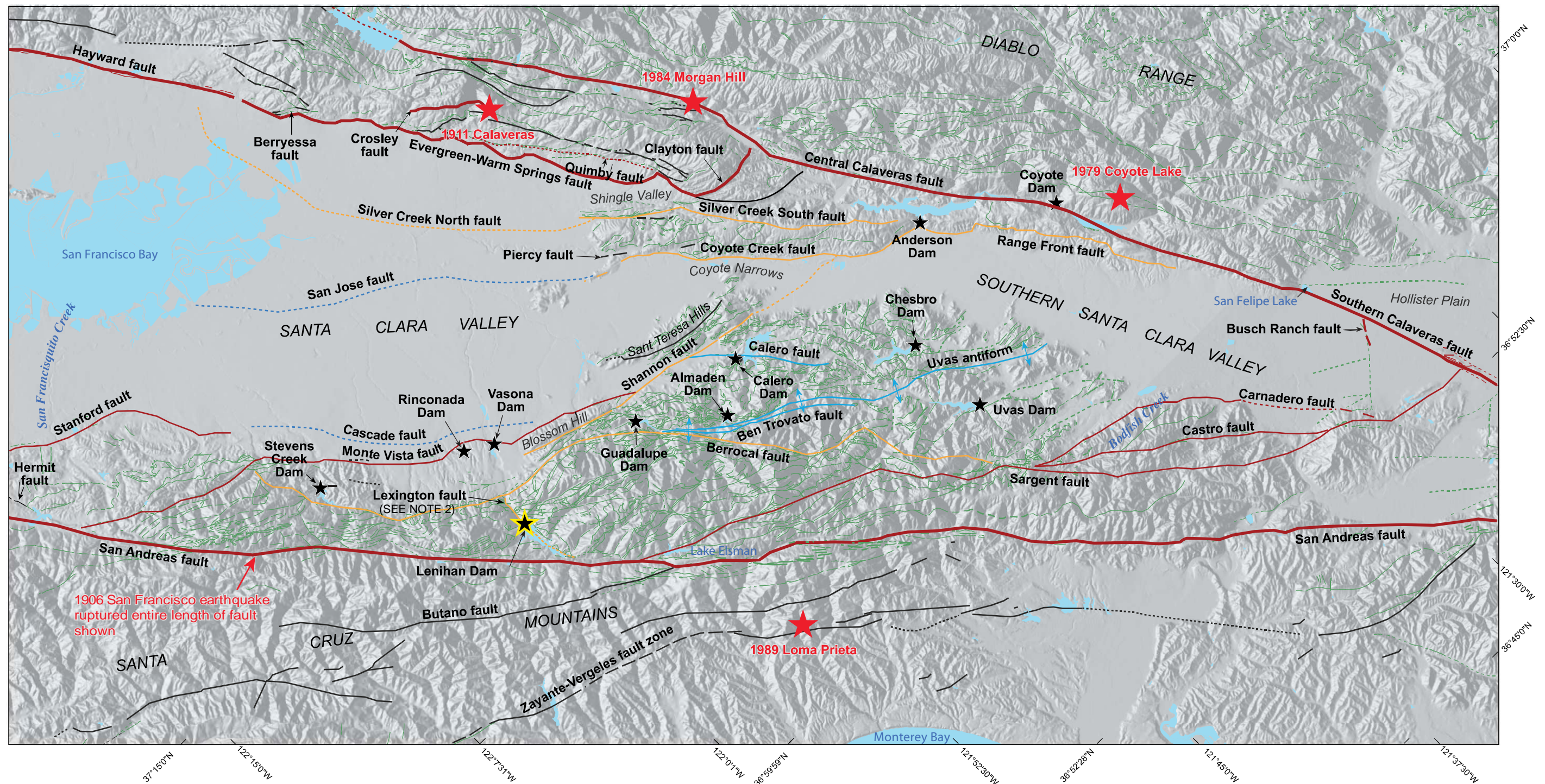


Rev. 1 03/28/2011 SSE2-WP-1LN










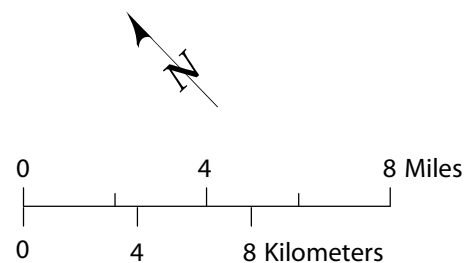






Explanation

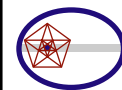
-  Active fault; dotted where concealed.  
 Conditionally Active fault; dotted where concealed  
 Other faults; dotted where concealed  
 Jennings (1992) detailed faults  
 Inactive Faults; dashed where inferred, dotted where concealed  
 SCVWD Dams  
 Historically significant earthquake



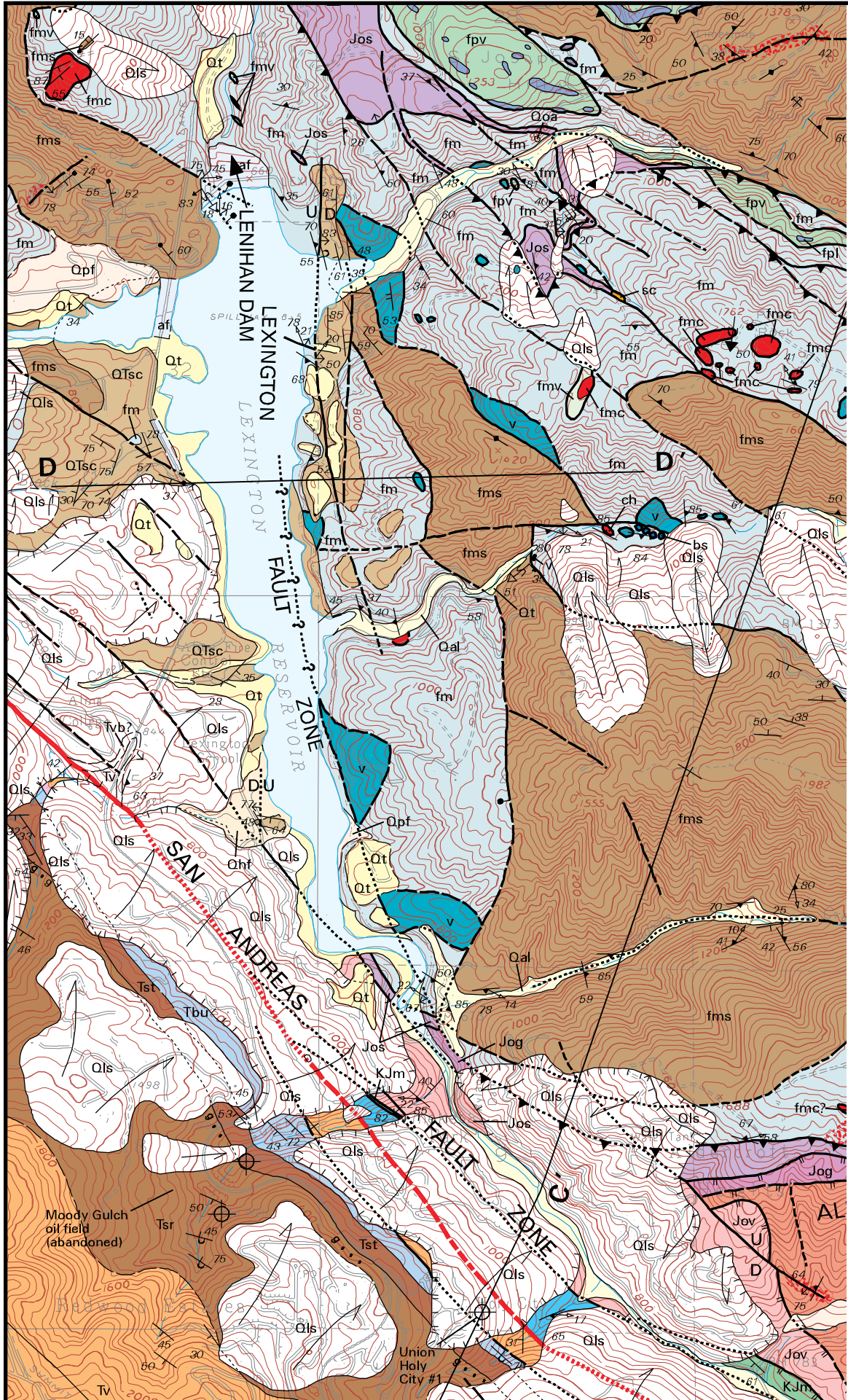
NOTES:  
1) FIGURE EXCERPTED FROM FINAL TECHNICAL MEMORANDUM  
BY WILLIAM LETTIS & ASSOCIATES, INC. (LETTIS, 2008)  
2) LEXINGTON FAULT RECENTLY ESTABLISHED AS INACTIVE BY  
DSOD (DSOD 2010b)

REGIONAL FAULT MAP  
LENIHAN DAM  
SEISMIC STABILITY EVALUATIONS (SSE2)

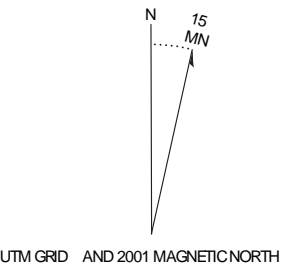
Figure  
3-1







QUATERNARY TO LATE TERTIARY UNITS	
md	Mine dump (Holocene)
gp	Gravel pit (Holocene)
pp	Percolation pond (Holocene)
af	Artificial fill (Holocene)
Qal	Alluvium, undivided (Holocene and Pleistocene)
Qls	Landslide deposits, undivided (Holocene and Pleistocene)
Qt	Alluvial terrace deposits, undivided (Holocene and Pleistocene)
Qhf	Alluvial fan deposits (Holocene)
Qhb	Basin deposits (Holocene)
Qhl	Levee deposits (Holocene)
Qhfp	Floodplain deposits (Holocene)
Qhc	Stream channel deposits (Holocene)
Qa	Aromas Sand (Pleistocene) - Locally divided into:
Qad	Dune deposits
Qaf	Fluvial deposits
Qof	Old floodplain deposits (Pleistocene?)
Qmt	Marine terrace deposits (Pleistocene)
Qoa	Old alluvium, undivided (Pleistocene)
Qpf	Alluvial fan deposits (Pleistocene)
QTf	Fluvial deposits, undivided (Pleistocene and Pliocene?)
QTsc	Santa Clara Formation (Pleistocene and Pliocene)



FROM:  
R.J. MCLAUGHLIN, J.C. CLARK, E.E. BRABB,  
E.J. HELLY, AND C.J. COLON - 2001

## EXPLANATION

### TERTIARY AND OLDER ROCK UNITS Northeast of San Andreas fault New Almaden Block

sc	Silica-carbonate rock (Miocene?)
Tus	Unnamed sandstone (middle Miocene or younger)
Tms	Monterey Shale (middle and lower Miocene)
Tt	Temblor Sandstone (middle Miocene to Oligocene?) - Locally includes:
Ttv	Volcanic and intrusive rocks (middle Miocene)
Jos	Serpentinized ultramafic rocks (Jurassic)

#### Franciscan Complex (Cretaceous and Jurassic) - Consists of:

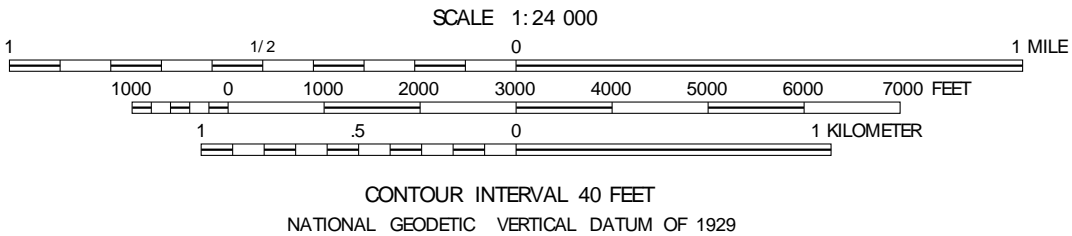
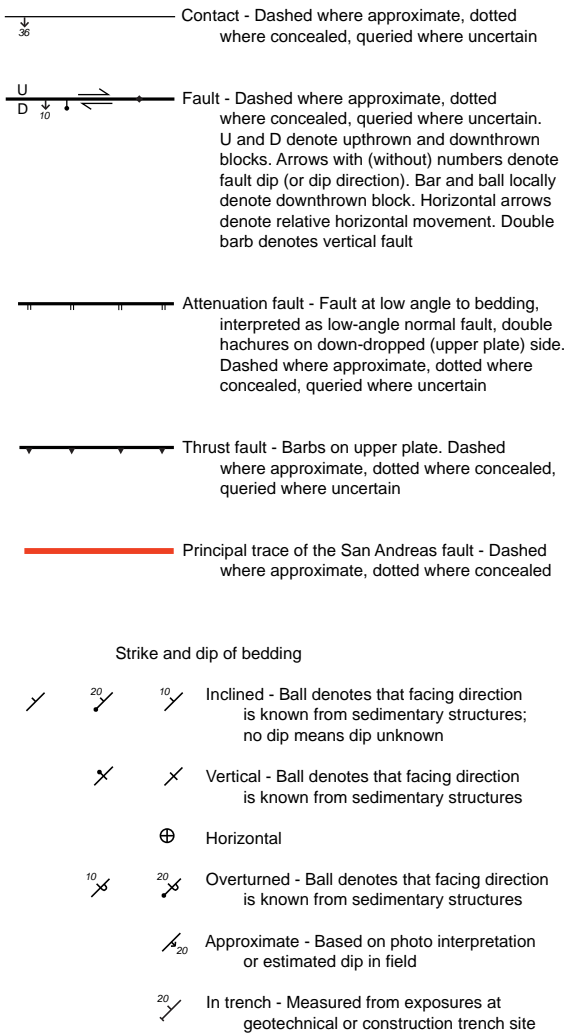
fm	Melange of the Central belt (Upper Cretaceous) - Includes:
bs	Blueschist blocks
am	Amphibolite blocks
ch	Chert blocks
v	Basaltic volcanic rock blocks
cg	Conglomerate block
mdi	Metadiorite block

#### Permanente terrane (Cretaceous) - Divided into:

fpl	Foraminiferal limestone (Upper and Lower Cretaceous)
fpv	Volcanic rocks (Lower Cretaceous)
fpt	Siliceous radiolarian-bearing tuff

#### Marin Headlands terrane (Cretaceous and Jurassic) - Divided into:

fms	Sandstone (Upper and (or) Lower Cretaceous)
fmc	Radiolarian chert (Lower Cretaceous and Jurassic)
fmv	Basaltic volcanic rocks (Lower Jurassic)



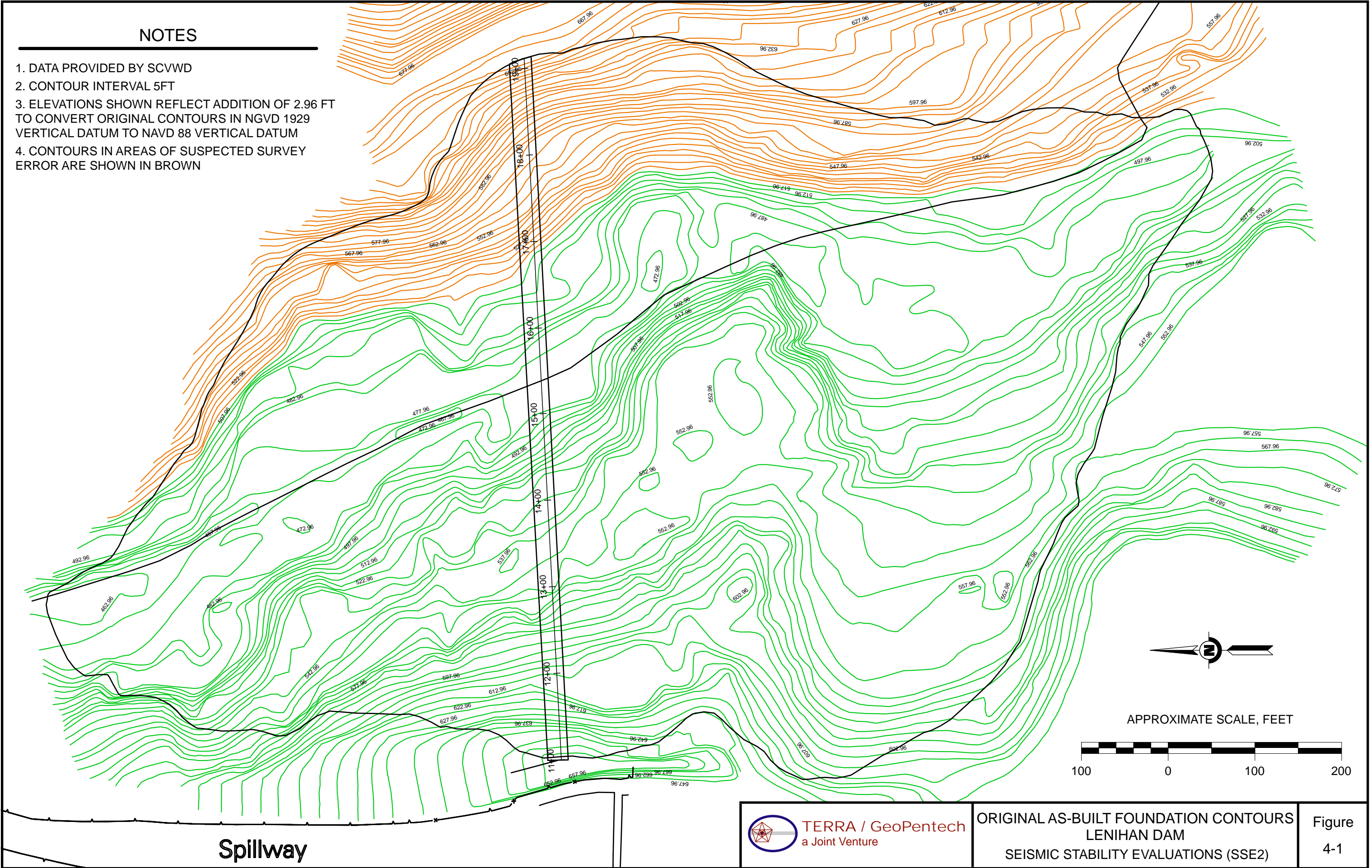
LOCAL REGION GEOLOGIC MAP  
LENIHAN DAM  
SEISMIC STABILITY EVALUATIONS (SSE2)

Figure  
3-2



NOTES

- 1. DATA PROVIDED BY SCVWD
- 2. CONTOUR INTERVAL 5FT
- 3. ELEVATIONS SHOWN REFLECT ADDITION OF 2.96 FT TO CONVERT ORIGINAL CONTOURS IN NGVD 1929 VERTICAL DATUM TO NAVD 88 VERTICAL DATUM
- 4. CONTOURS IN AREAS OF SUSPECTED SURVEY ERROR ARE SHOWN IN BROWN



Rev. 1 03/28/2011 SSE2-WP-1LN

Spillway



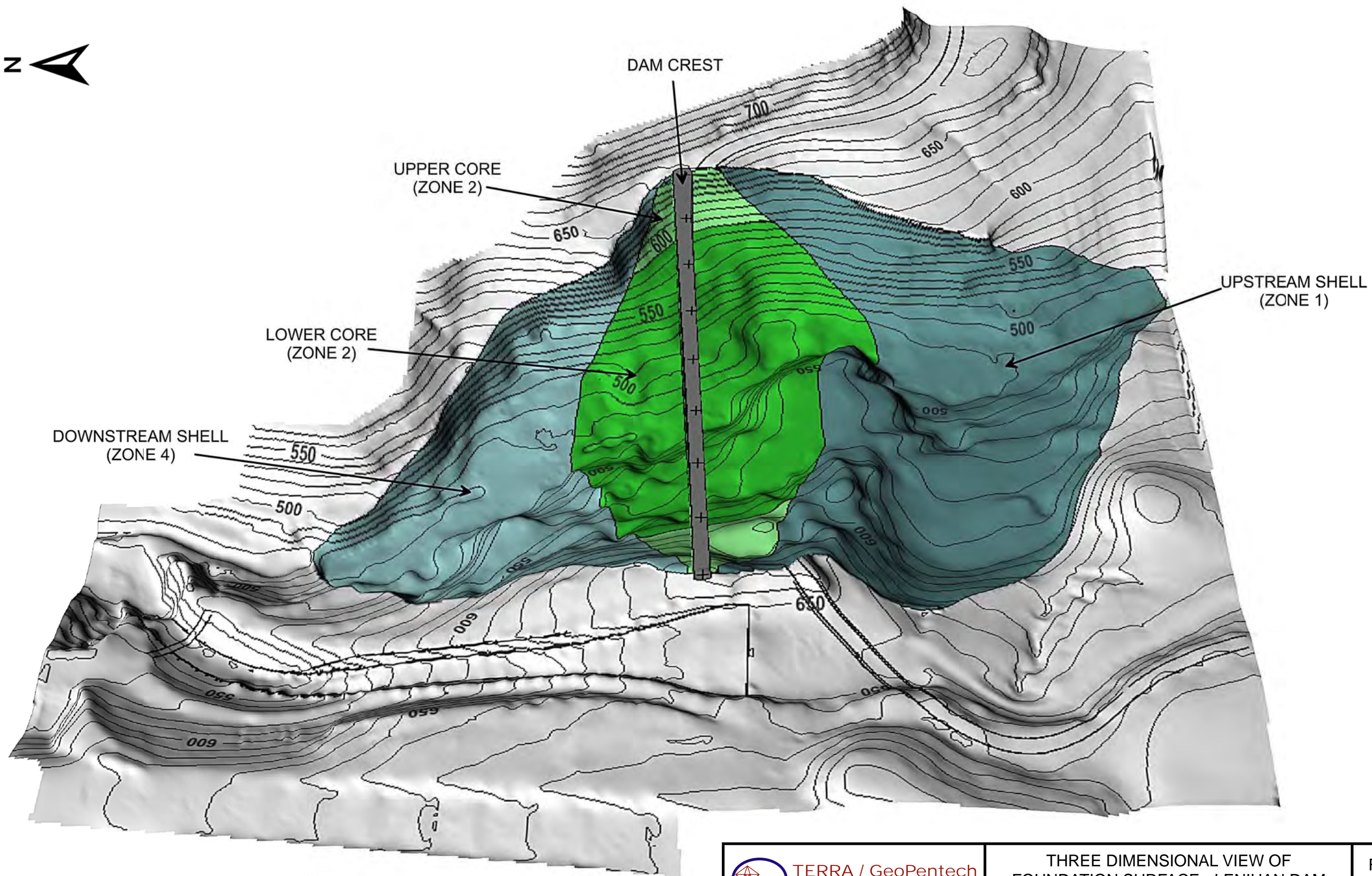
TERRA / GeoPentech  
a Joint Venture

ORIGINAL AS-BUILT FOUNDATION CONTOURS  
LENIHAN DAM  
SEISMIC STABILITY EVALUATIONS (SSE2)

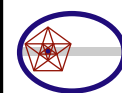
Figure  
4-1



0' 100' 200' 300' 400'



Note:  
1. Contacts of various dam zones with foundation surface are shown.



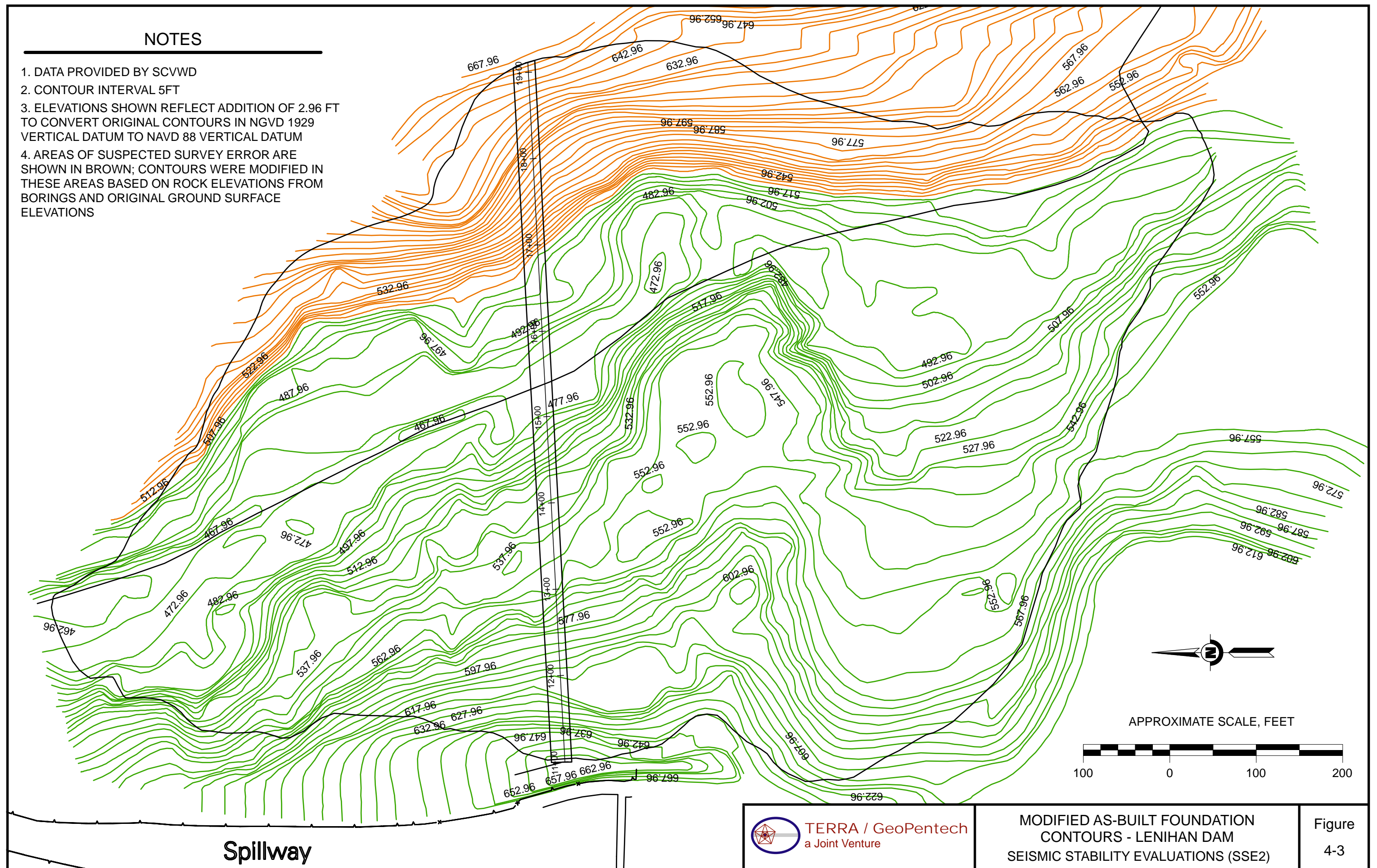
TERRA / GeoPentech  
a Joint Venture

THREE DIMENSIONAL VIEW OF  
FOUNDATION SURFACE - LENIHAN DAM  
SEISMIC STABILITY EVALUATIONS (SSE2)

Figure  
4-2

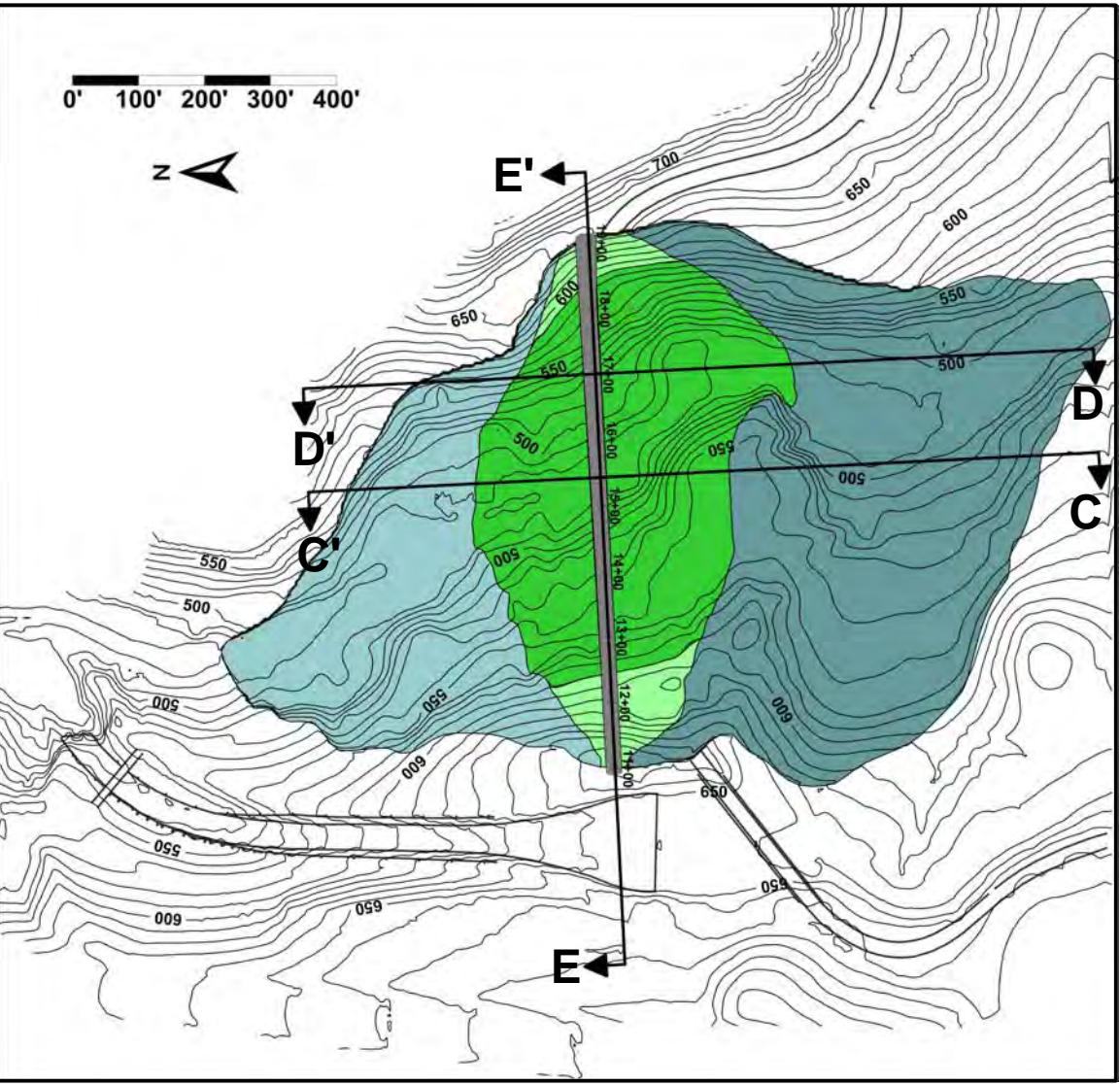


1. DATA PROVIDED BY SCVWD
2. CONTOUR INTERVAL 5FT
3. ELEVATIONS SHOWN REFLECT ADDITION OF 2.96 FT TO CONVERT ORIGINAL CONTOURS IN NGVD 1929 VERTICAL DATUM TO NAVD 88 VERTICAL DATUM
4. AREAS OF SUSPECTED SURVEY ERROR ARE SHOWN IN BROWN; CONTOURS WERE MODIFIED IN THESE AREAS BASED ON ROCK ELEVATIONS FROM BORINGS AND ORIGINAL GROUND SURFACE ELEVATIONS



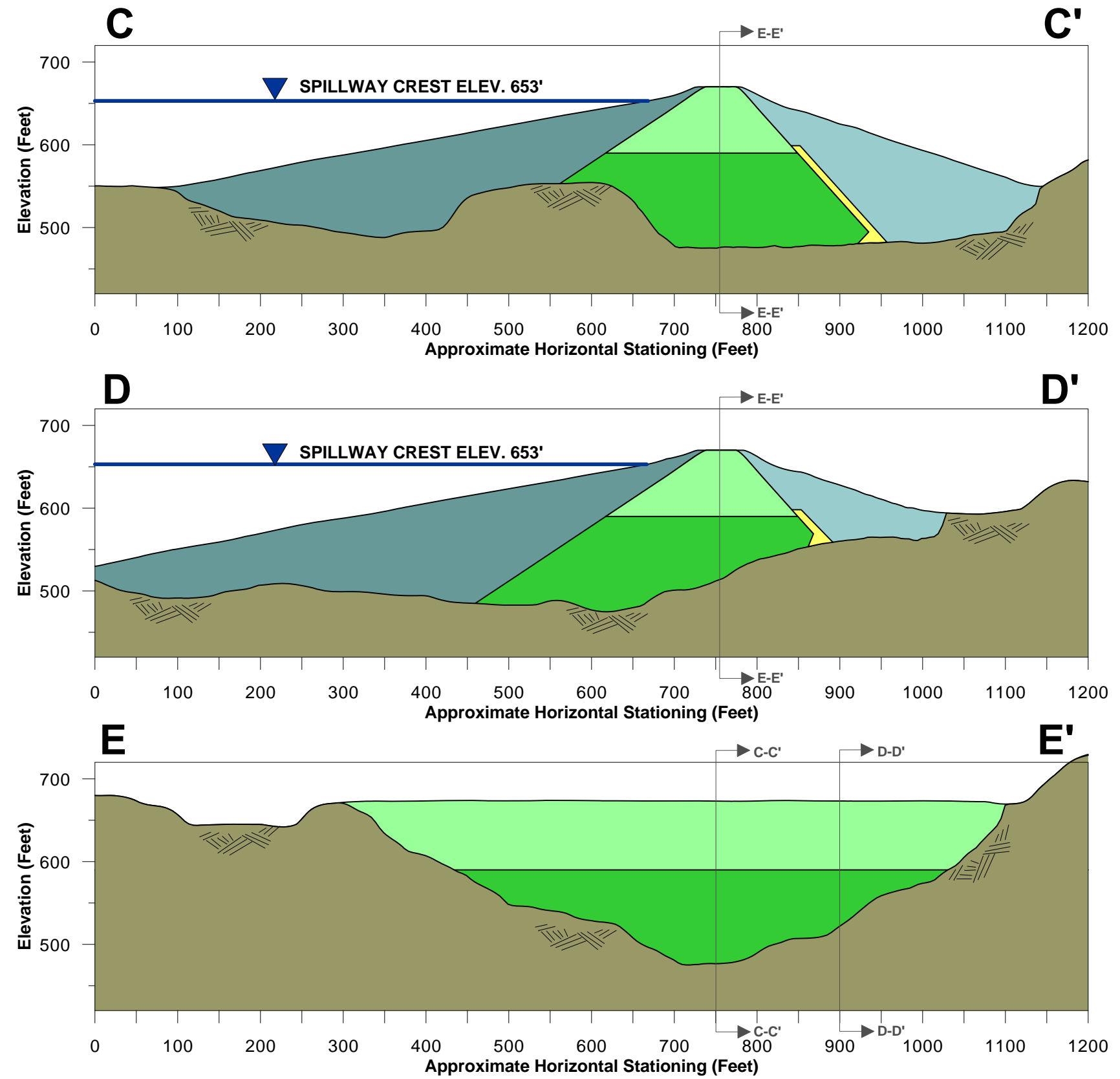


# CROSS SECTION LOCATION MAP

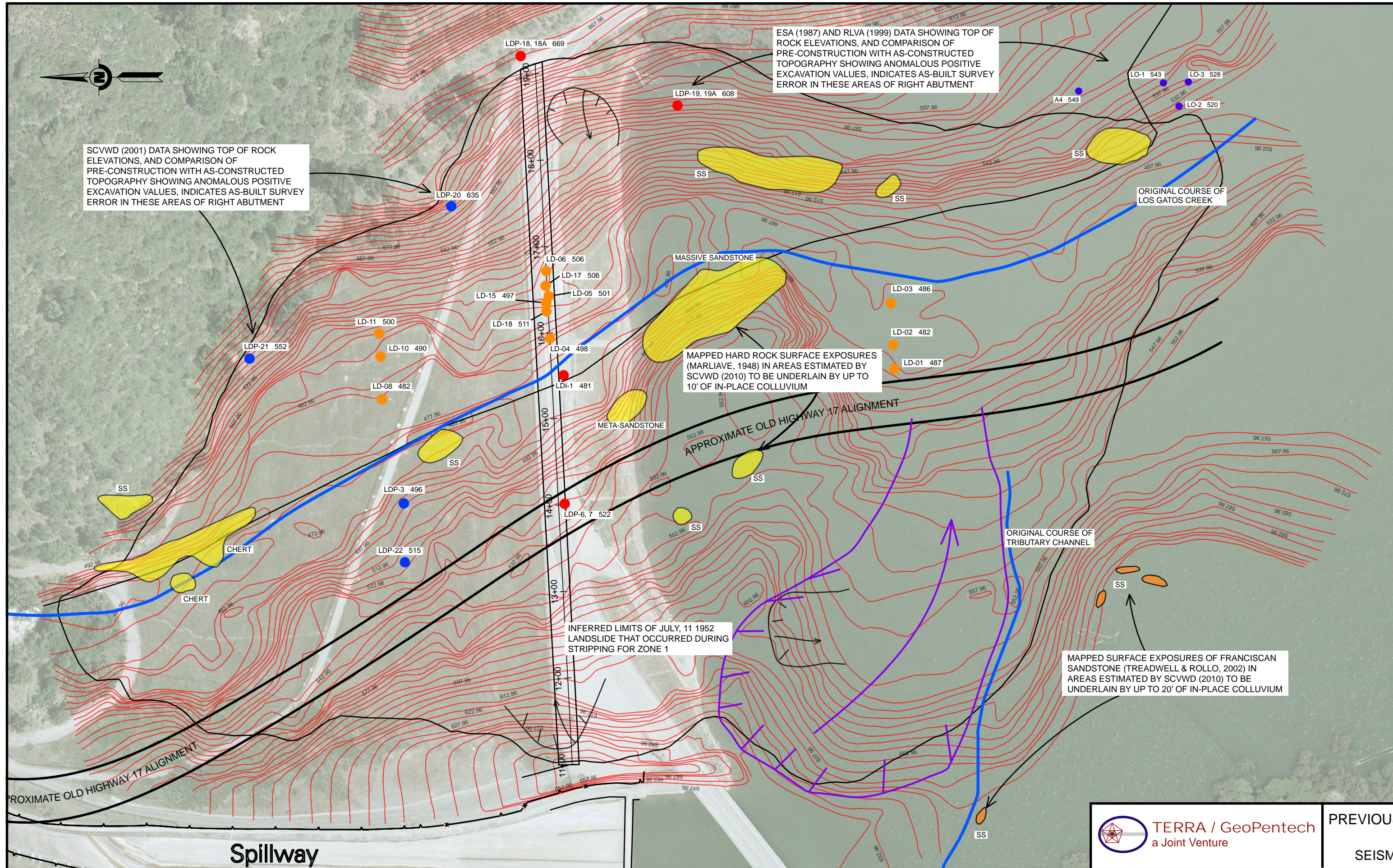


## LEGEND

- Upstream Shell (Zone 1)
- Lower Core (Zone 2, Below El. 590)
- Upper Core (Zone 2, Above El. 590)
- Drain Zone (Zone 3)
- Downstream Shell (Zone 4)
- Franciscan Complex Bedrock







## EXPLANATION

BORINGS FROM PREVIOUS INVESTIGATIONS AND CURRENT INSTRUMENTATION (WITH ELEVATION OF TOP OF ROCK INDICATED):

- WAHLER 1982 BORINGS
- ESA 1987 BORINGS
- VOLPE 1999 BORINGS
- DISTRICT 2001 BORINGS

● HARD ROCK OUTCROP (MOSTLY FRANCISCAN SANDSTONE) MAPPED IN DAMSITE AREA PRIOR TO CONSTRUCTION (MARLIVAE, 1948)

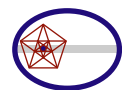
▲ LANDSLIDE MAPPED PRIOR TO CONSTRUCTION (MARLIVAE, 1948)

— AS-BUILT FOUNDATION ELEVATION CONTOUR (FROM AS-CONSTRUCTED GENERAL PLAN-SCVWD 1955; CORRECTED TO 1988 NAVD)

APPROXIMATE SCALE, FEET



- NOTES:
- 1) ONLY THOSE BORINGS THAT WERE EXTENDED INTO THE FOUNDATION ARE DEPICTED.
  - 2) BORING LOCATIONS FROM WAHLER 1982, RLVA 1999, SCVWD 2001 EXPLORATION PLANS, AND SCVWD 2010 SURVEILLANCE REPORT
  - 3) REFER TO SECTION 4.0 FOR DISCUSSION OF INFERRED FOUNDATION CONDITIONS AND COMPARISON WITH SCVWD 2010 FOUNDATION ANALYSIS REPORT.

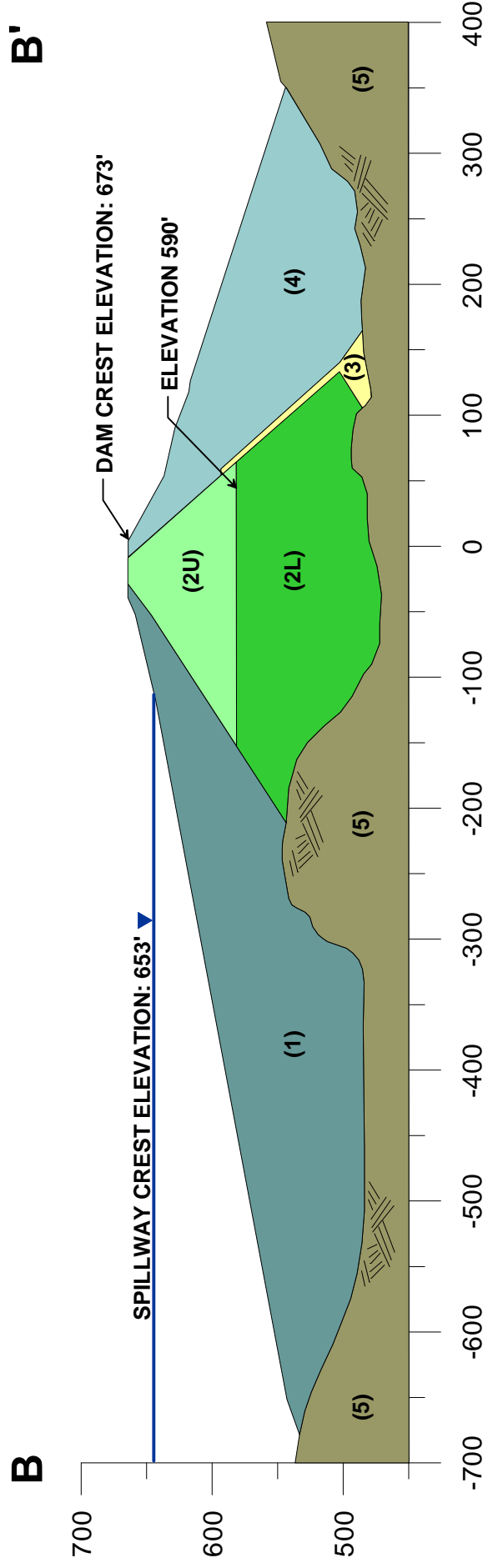


**TERRA / GeoPentech**  
a Joint Venture

PREVIOUS FOUNDATION EXPLORATION DATA  
LENIHAN DAM  
SEISMIC STABILITY EVALUATIONS (SSE2)

Figure  
4-5





Zone	Color Code	Material Description	Predominant Soil Classification
1		Upstream Shell	Gravely Clayey Sands (SC) to Sandy Clays (CL)
2U		Upper Core (Above El. 590)	Gravely Clayey Sands (SC) to Clayey Gravels (GC)
2L		Lower Core (Below El. 590)	Sandy Highly Plastic Clays (CH) to Silty Sands-Sandy Highly Plastic Silts (SM/MH)
3		Drain	N/A
4		Downstream Shell	Gravely Clayey Sands (SC) to Clayey Gravels (GC)
5		Bedrock	Franciscan Complex

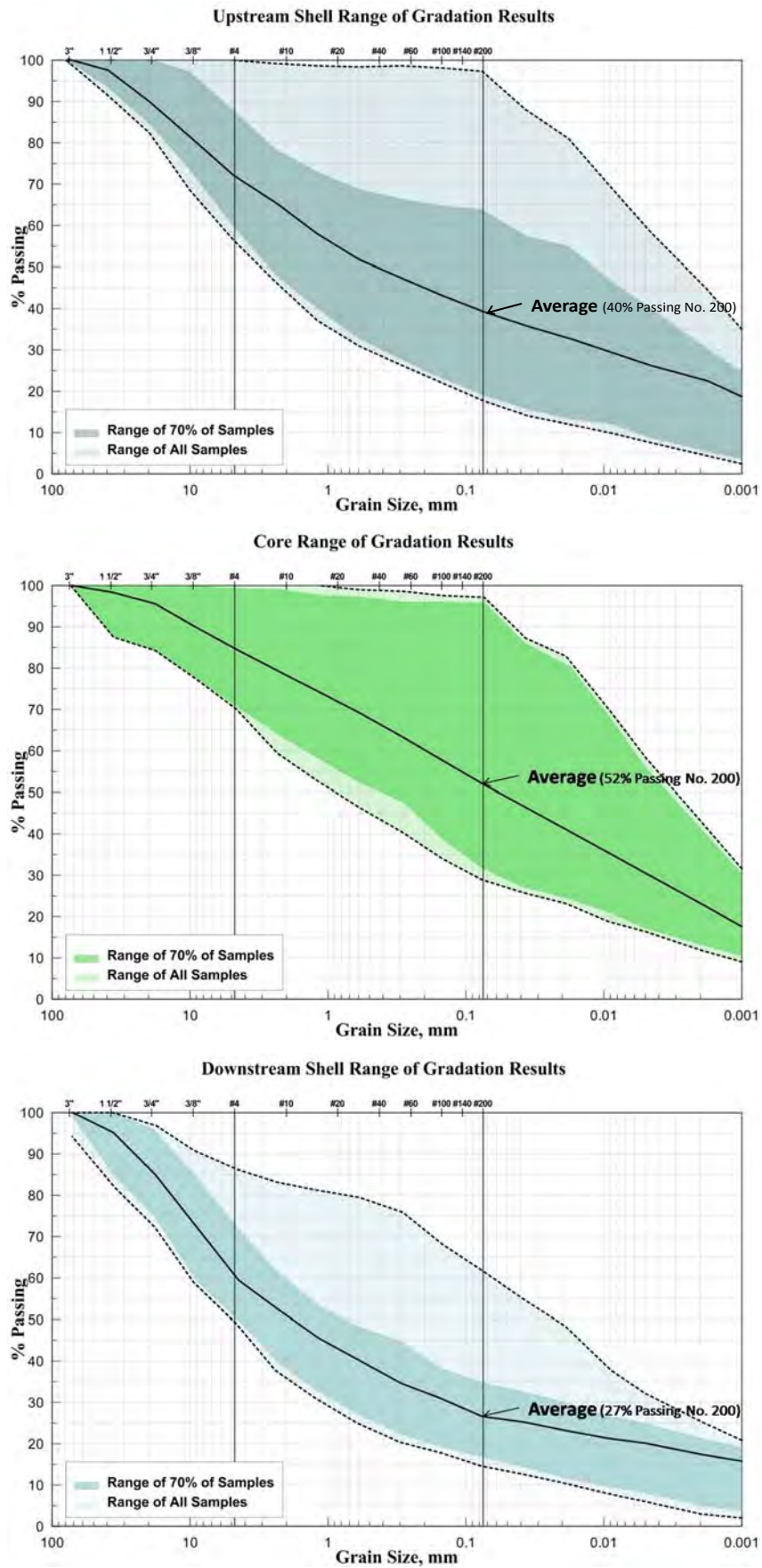
Note: See Figure 2-2A for location of section B-B', see Figure 2-3 for piezometric data.



MAXIMUM CROSS SECTION B-B'  
LENIHAN DAM  
SEISMIC STABILITY EVALUATIONS (SSE2)

Figure  
5-1

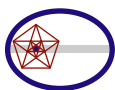
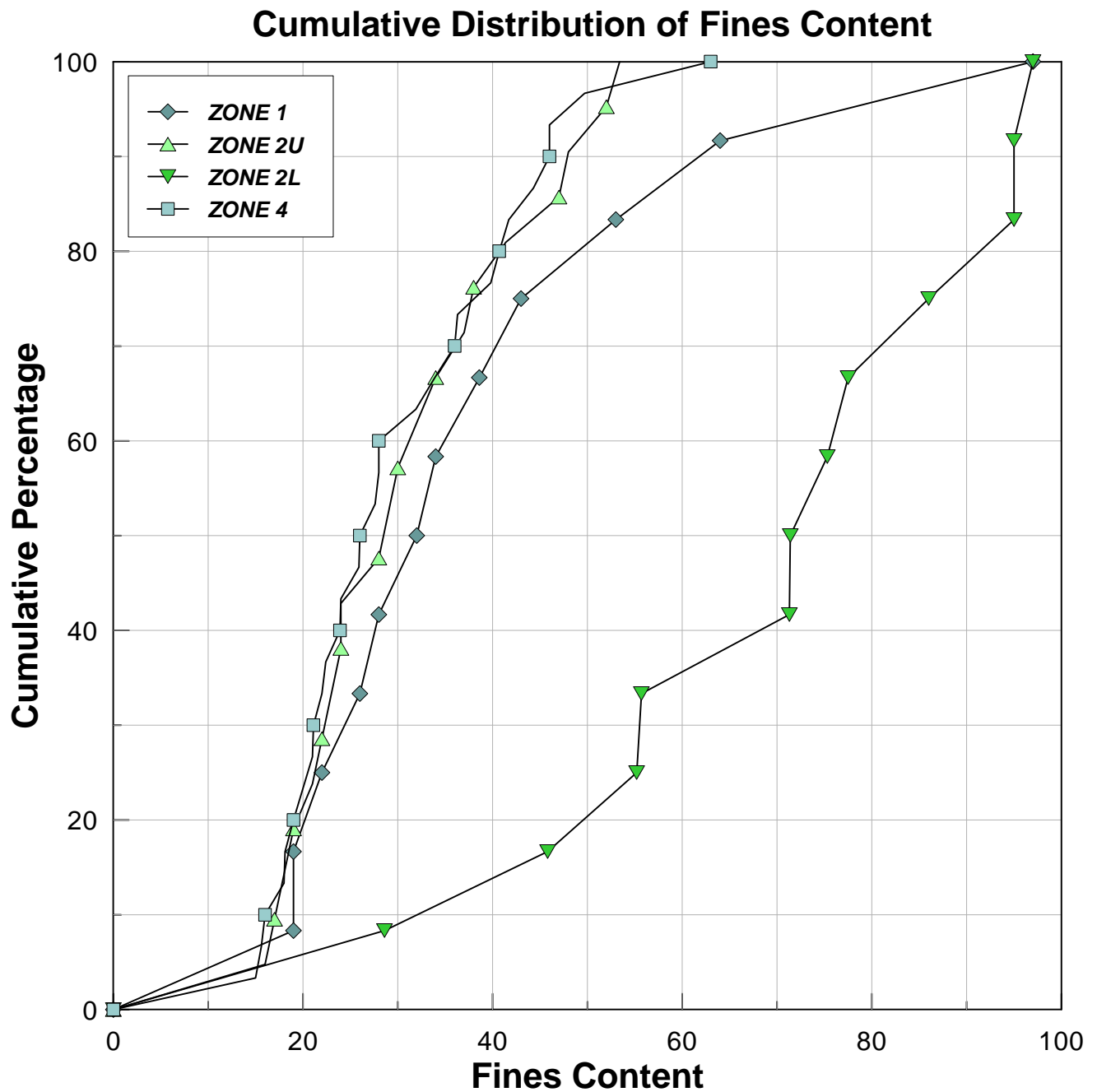


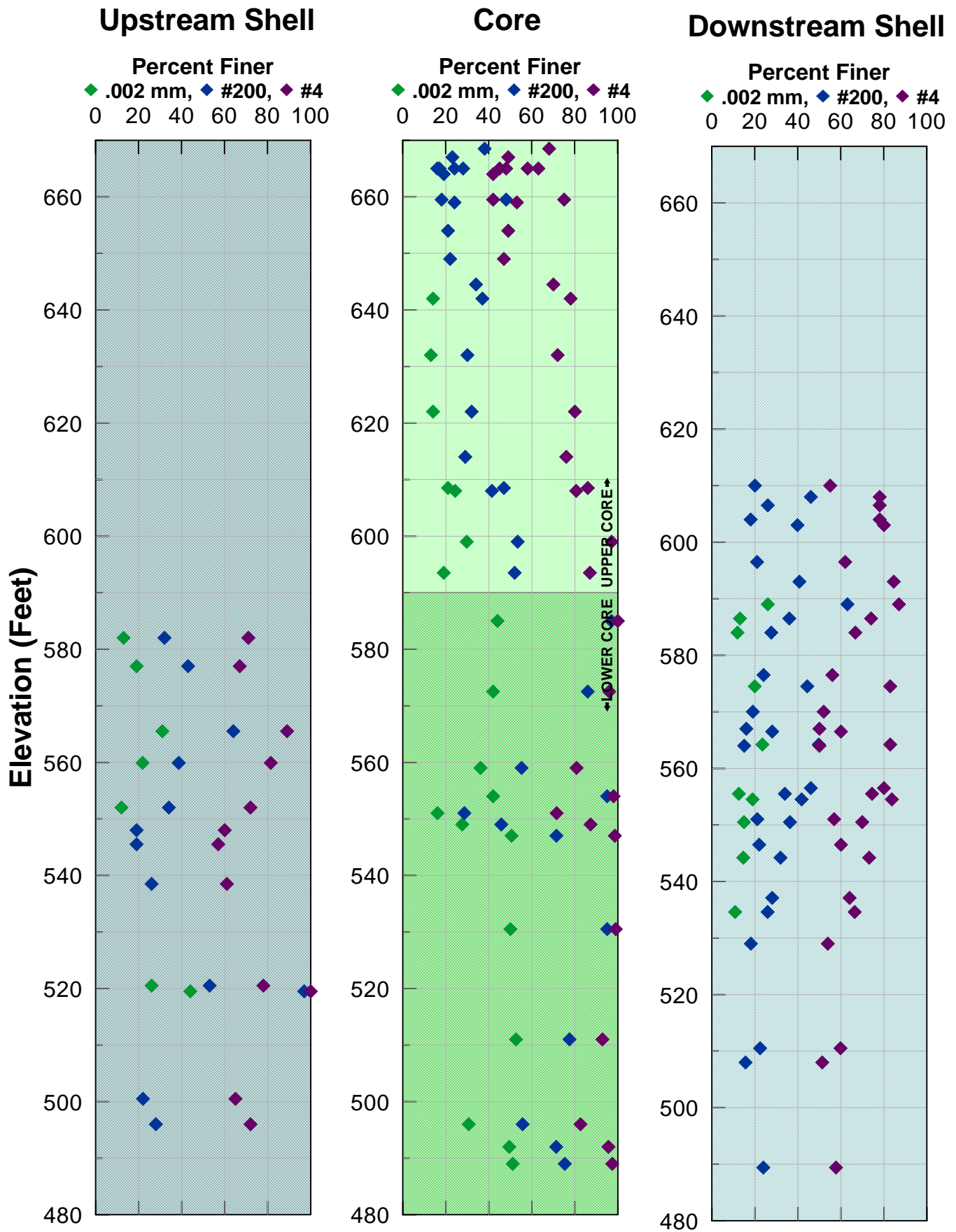


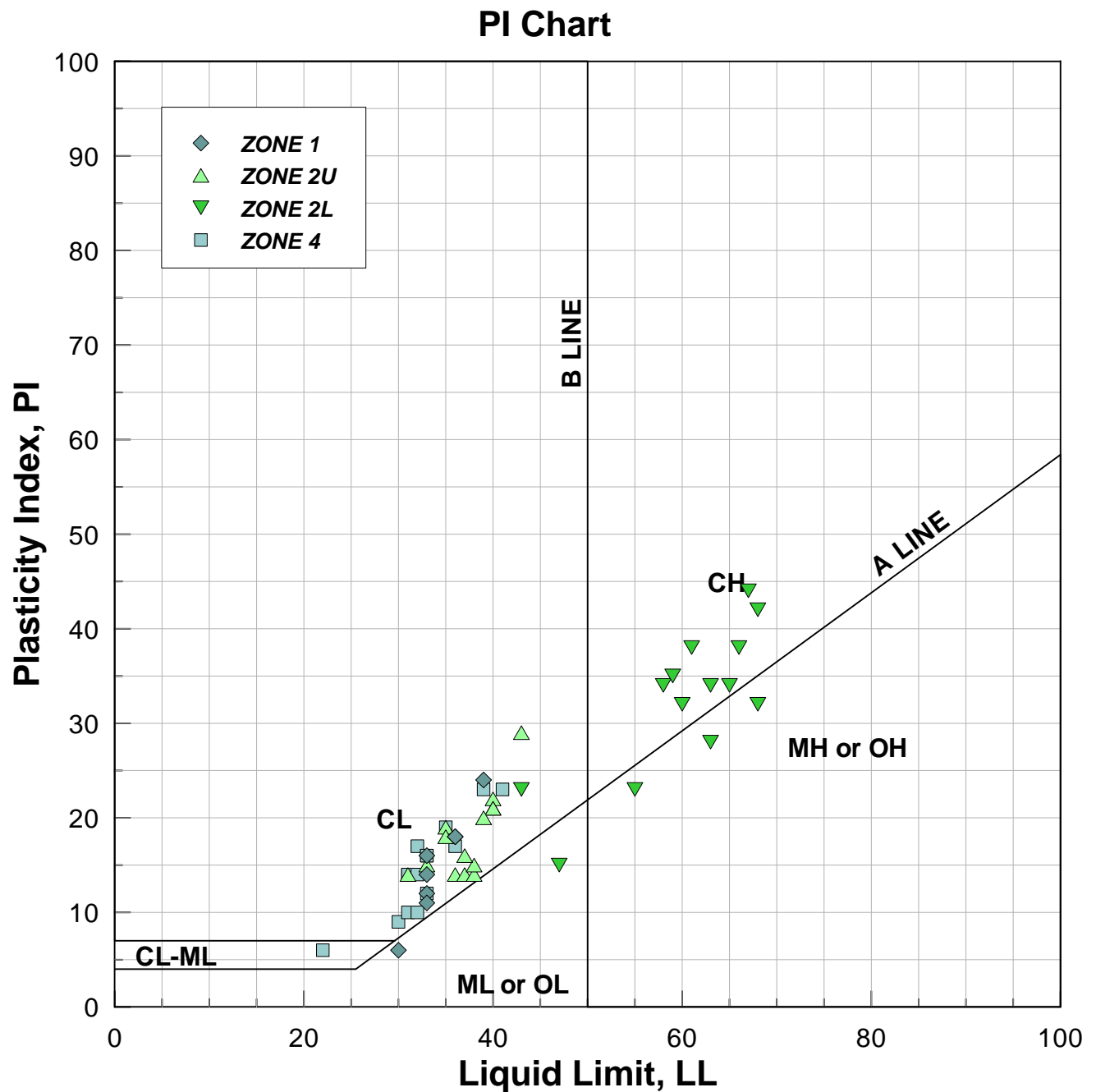
**TERRA / GeoPentech**  
a Joint Venture

**GRADATION RANGES  
LENIHAN DAM  
SEISMIC STABILITY EVALUATIONS (SSE2)**

**Figure  
5-2**



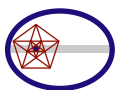
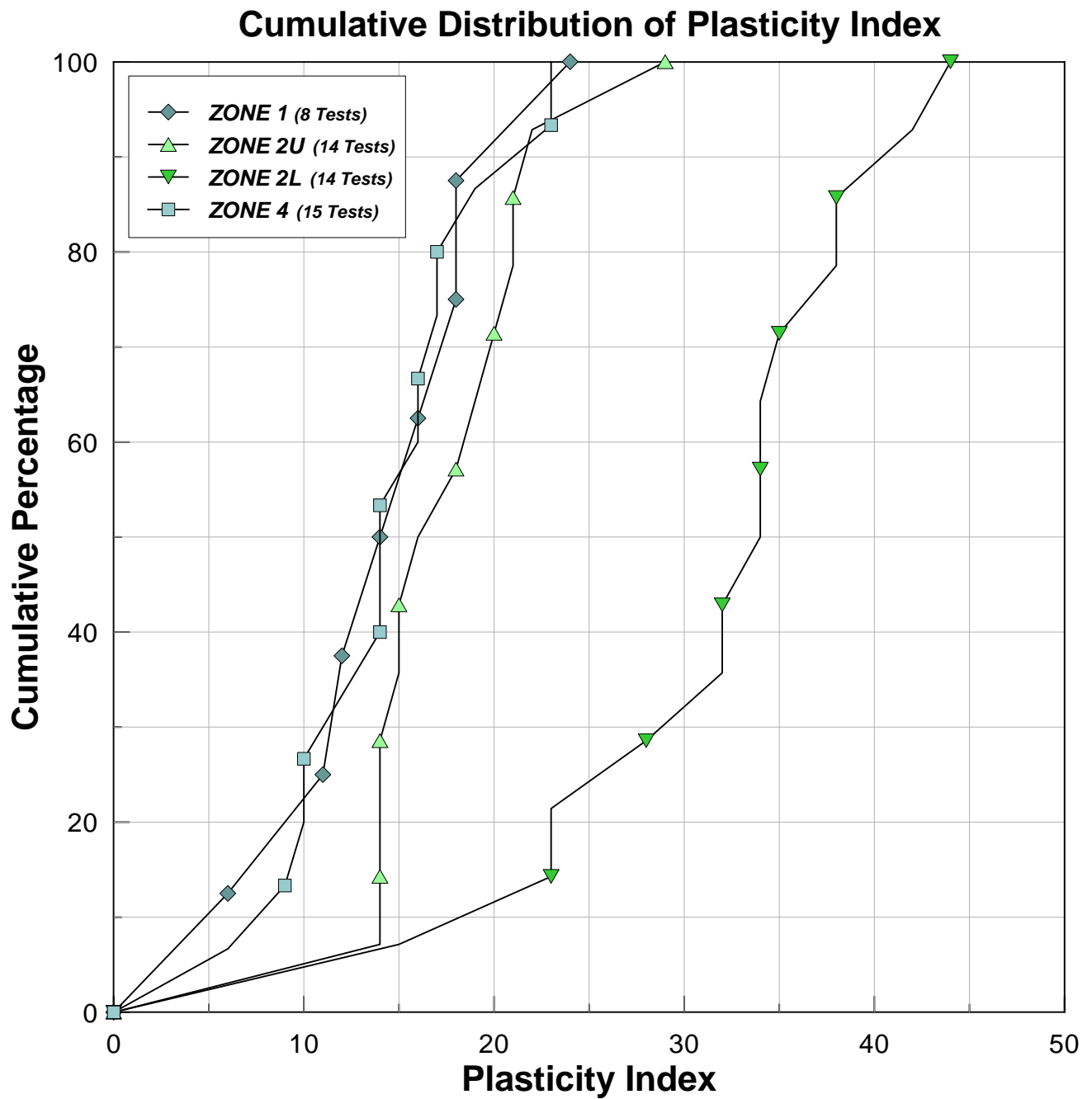




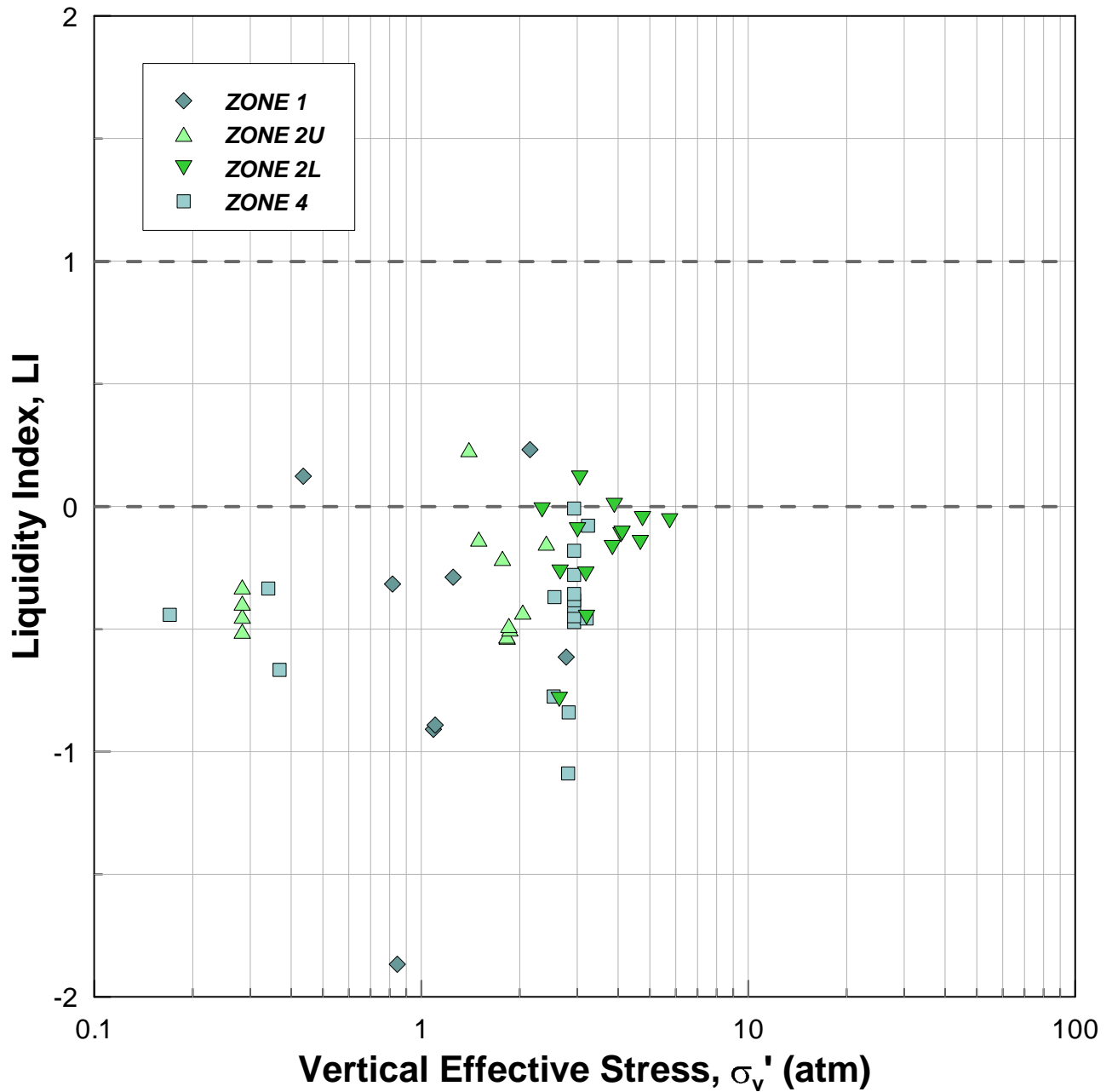
**SUMMARY OF ATTERBERG LIMITS TEST RESULTS**

Zone	Material	Material Description	No. Tests	Range of LL	Median LL	Range of PI	Median PI
1	Upstream Shell	SC-CL	8	30 to 39	33	6 to 24	15
2U	Upper Core	SC-GC-SM-CL	13	31 to 43	38	14 to 29	17
2L	Lower Core	CH-CL-MH-SM-CL	14	43 to 68	62	15 to 44	34
4	Downstream Shell	SC-GC-SP-CL-GM	17	22 to 41	32	6 to 23	14





## Liquidity Chart

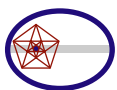
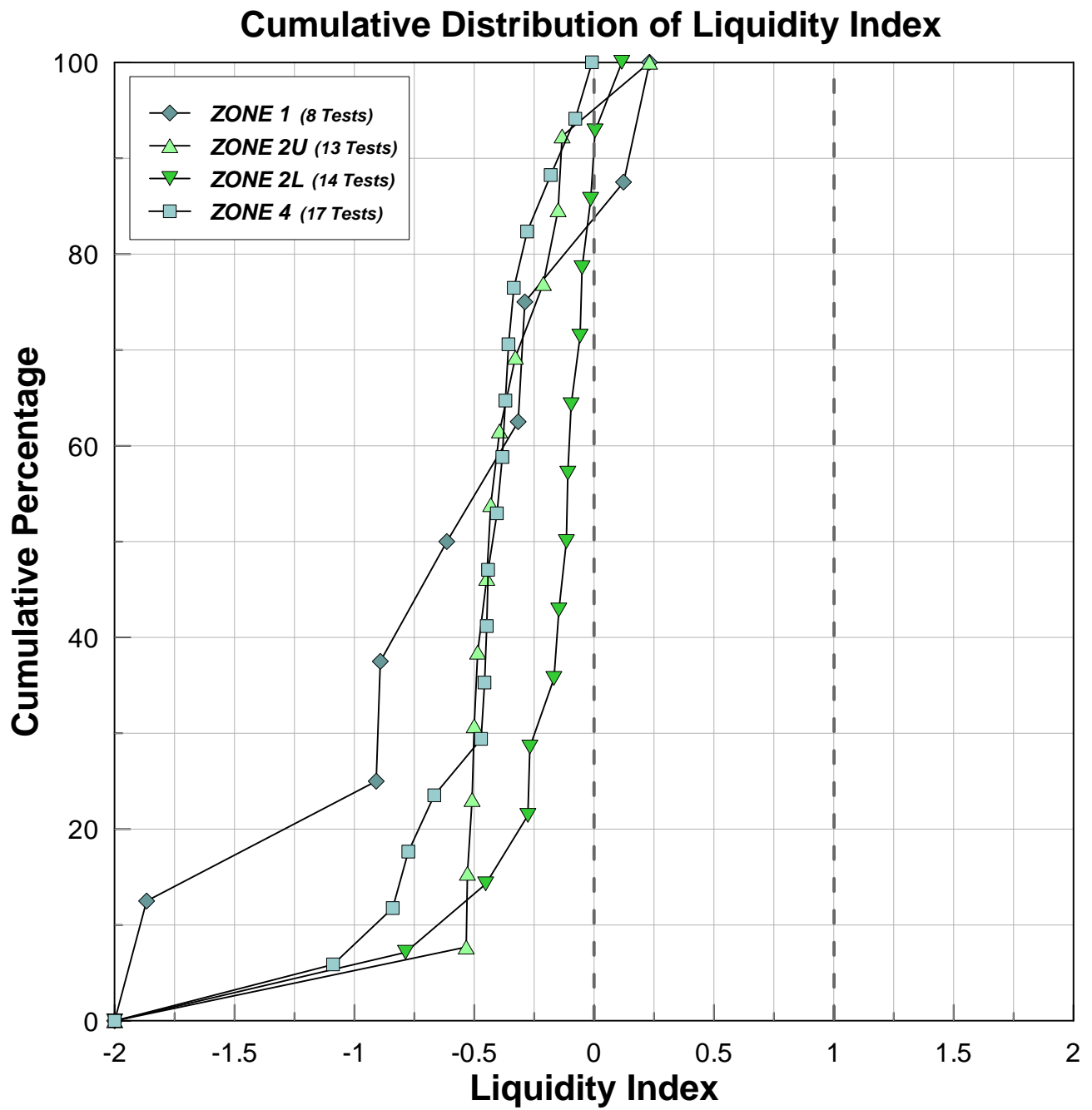


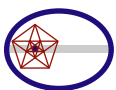
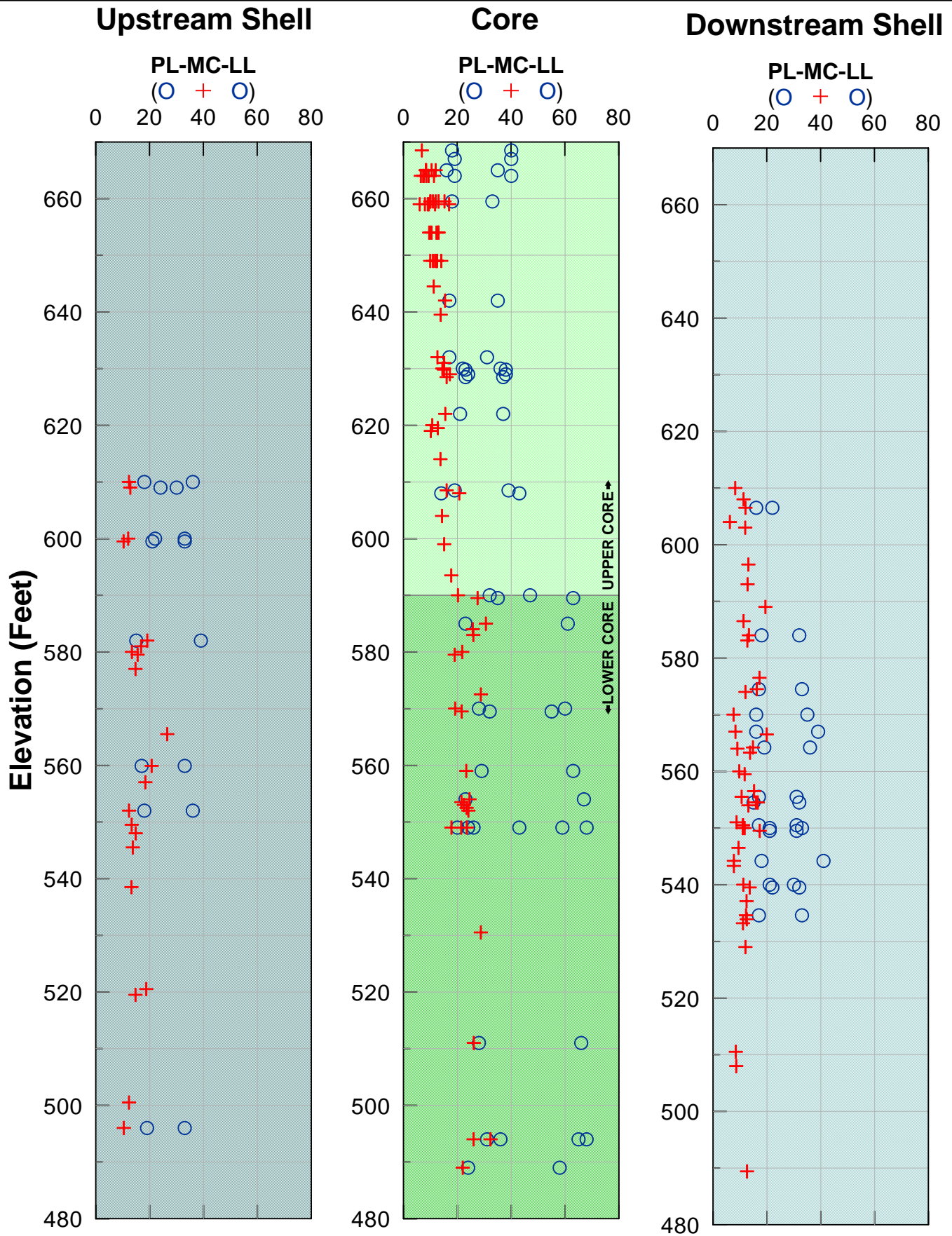
### SUMMARY OF LIQUIDITY INDEX TEST RESULTS

Zone	Material	Material Description	No. Tests	Range of LI	Median LI
1	Upstream Shell	SC-CL	8	-1.87 to 0.23	-0.47
2U	Upper Core	SC-GC-SM-CL	13	-0.53 to 0.23	-0.43
2L	Lower Core	CH-CL-MH-SM-CL	14	-0.79 to 0.12	-0.11
4	Downstream Shell	SC-GC-SP-CL-GM	17	-1.09 to -0.01	-0.41

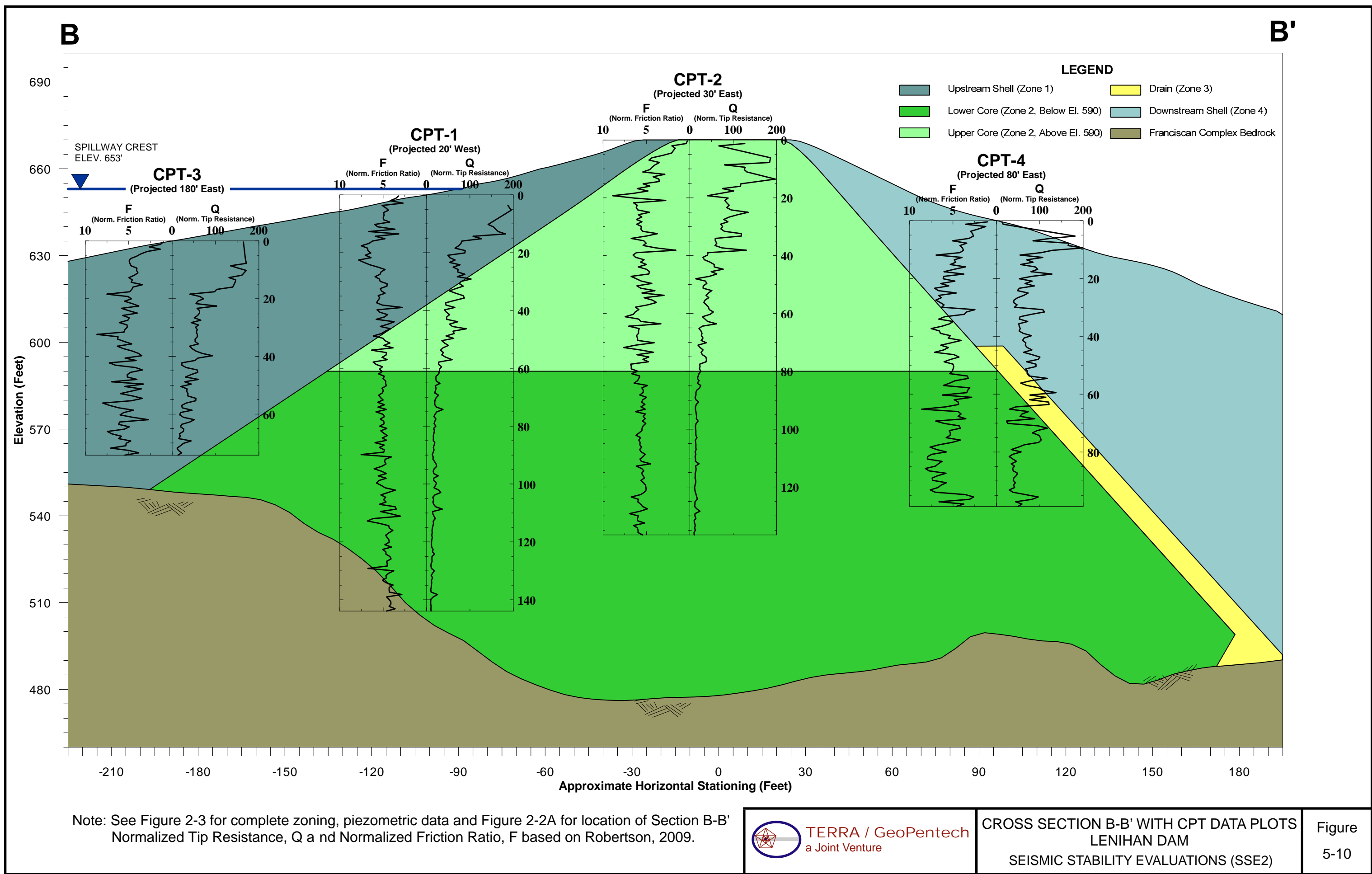






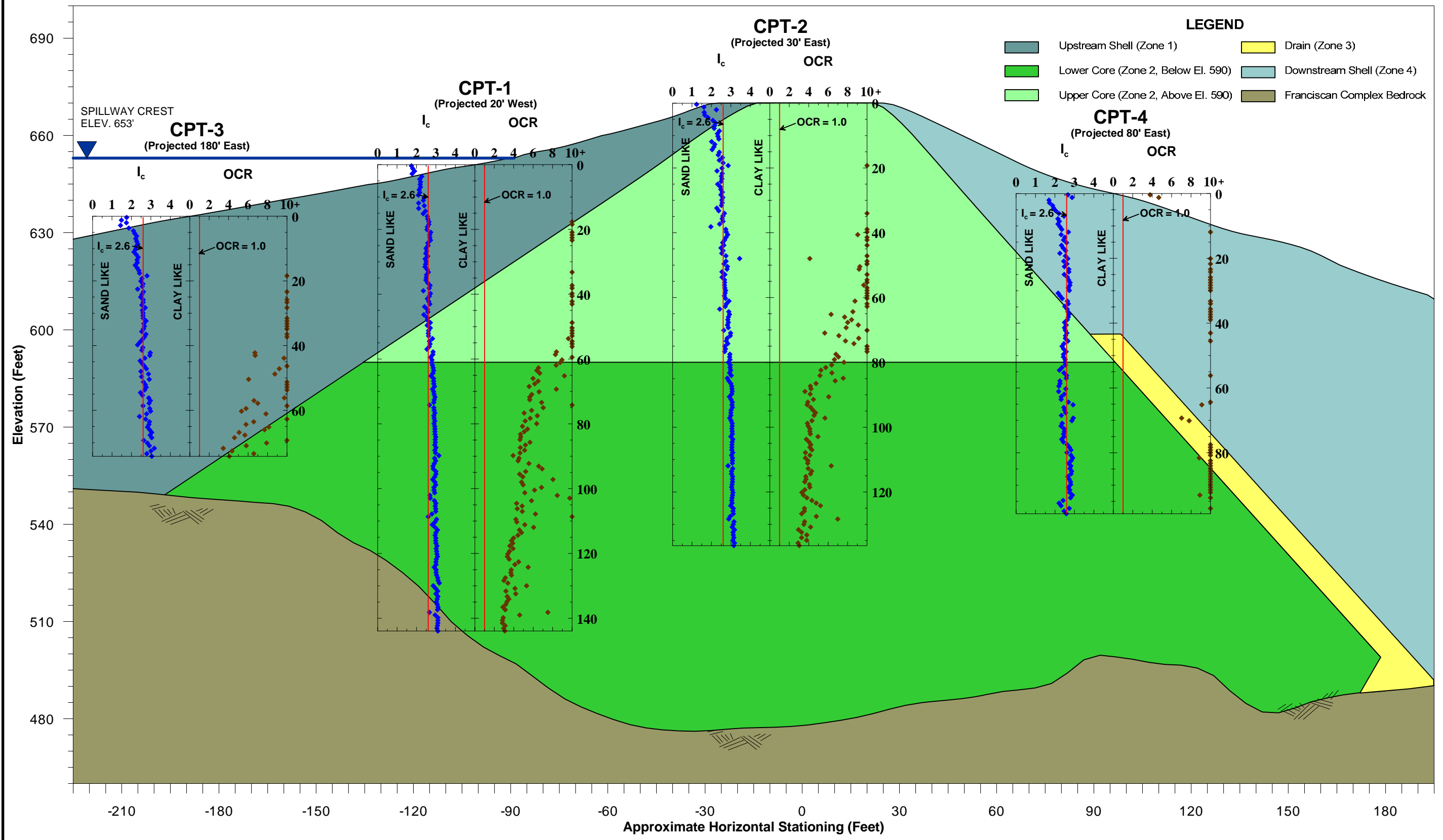


Rev. 2 03/28/2011 SSE2-WP-1LN



B

B'



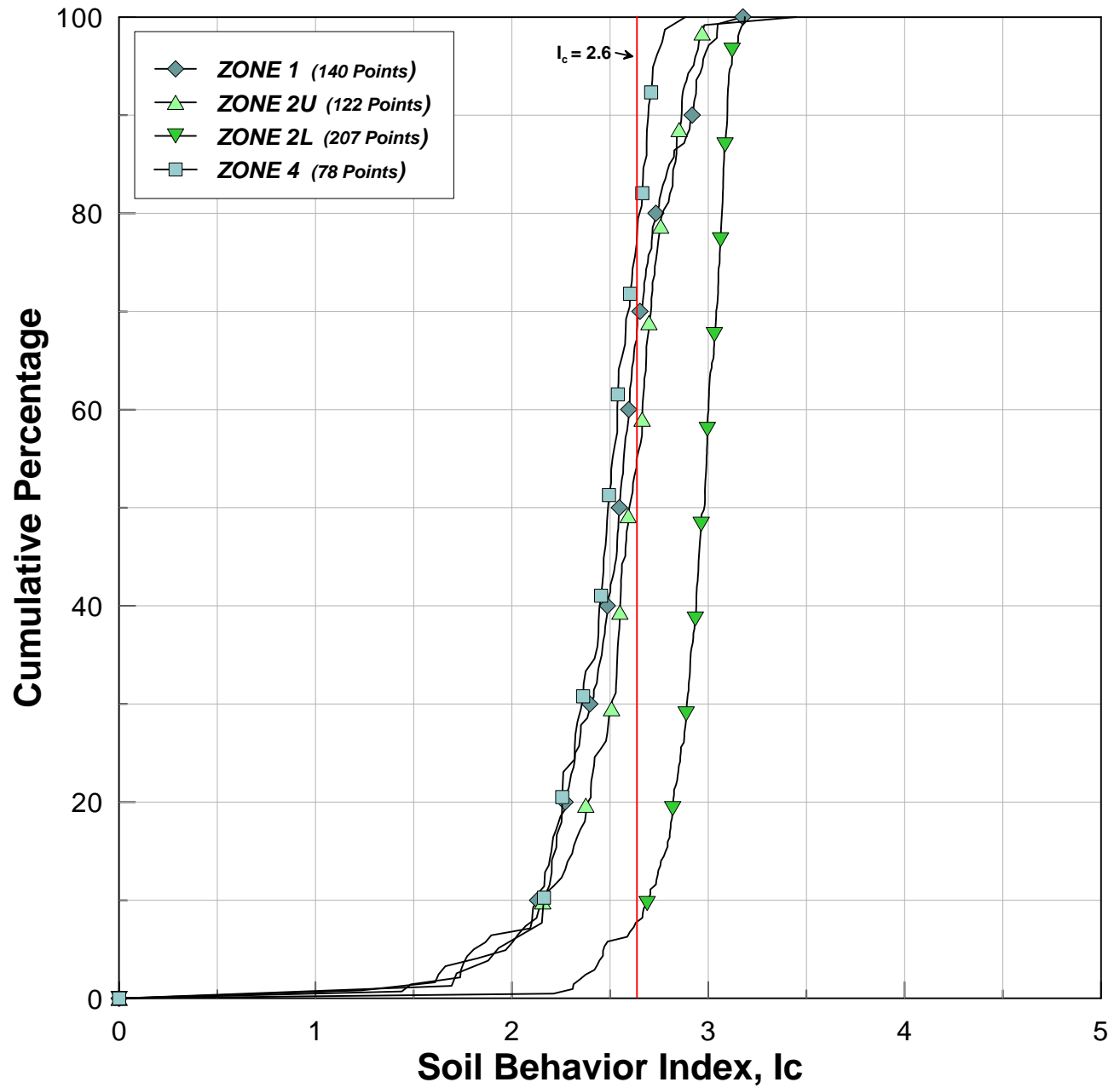
Note: See Figure 2-3 for complete zoning, piezometric data and Figure 2-2A for location of Section B-B'  
Soil Behavior Type Index,  $I_c$  and Inferred OCR based on Robertson, 2009.



CROSS SECTION B-B' WITH  
CPT INTERPRETATIONS - LENIHAN DAM  
SEISMIC STABILITY EVALUATIONS (SSE2)

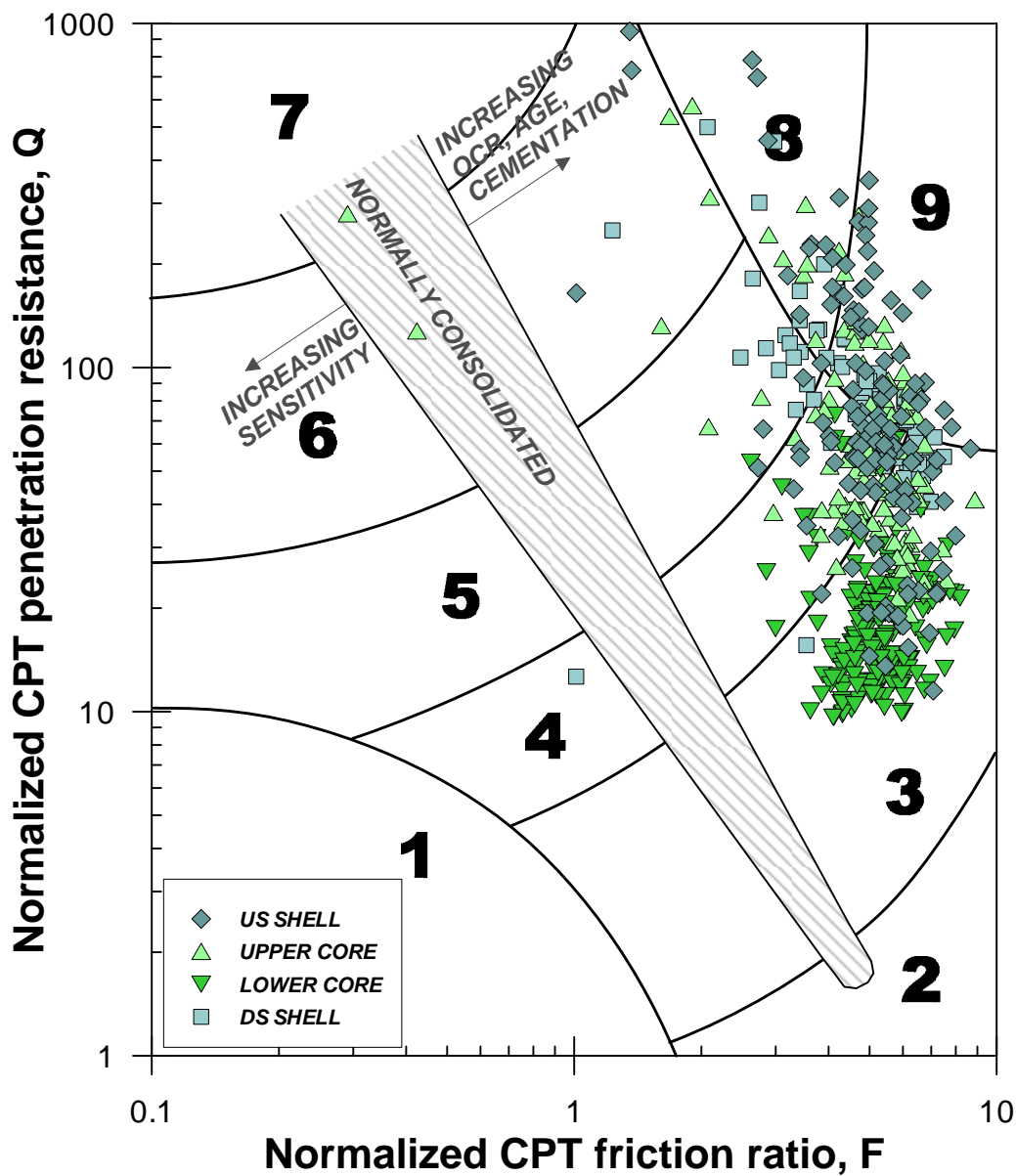
Figure  
5-11

## Cumulative Distribution of Soil Behavior Index, $I_c$



Zone	Soil Behavior Type	$I_c$
1	Sensitive, fine grained	N/A
2	Organic soils – peats	> 3.6
3	Clays – silty clay to clay	2.95 – 3.6
4	Silt mixtures – clayey silt to silty clay	2.60 – 2.95
5	Sand mixtures – silty sand to sandy silt	2.05 – 2.6
6	Sands – clean sand to silty sand	1.31 – 2.05
7	Gravelly sand to dense sand	< 1.31
8	Very stiff sand to clayey sand*	N/A
9	Very stiff, fine grained*	N/A

\* Heavily overconsolidated or cemented



Notes: Soil Behavior Type Index Chart based on Robertson (2009)



**TERRA / GeoPentech**  
a Joint Venture

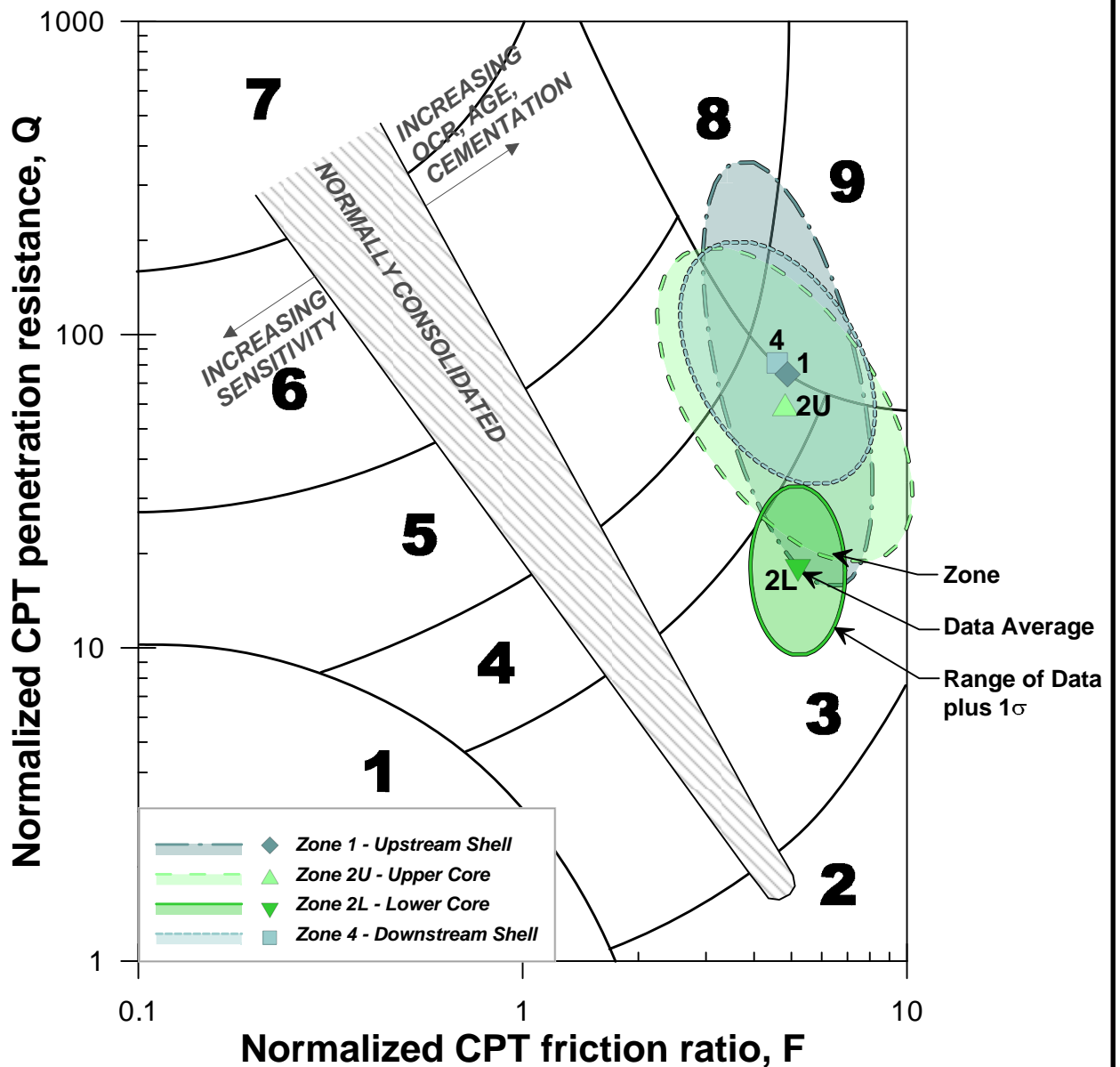
SOIL BEHAVIOR TYPE CHART WITH DATA  
LENIHAN DAM  
SEISMIC STABILITY EVALUATIONS (SSE2)

Figure  
5-13

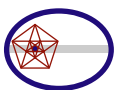


Zone	Soil Behavior Type	$I_c$
1	Sensitive, fine grained	N/A
2	Organic soils – peats	> 3.6
3	Clays – silty clay to clay	2.95 – 3.6
4	Silt mixtures – clayey silt to silty clay	2.60 – 2.95
5	Sand mixtures – silty sand to sandy silt	2.05 – 2.6
6	Sands – clean sand to silty sand	1.31 – 2.05
7	Gravelly sand to dense sand	< 1.31
8	Very stiff sand to clayey sand*	N/A
9	Very stiff, fine grained*	N/A

\* Heavily overconsolidated or cemented



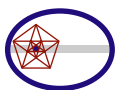
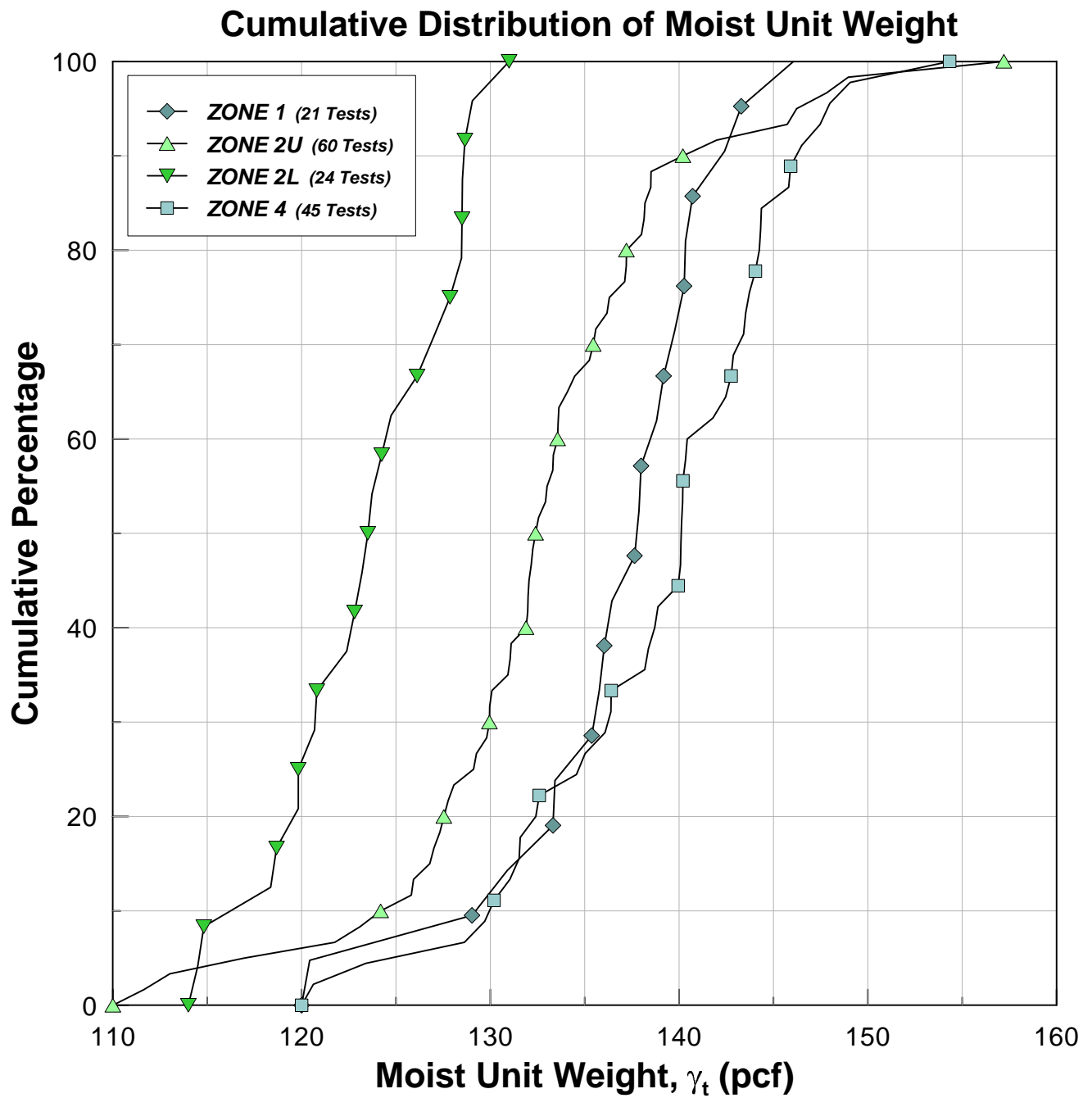
Notes: Soil Behavior Type Index Chart based on Robertson (2009)

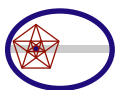
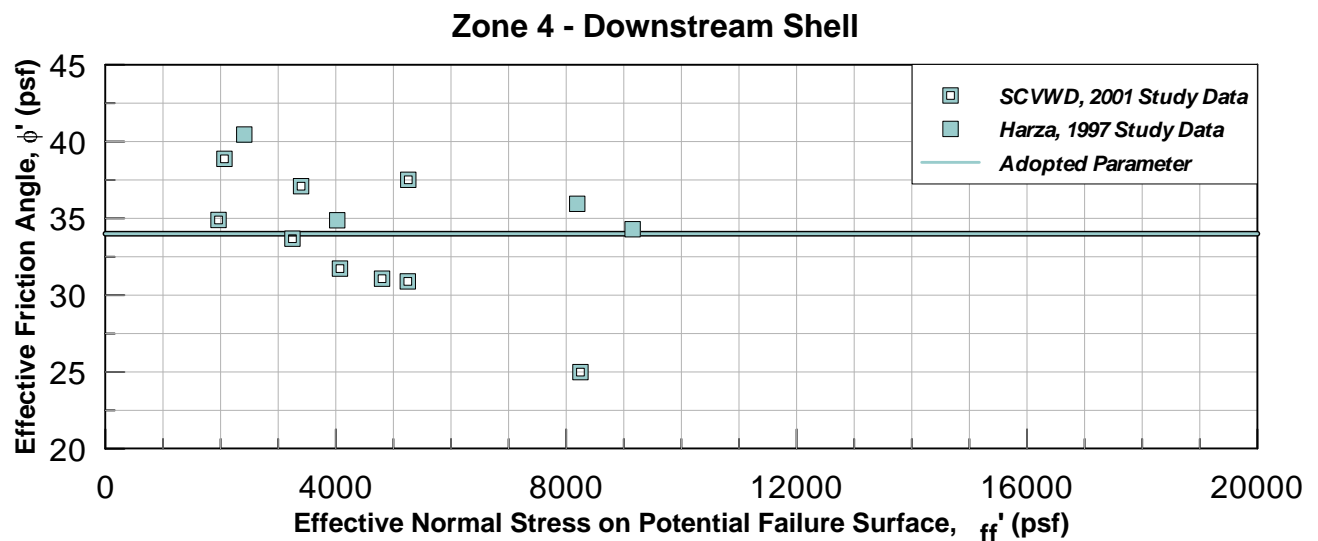
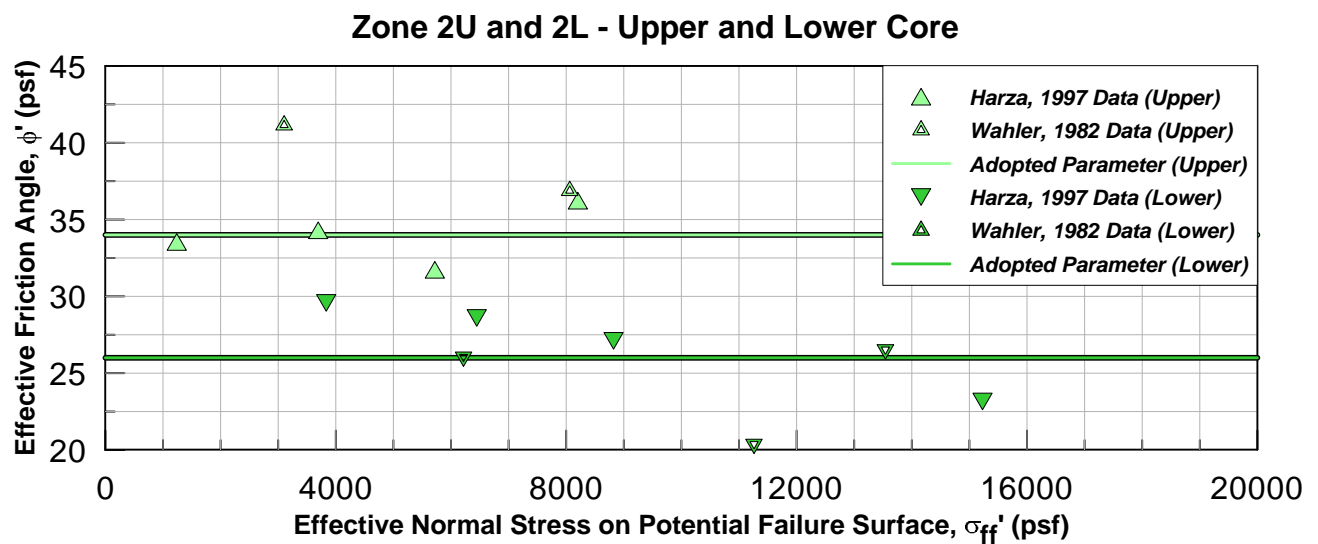
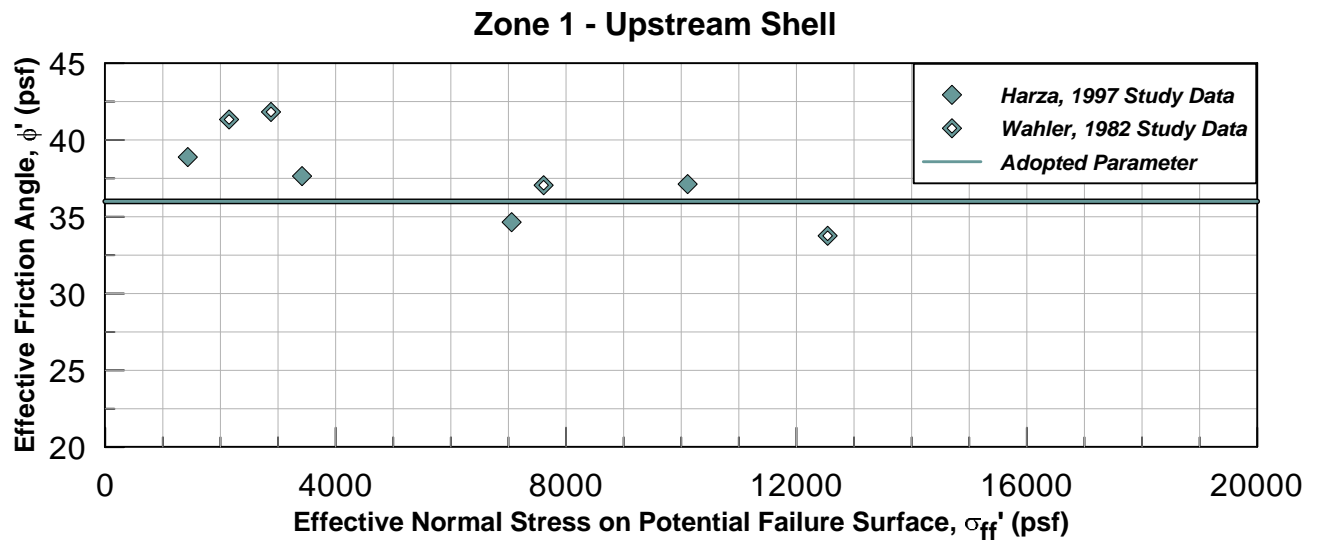


**TERRA / GeoPentech**  
a Joint Venture

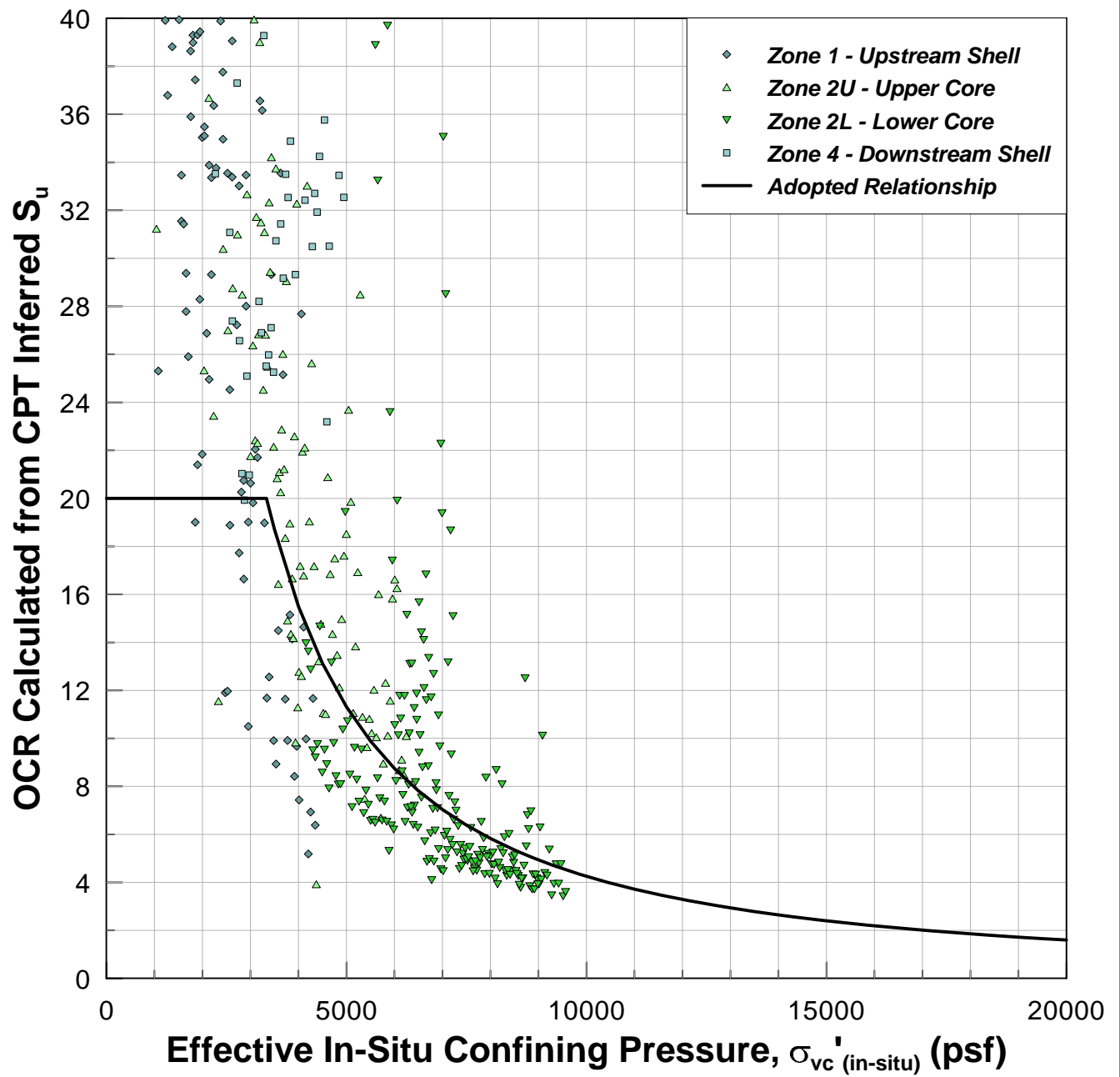
SOIL BEHAVIOR TYPE CHART WITH  
STATISTICAL VALUES - LENIHAN DAM  
SEISMIC STABILITY EVALUATIONS (SSE2)

Figure  
5-14



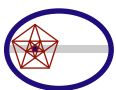


## OCR for All Zones

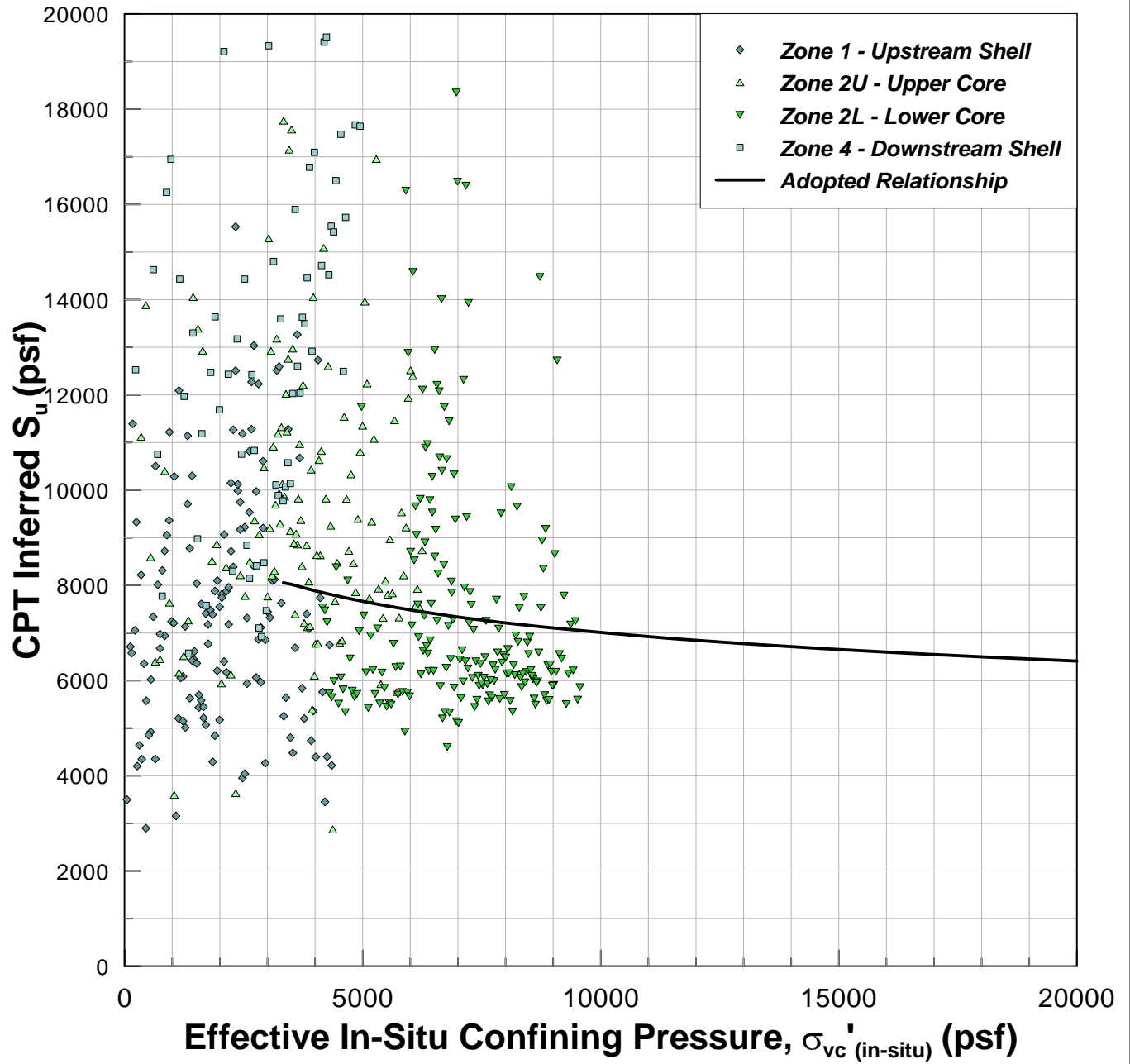


**Adopted Relationship**

$$\text{OCR} = e^{(-1.41 \cdot \ln(\sigma_{vc}') + 14.44)}$$

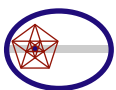


## Undrained Strength Comparison



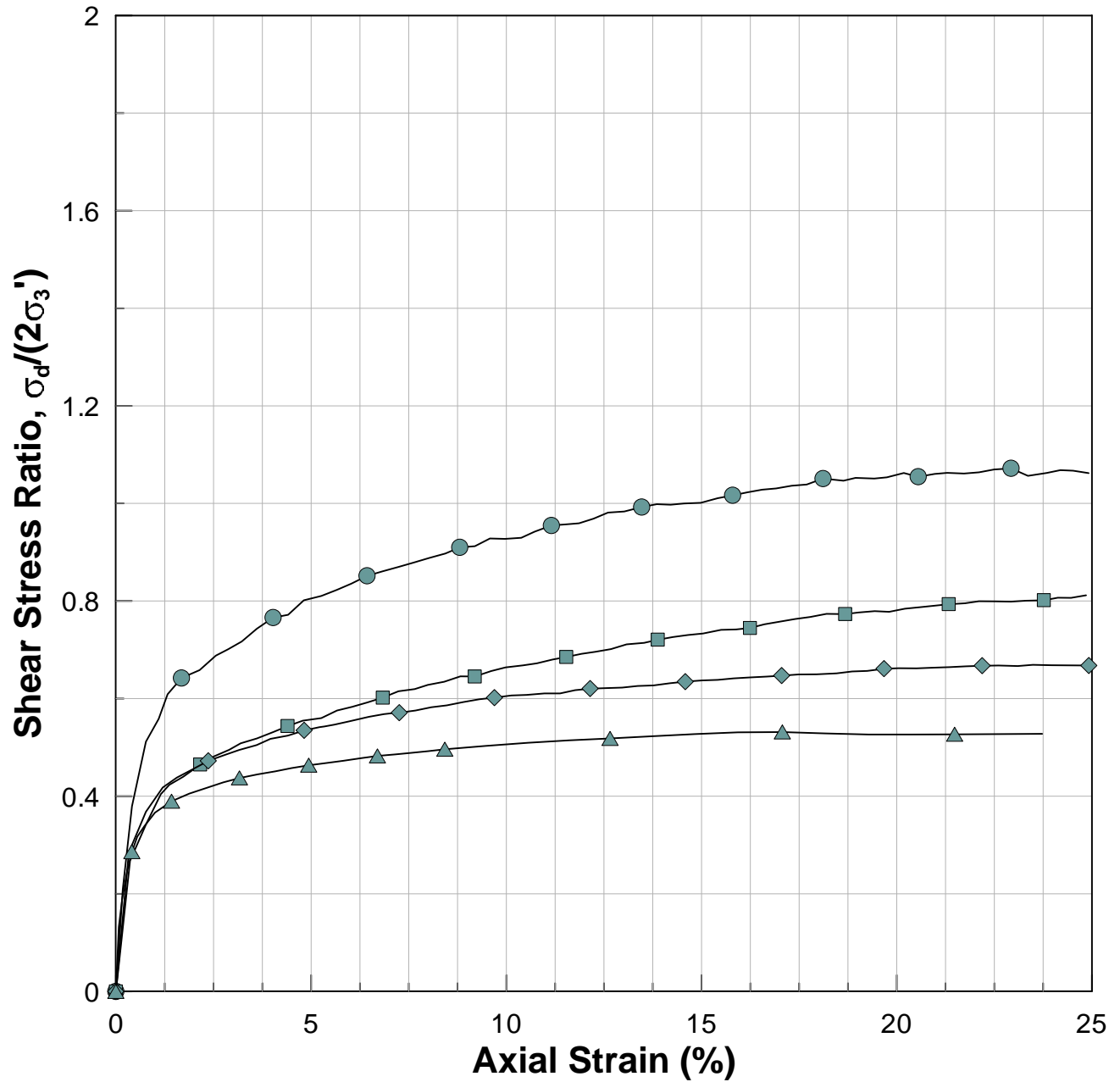
### Adopted Parameter

$$S_u / \sigma_{vc}' = 0.22 * (OCR)^{0.8}$$



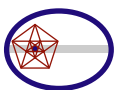


## Strain-Strength Plot for Upstream Shell

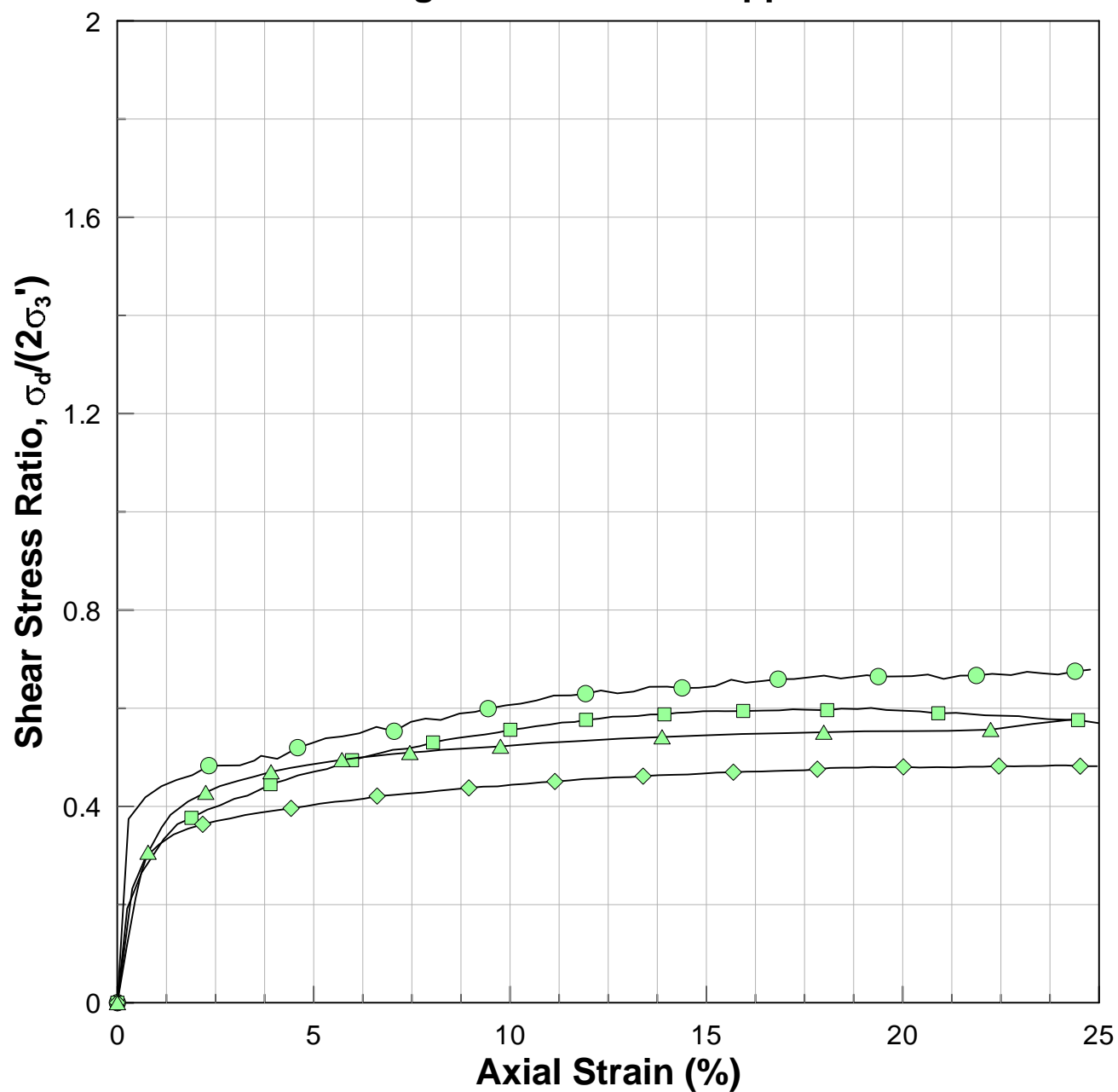


- Cons. @ 2 ksf,  $\sigma_{vc}'(\text{tested})/\sigma_{vc}'(\text{in-situ}) \sim 1.1$
- Cons. @ 6 ksf,  $\sigma_{vc}'(\text{tested})/\sigma_{vc}'(\text{in-situ}) \sim 2.6$
- ◆ Cons. @ 10 ksf,  $\sigma_{vc}'(\text{tested})/\sigma_{vc}'(\text{in-situ}) \sim 4.3$
- ▲ Cons. @ 18.2 ksf,  $\sigma_{vc}'(\text{tested})/\sigma_{vc}'(\text{in-situ}) \sim 10.2$

Note: In-situ confining pressure for samples was estimated based on available information, original data was not recoverable.



## Strain-Strength Ratio Plot for Upper Core

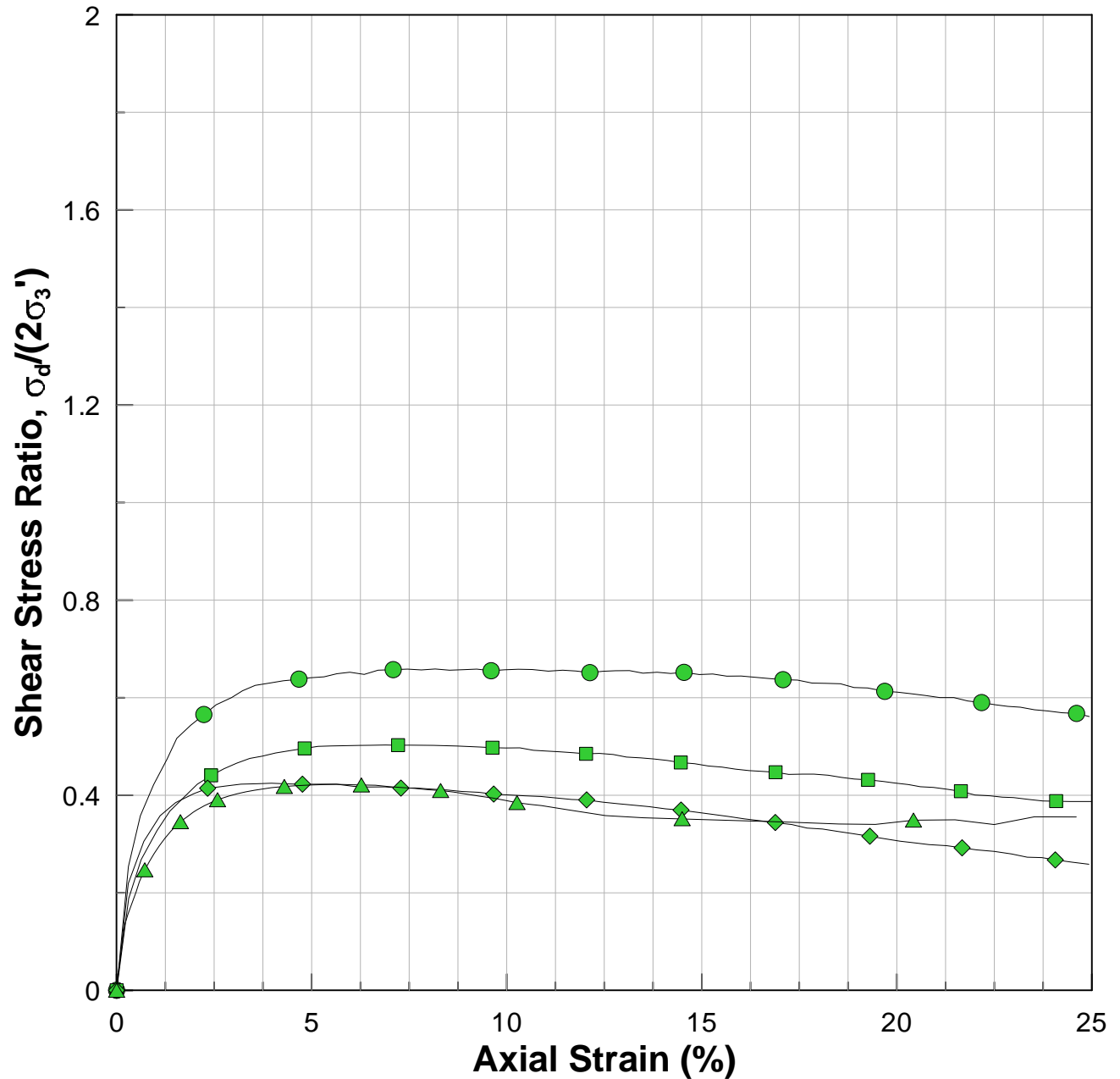


- Cons. @ 2 ksf,  $\sigma_{vc}'(\text{tested})/\sigma_{vc}'(\text{in-situ}) \sim 0.5$
- Cons. @ 2 ksf,  $\sigma_{vc}'(\text{tested})/\sigma_{vc}'(\text{in-situ}) \sim 1.5$
- ◇— Cons. @ 10 ksf,  $\sigma_{vc}'(\text{tested})/\sigma_{vc}'(\text{in-situ}) \sim 2.5$
- ▲— Cons. @ 15.2 ksf,  $\sigma_{vc}'(\text{tested})/\sigma_{vc}'(\text{in-situ}) \sim 3.9$

Note: In-situ confining pressure for samples was estimated based on available information, original data was not recoverable.

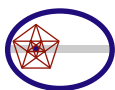


## Strain-Strength Plot for Lower Core



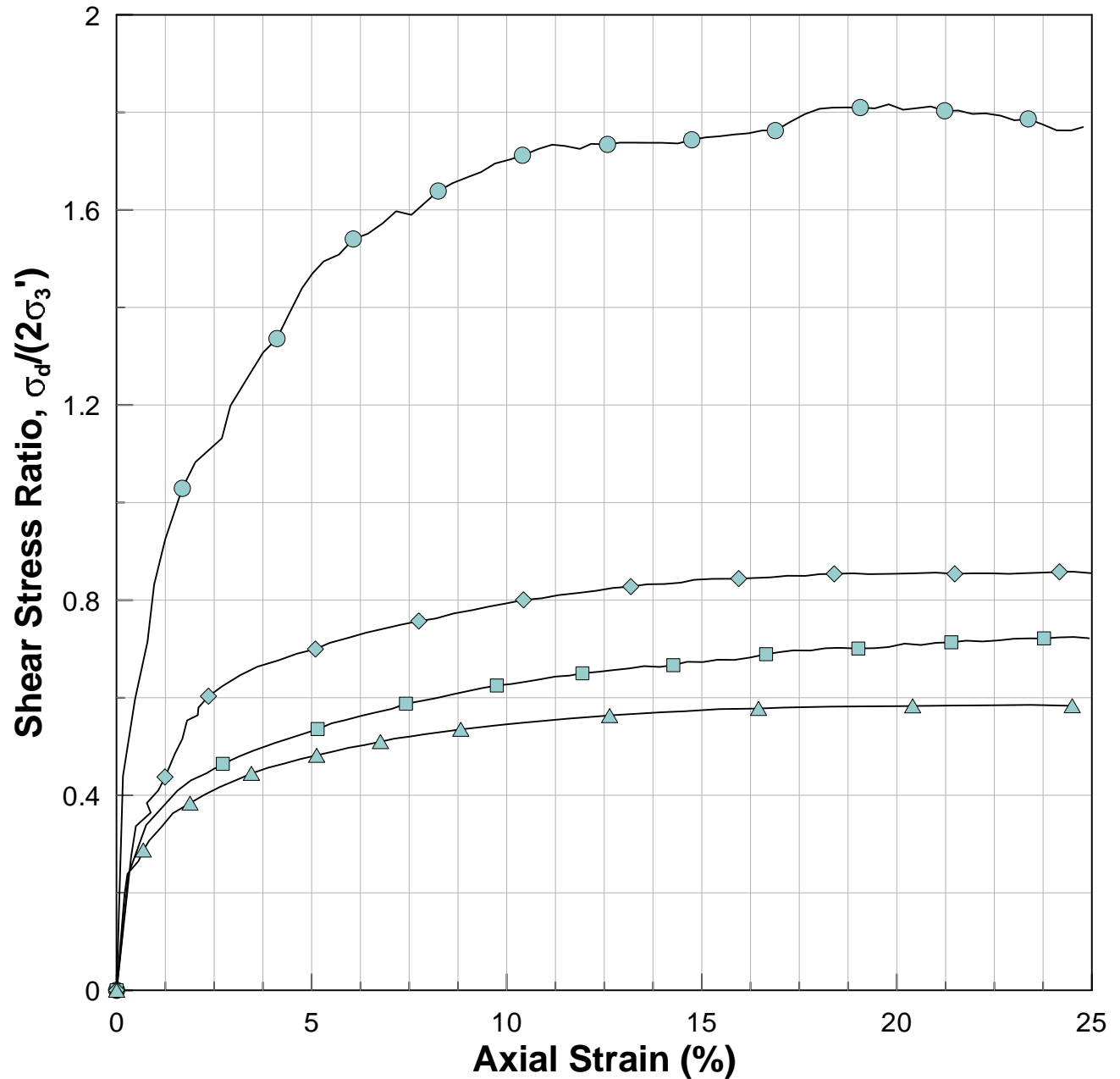
- Cons. @ 4 ksf,  $\sigma_{vc}'(\text{tested})/\sigma_{vc}'(\text{in-situ}) \sim 0.6$
- Cons. @ 8 ksf,  $\sigma_{vc}'(\text{tested})/\sigma_{vc}'(\text{in-situ}) \sim 1.4$
- ◆ Cons. @ 12 ksf,  $\sigma_{vc}'(\text{tested})/\sigma_{vc}'(\text{in-situ}) \sim 2.3$
- ▲ Cons. @ 16.8 ksf,  $\sigma_{vc}'(\text{tested})/\sigma_{vc}'(\text{in-situ}) \sim 2.5$

Note: In-situ confining pressure for samples was estimated based on available information, original data was not recoverable.



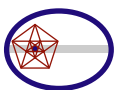


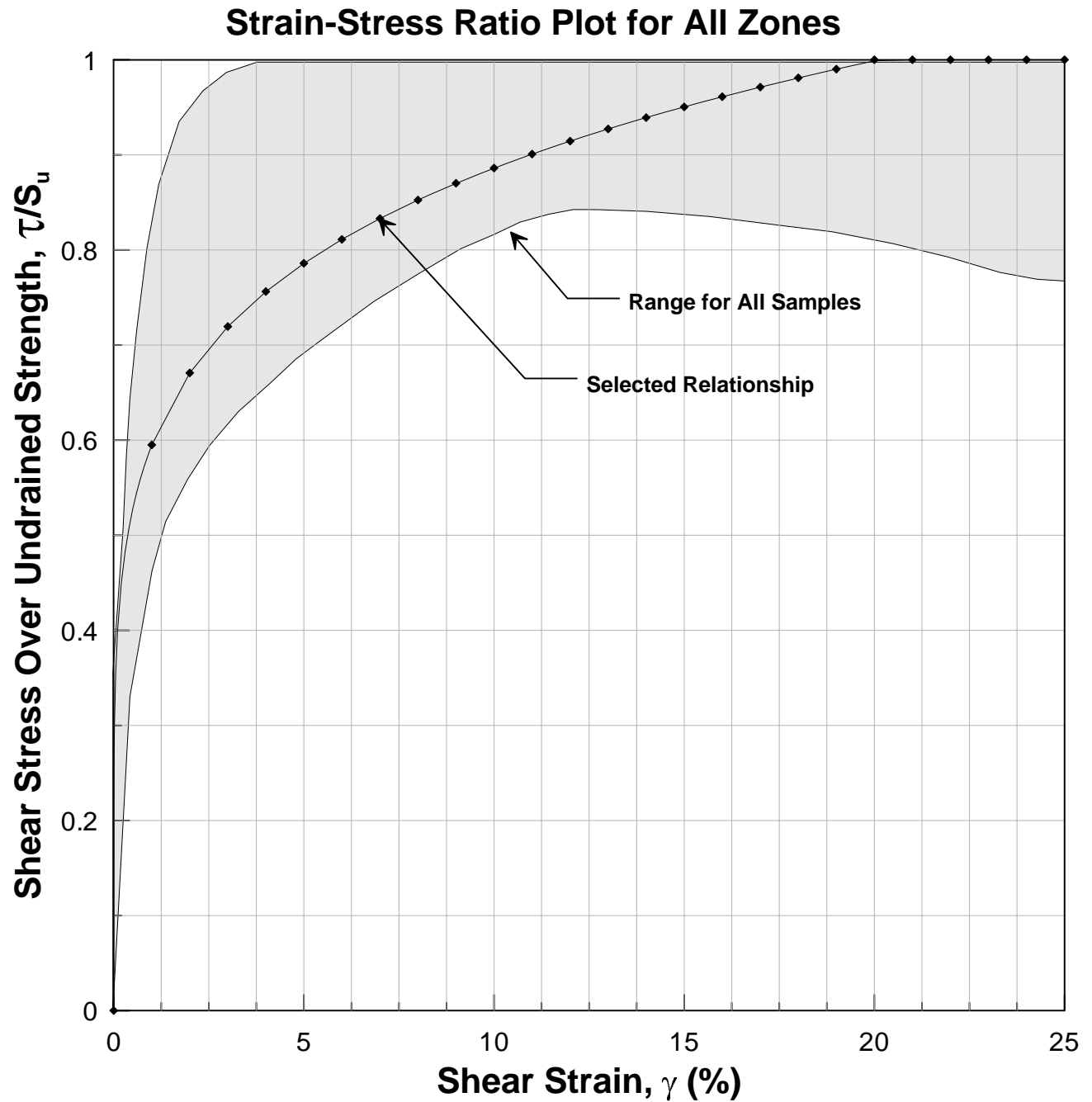
## Strain-Strength Ratio Plot for Downstream Shell



- **Cons. @ 2 ksf,  $\sigma_{vc}'(\text{tested})/\sigma_{vc}'(\text{in-situ}) \sim 0.4$**
- **Cons. @ 6 ksf,  $\sigma_{vc}'(\text{tested})/\sigma_{vc}'(\text{in-situ}) \sim 1.0$**
- ◆— **Cons. @ 10 ksf,  $\sigma_{vc}'(\text{tested})/\sigma_{vc}'(\text{in-situ}) \sim 1.7$**
- ▲— **Cons. @ 14.4 ksf,  $\sigma_{vc}'(\text{tested})/\sigma_{vc}'(\text{in-situ}) \sim 2.7$**

Note: In-situ confining pressure for samples was estimated based on available information, original data was not recoverable.

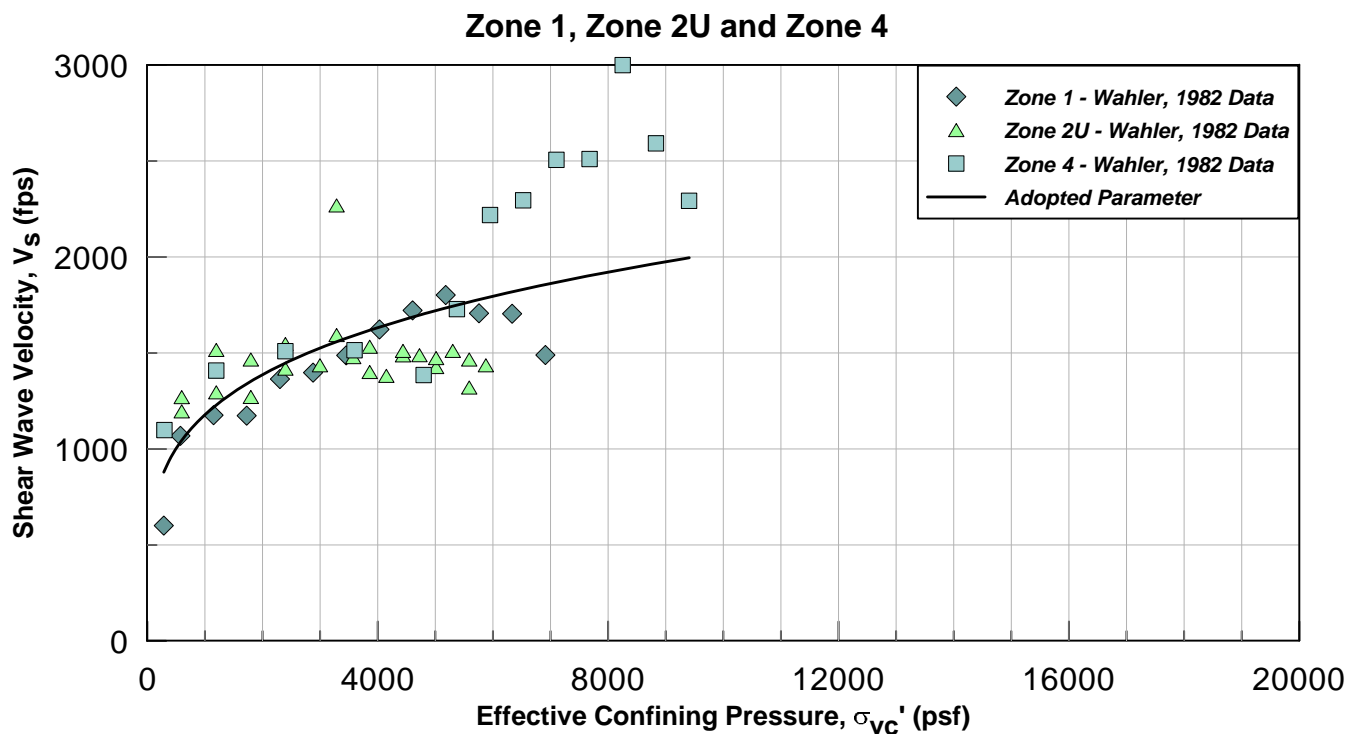




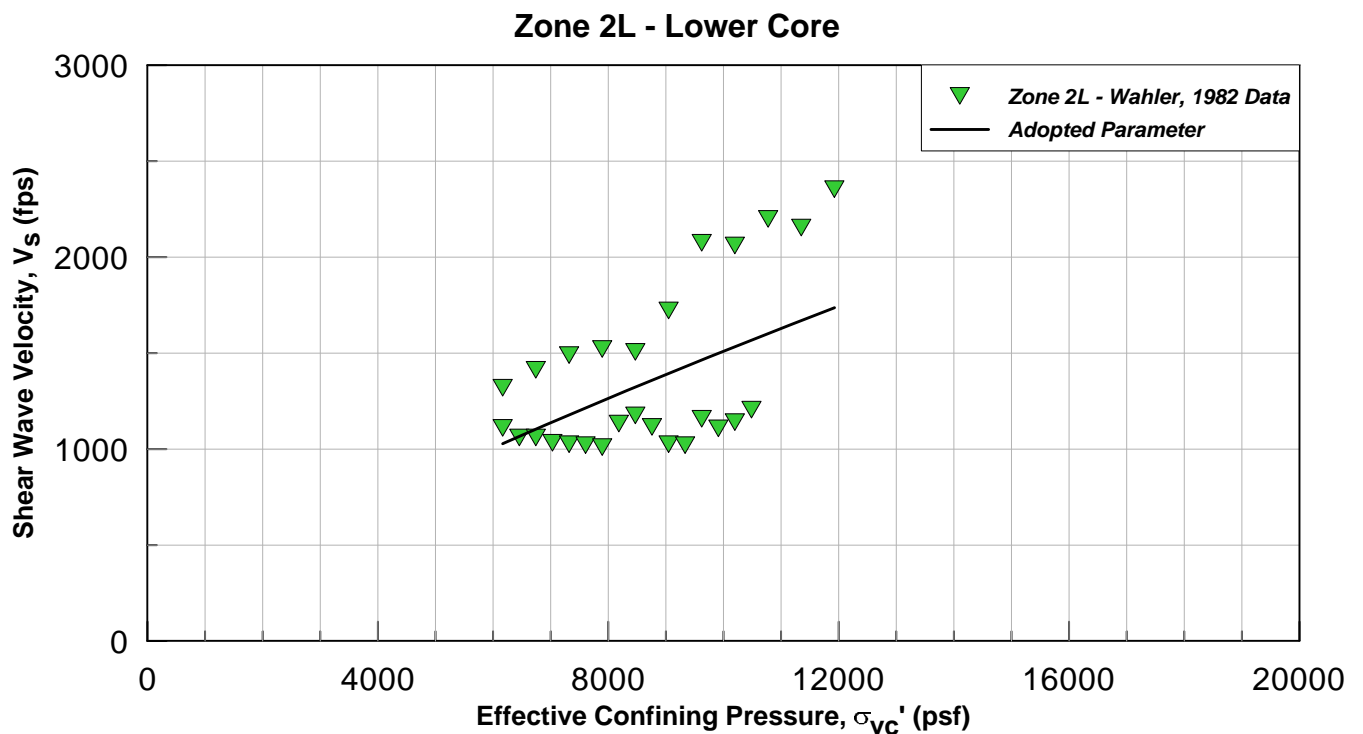
**Adopted Relationship**

$$\tau = S_u * e^{(0.17 * \ln(\gamma) - 0.52)}$$

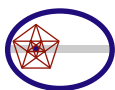




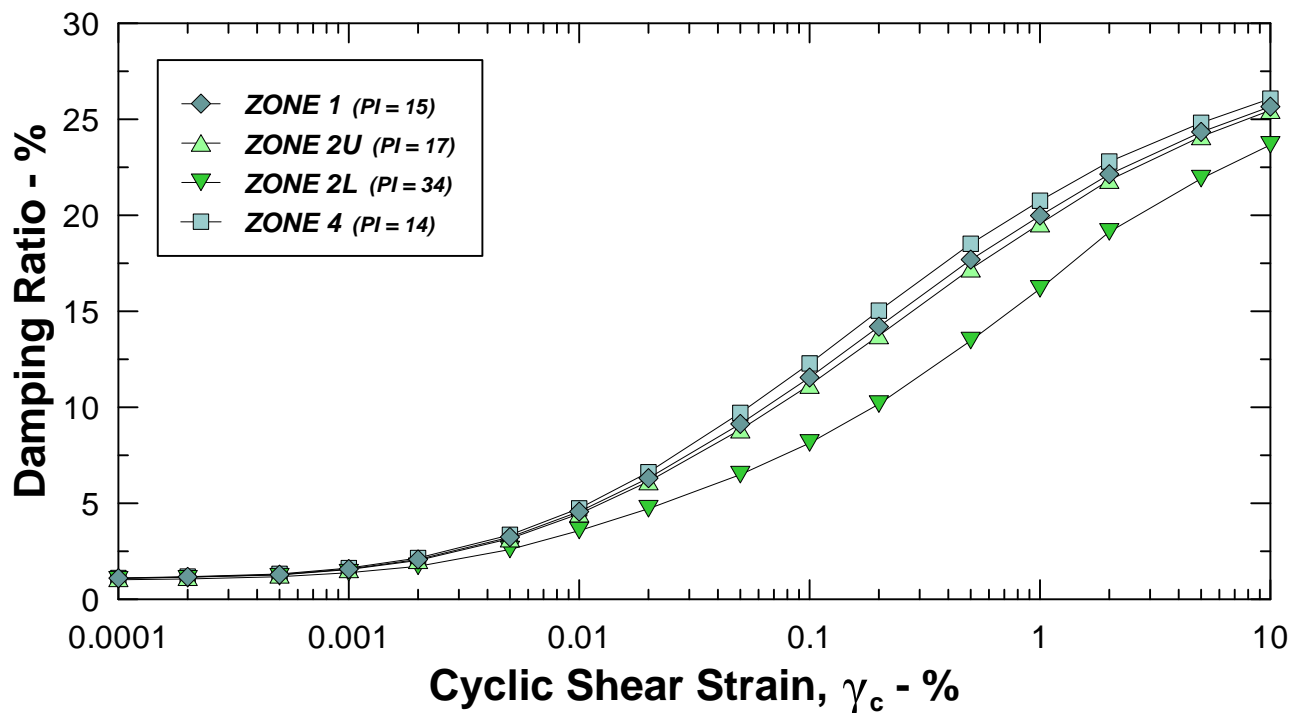
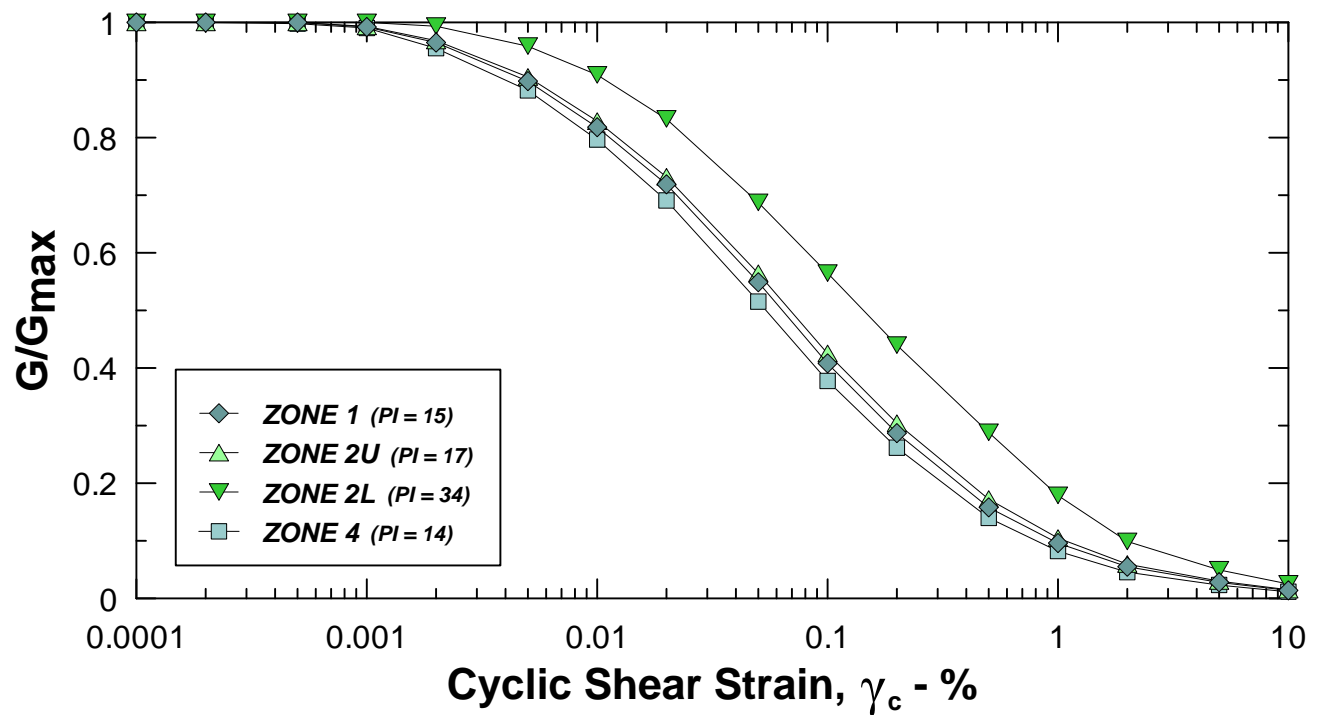
**Zone 1, 2U, 4 - Adopted Parameter:  $V_s = e^{(0.24 \cdot \ln(\sigma_{vc}') + 5.4)}$**



**Zone 2L - Adopted Parameter:  $V_s = e^{(0.79 \cdot \ln(\sigma_{vc}') + 5.4)}$**







Note: Modulus reduction and damping ratio curves are based on Vucetic and Dobry, 1991



**TERRA / GeoPentech**  
a Joint Venture

MODULUS REDUCTION AND DAMPING  
RATIO CURVES - LENIHAN DAM  
SEISMIC STABILITY EVALUATIONS (SSE2)

Figure  
5-22

Deformation from Survey Measurement

Crest Station	Horizontal Change* (Between 7/11/89 and 10/18/89)	Vertical Change (Between 7/11/89 and 10/18/89)
11+00	0.03 ft	-0.15 ft
13+00	0.21 ft	-0.61 ft
14+00	0.25 ft	-0.74 ft
15+00	0.18 ft	-0.85 ft
16+00	0.10 ft	-0.78 ft
17+00	-0.01 ft	-0.63 ft
18+00	-0.12 ft	-0.46 ft
19+00	-0.12 ft	-0.35 ft

\*Positive indicates downstream movement, negative indicates upstream movement.

Wet Area Observed on Downstream Face<sup>2</sup>

Limits of Embankment

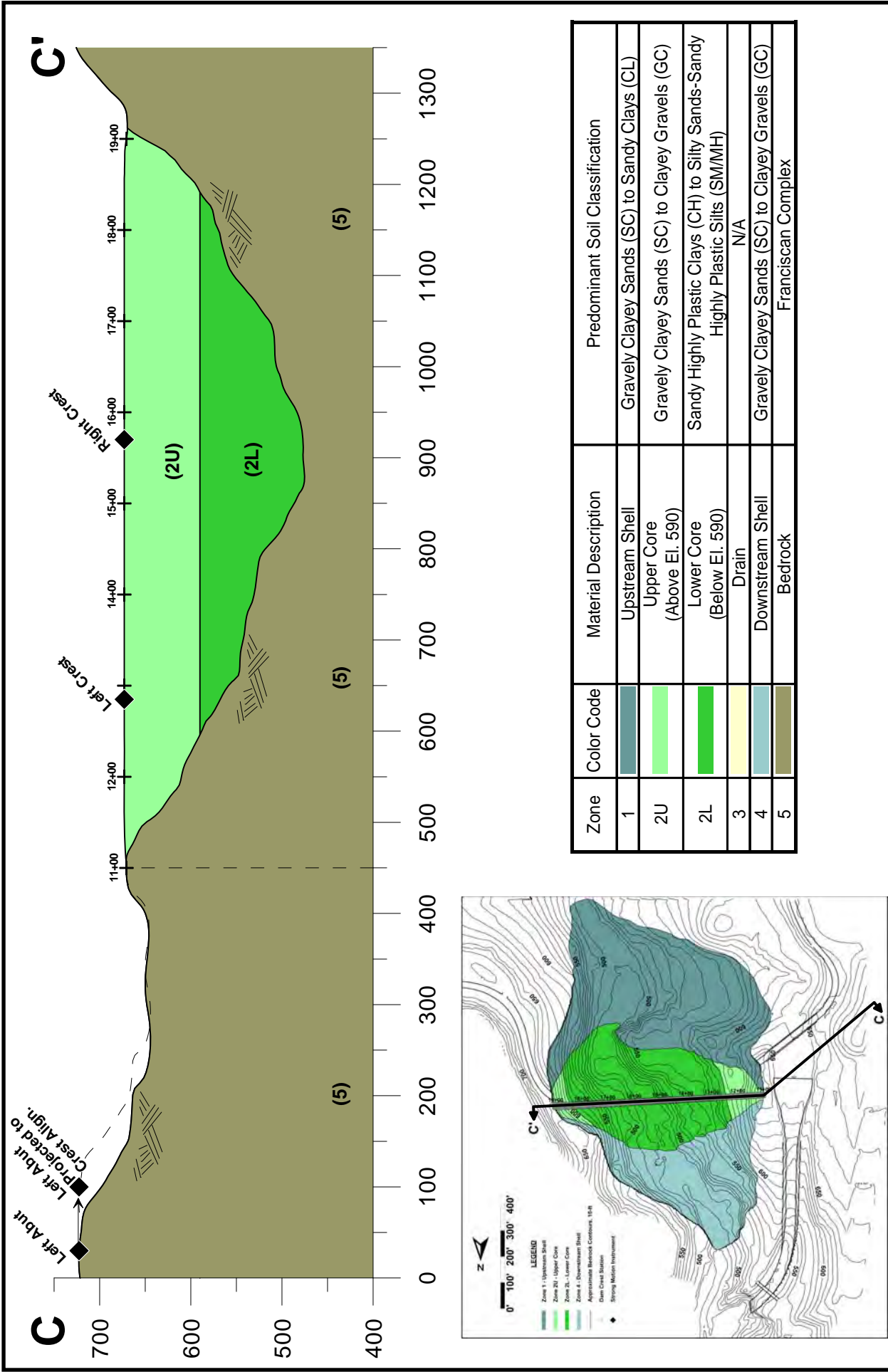
LEGEND

- Zone 1 - Upstream Shell
- Zone 2U - Upper Core
- Zone 2L - Lower Core
- Zone 4 - Downstream Shell
- Approximate Bedrock Contours, 10-ft
- Approximate Crack Location<sup>1</sup>
- Horizontal Movement (Magnitude: 1"=.25')
- Vertical Movement (Magnitde: ● = .8')
- Dam Crest Station
- Strong Motion Instrument

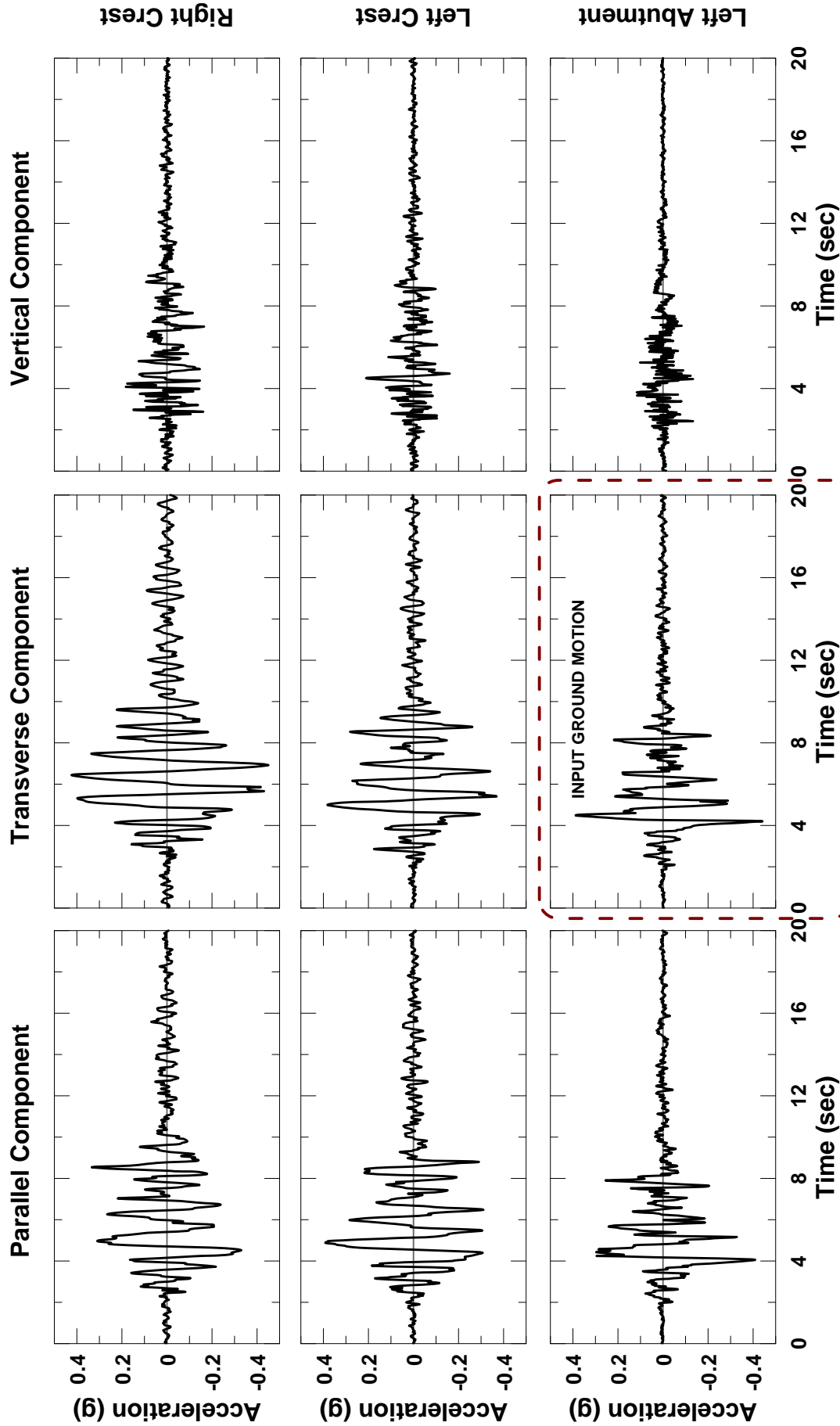


Notes:

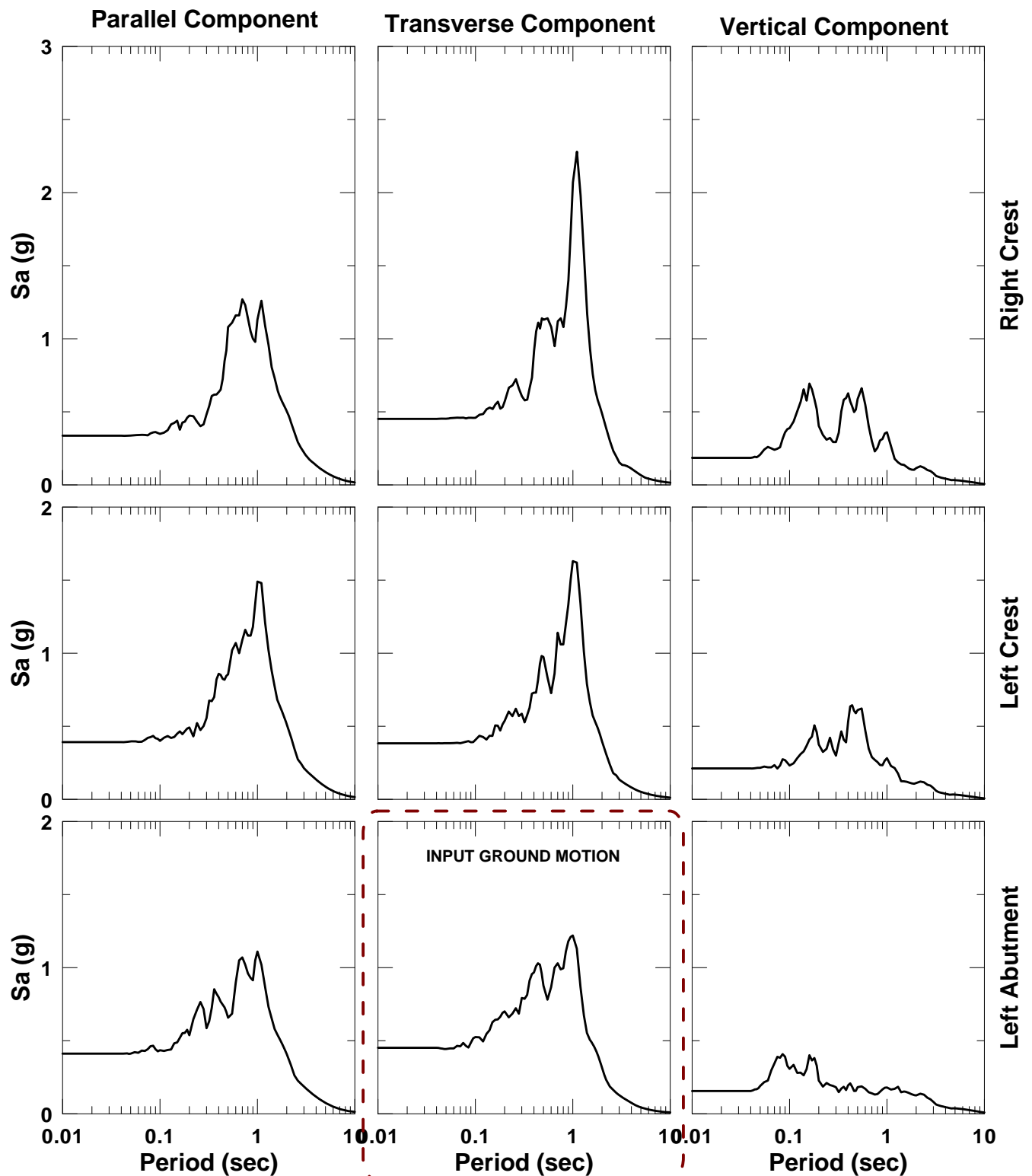
- 1. Approximate locations of cracks derive from Investigation of SCVWD Dams Affected by the Loma Prieta Earthquake of October 17, 1989 (RLVA, 1990).
- 2. Wet area speculated to be due to previously installed drill hole casing backfilled with pea gravel acting as a relief well for groundwater in the bedrock fracture system in response to the increased pressure induced by the shaking conditions. This hypothesis is documented in RLVA, 1990.







Acceleration Time Histories of  
Loma Prieta Recordings from CGS Strong Motion Center Database

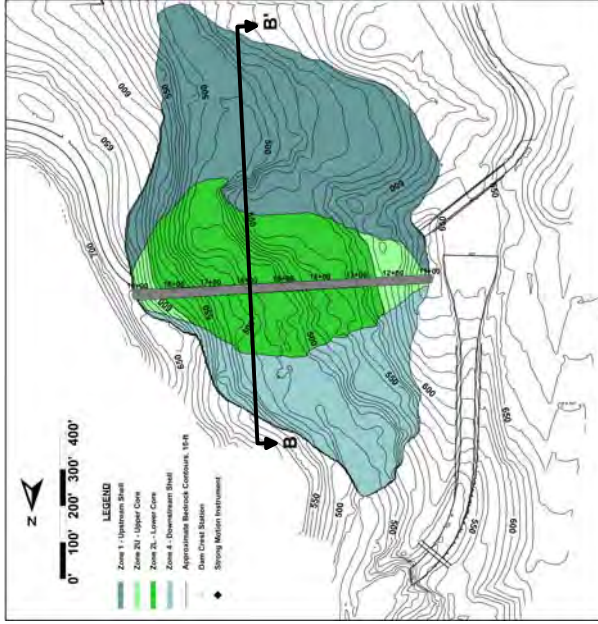
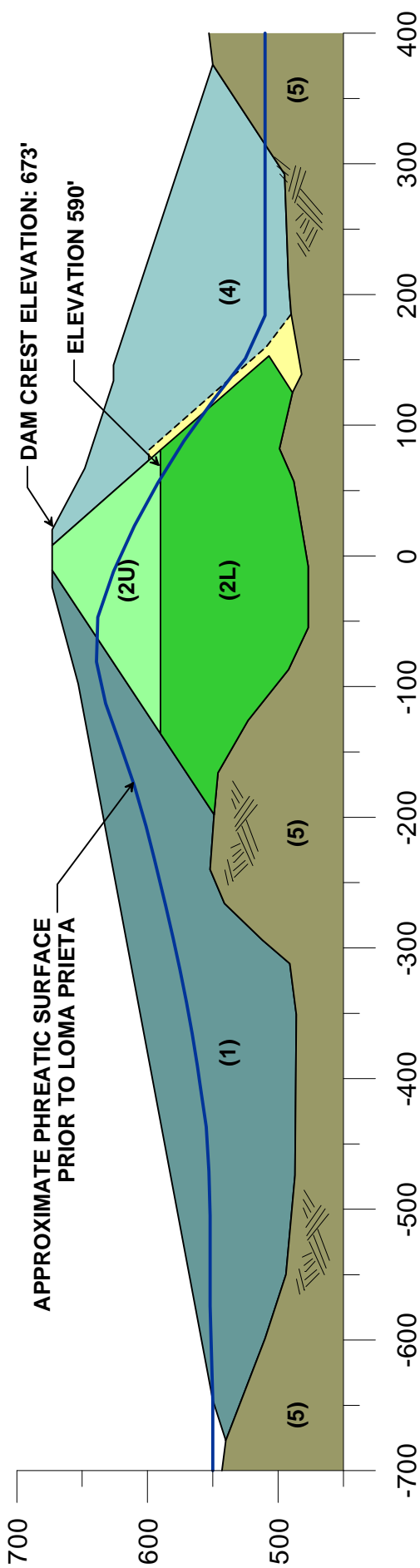


**Acceleration Response Spectra (5% Damped) of  
Loma Prieta Recordings from CGS Strong Motion Center Database**



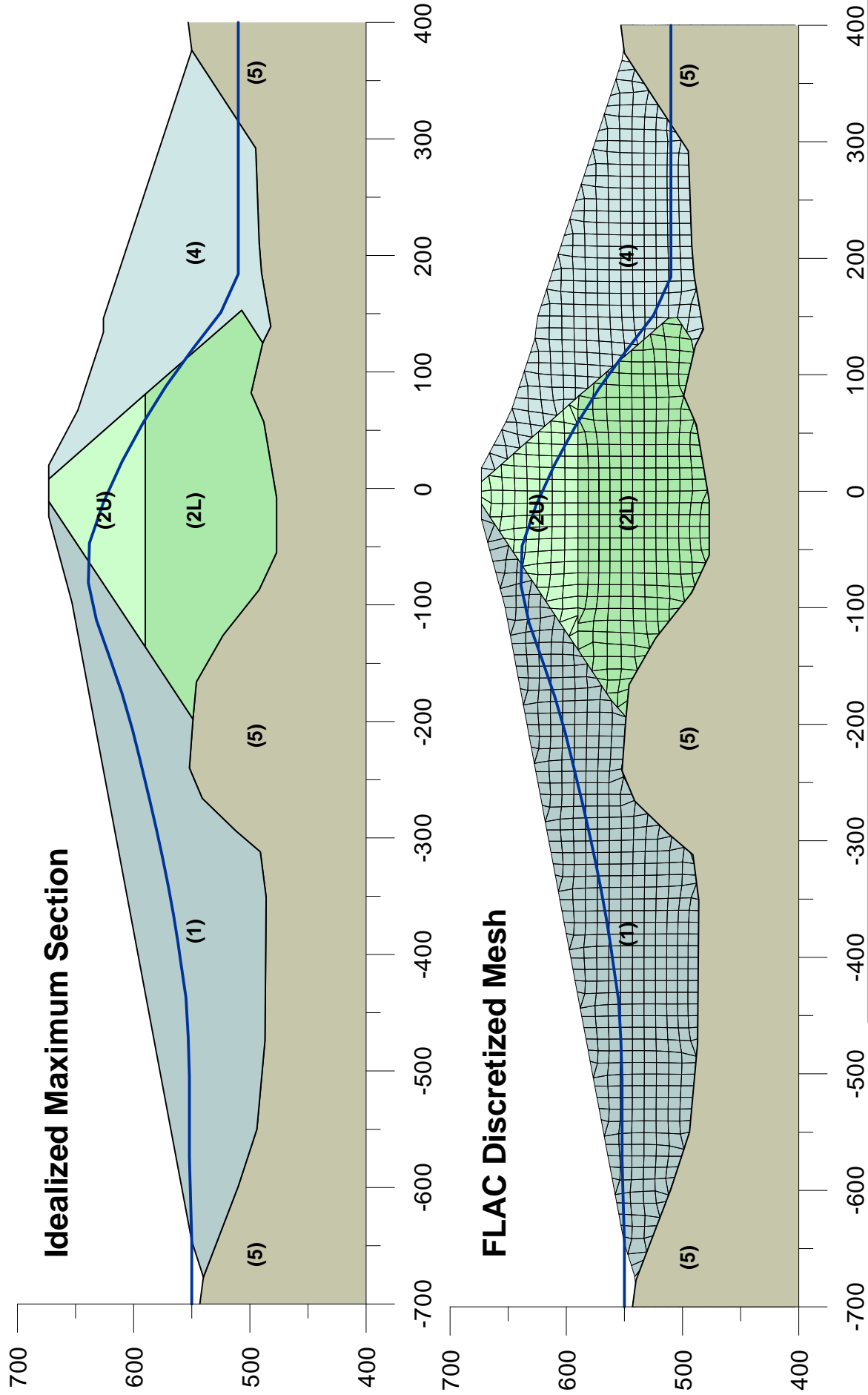
B

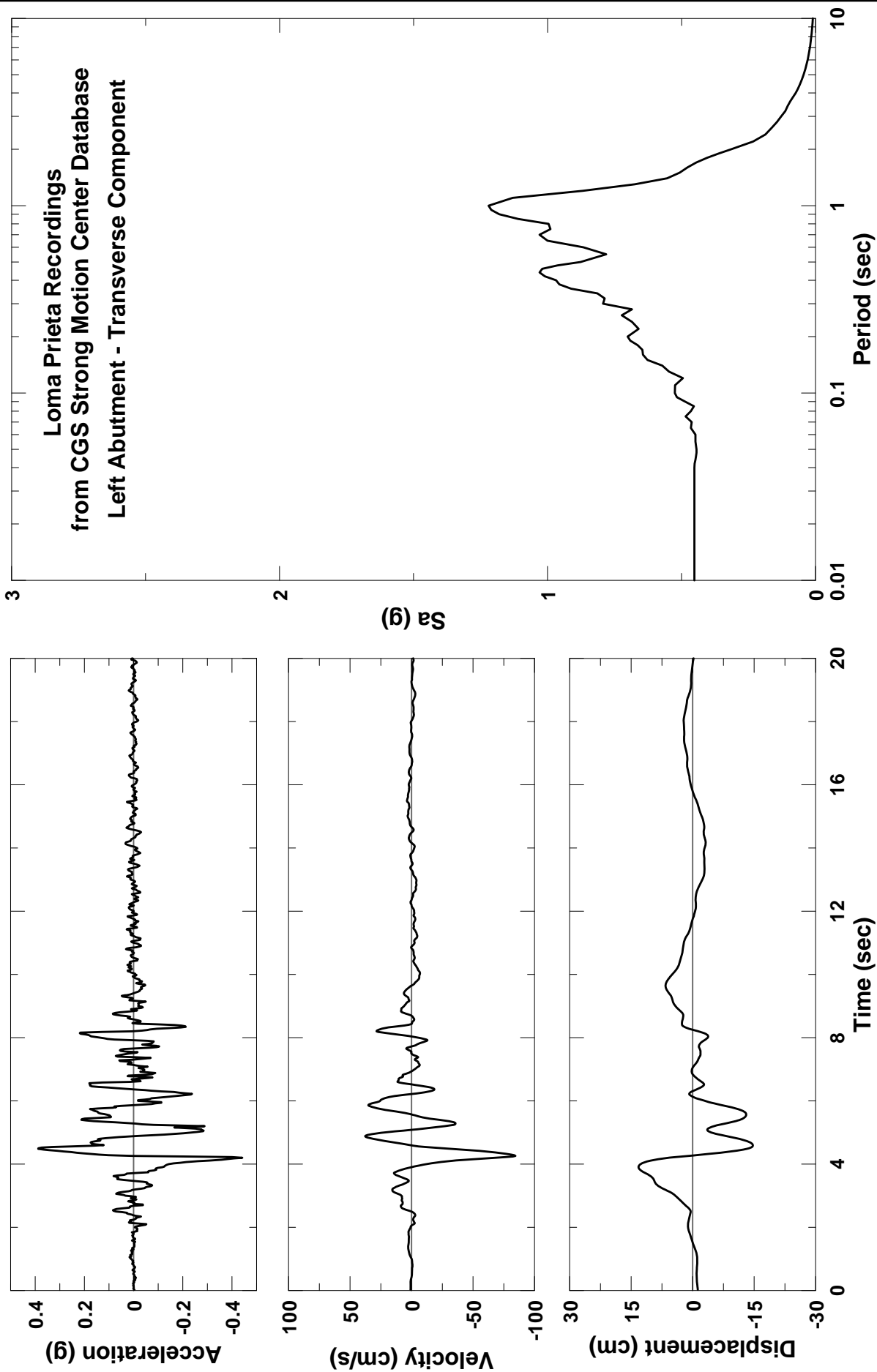
B'



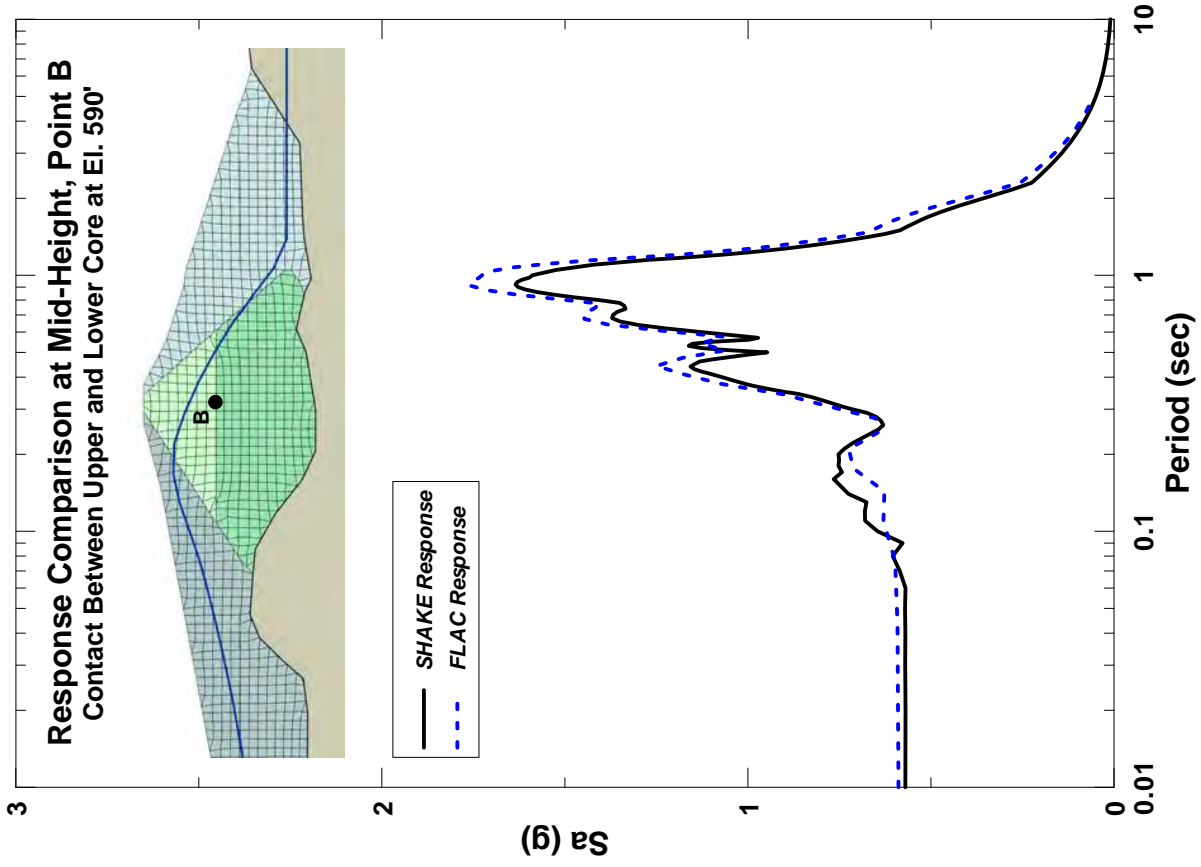
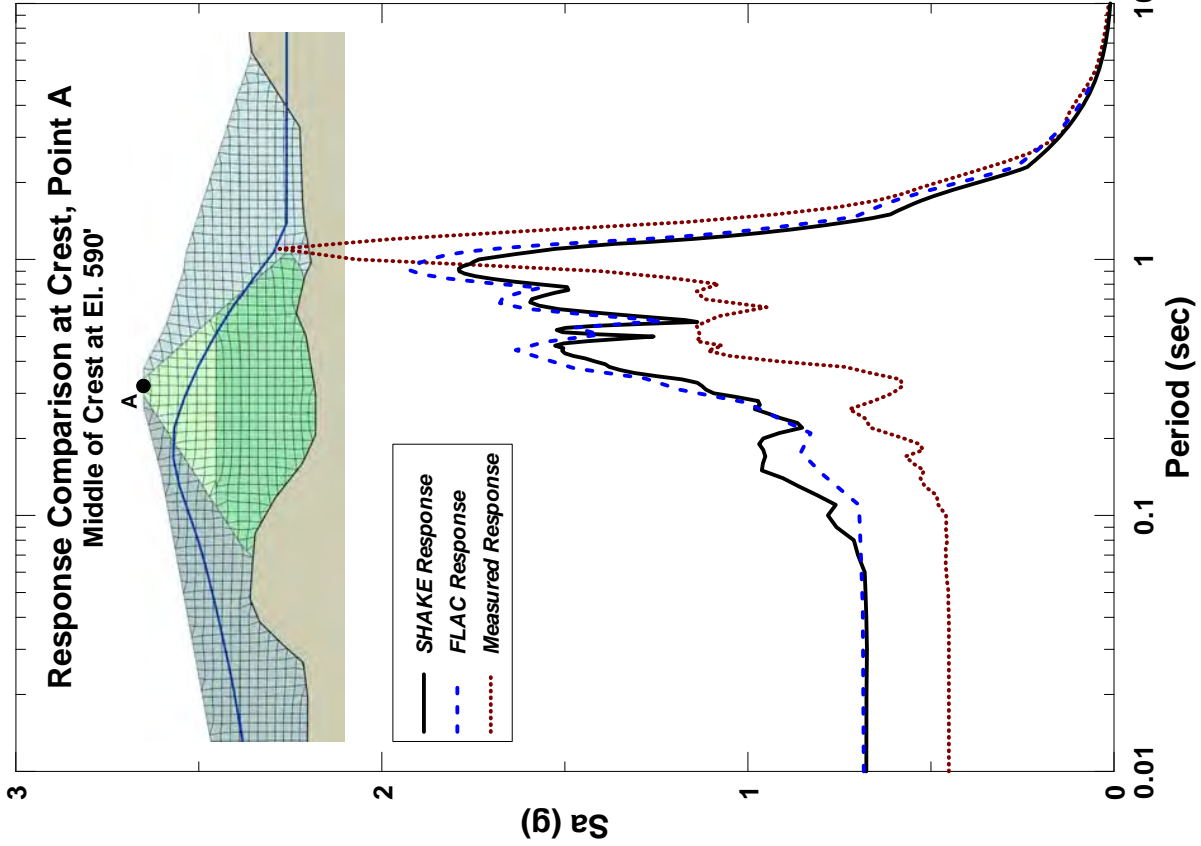
Zone	Color Code	Material Description	Predominant Soil Classification
1		Upstream Shell	Gravely Clayey Sands (SC) to Sandy Clays (CL)
2U		Upper Core (Above El. 590)	Gravely Clayey Sands (SC) to Clayey Gravels (GC)
2L		Lower Core (Below El. 590)	Sandy Highly Plastic Clays (CH) to Silty Sands-Sandy Highly Plastic Silts (SM/MH)
3		Drain	N/A
4		Downstream Shell	Gravely Clayey Sands (SC) to Clayey Gravels (GC)
5		Bedrock	Franciscan Complex







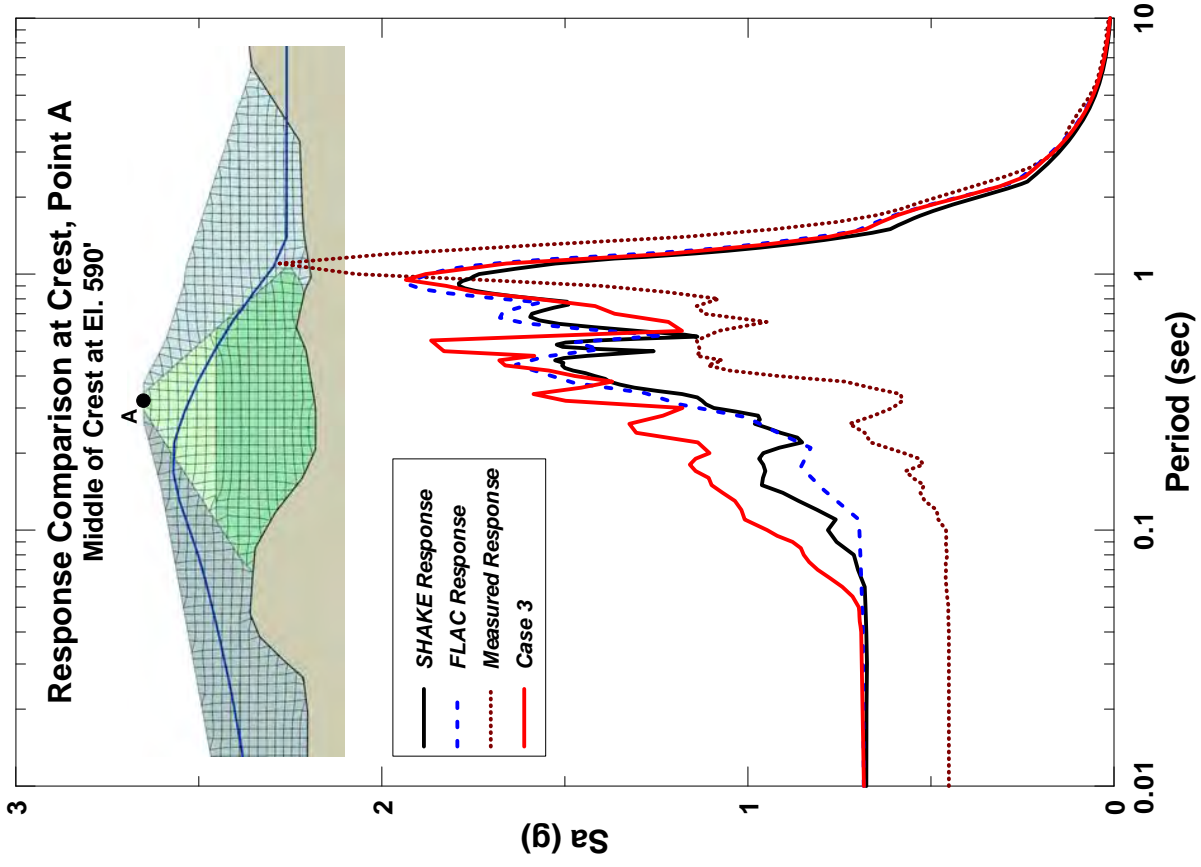
 <b>TERRA / GeoPentech</b> a Joint Venture	<b>INPUT MOTION FOR FLAC ANALYSES LENIHAN DAM SEISMIC STABILITY EVALUATIONS (SSE2)</b>	<b>Figure 6-7</b>
---	--	-----------------------



COMPARISON OF FLAC AND SHAKE  
RESPONSE SPECTRA - LENIHAN DAM  
SEISMIC STABILITY EVALUATIONS (SSE2)

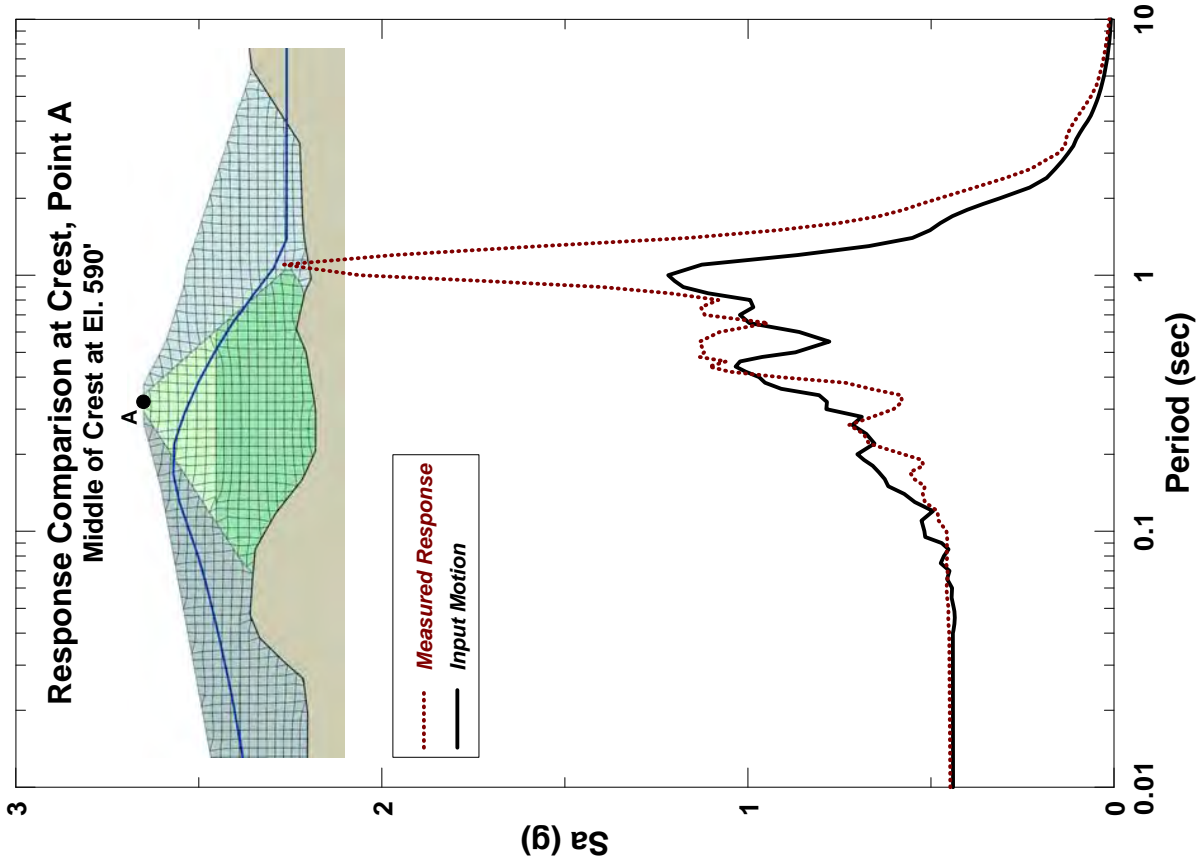
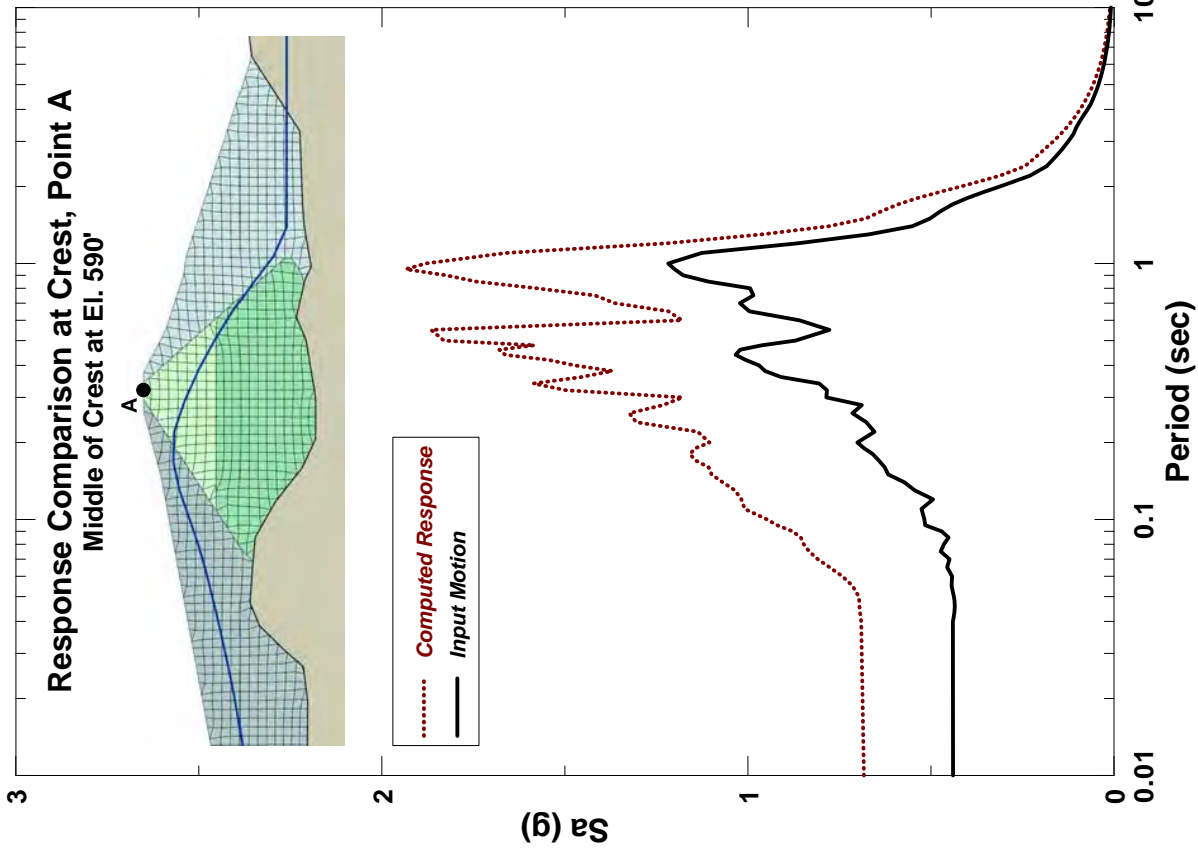
Figure  
6-8

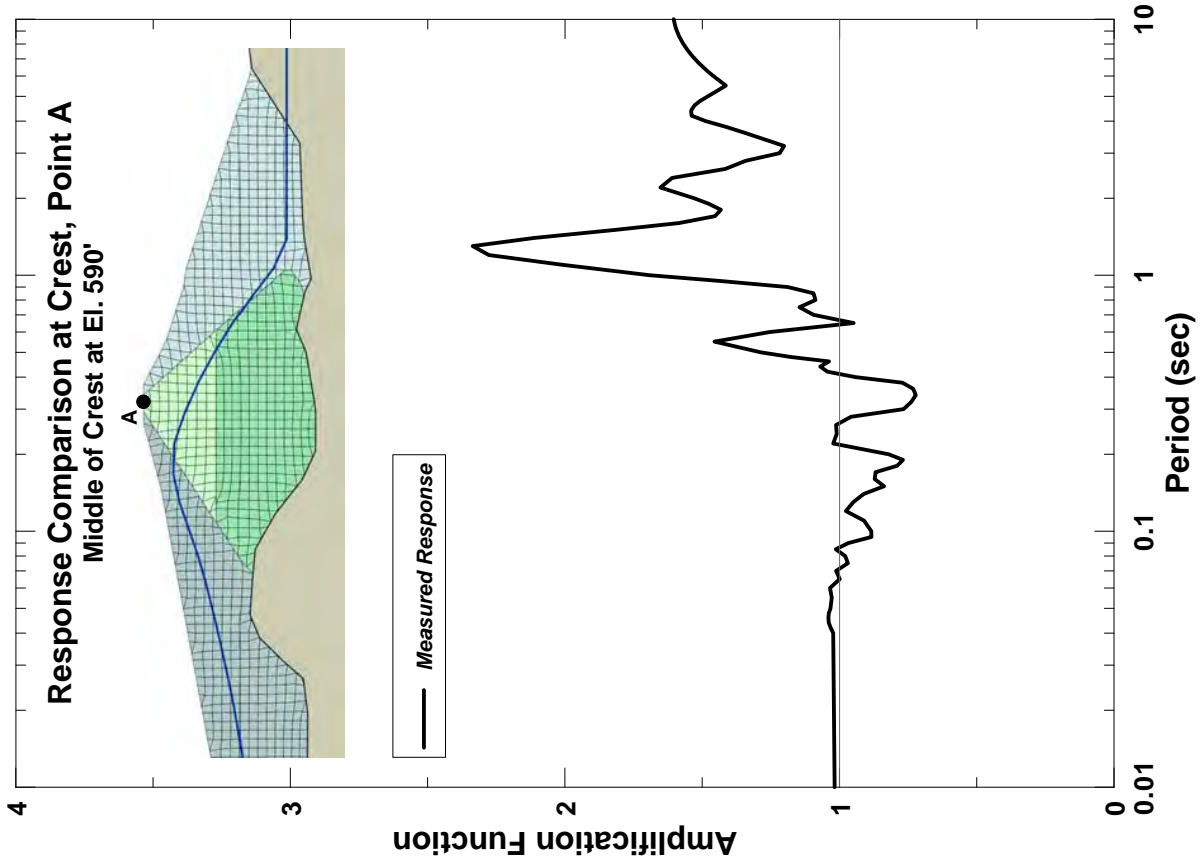
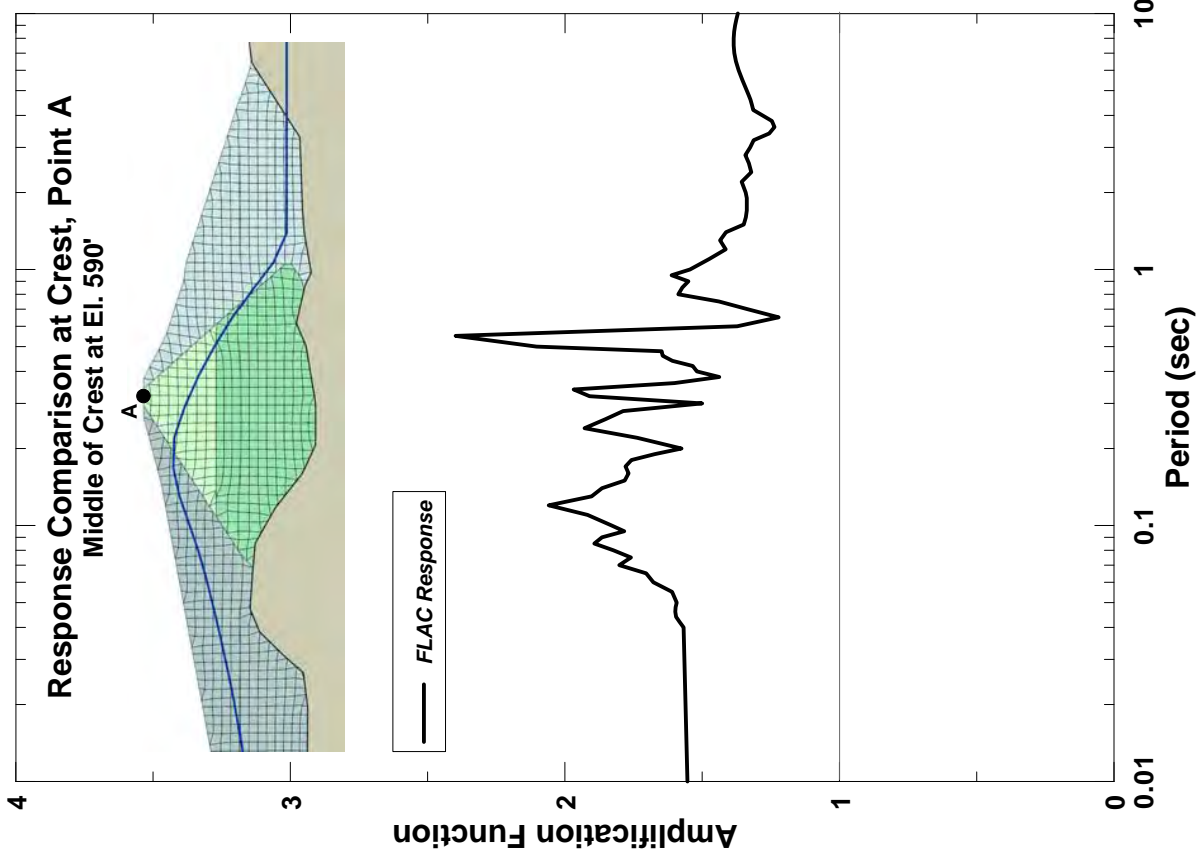




RESPONSE SPECTRA - COMPARISON WITH  
2-D CASE 3 - LENIHAN DAM  
SEISMIC STABILITY EVALUATIONS (SSE2)

Figure  
6-9





COMPARISON OF COMPUTED  
AMPLIFICATION FUNCTIONS - LENIHAN DAM  
SEISMIC STABILITY EVALUATIONS (SSE2)

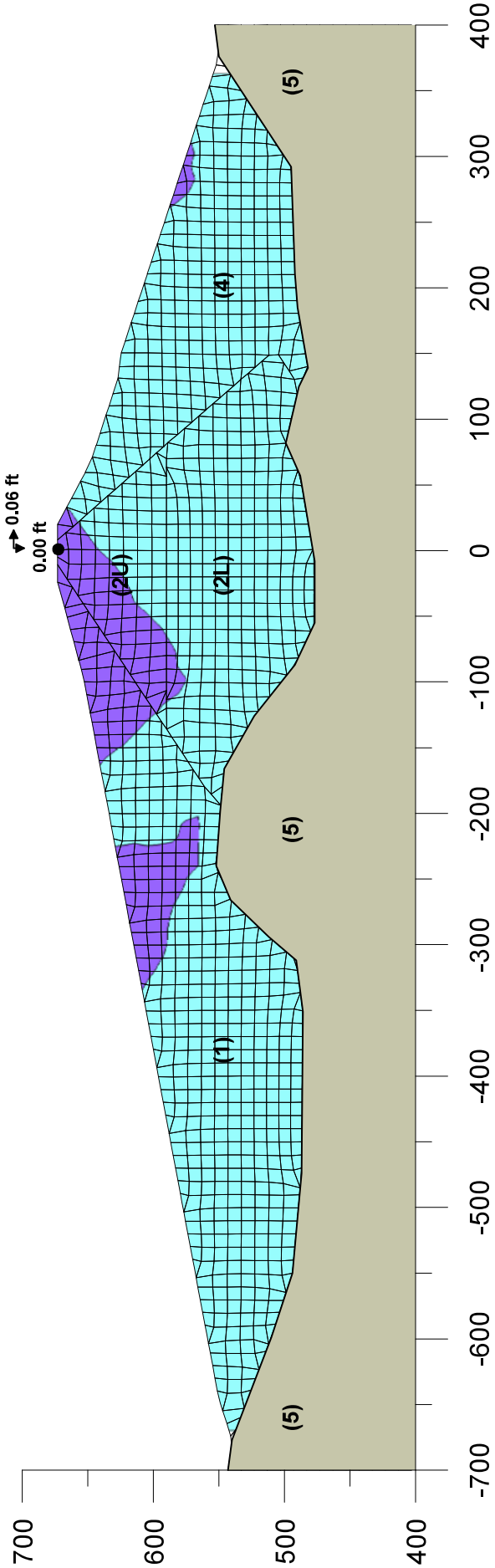
Figure  
6-11



Displacement  
Scale:  
(ft)

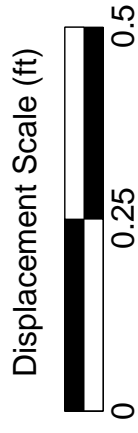
> 0.7
0.6-0.7
0.5-0.6
0.4-0.5
0.3-0.4
0.2-0.3
0.15-0.2
0.10-0.15
0.005-0.10
0.00-0.005

CASE 1 - Undrained Strength Below & Effective Strength Above WT

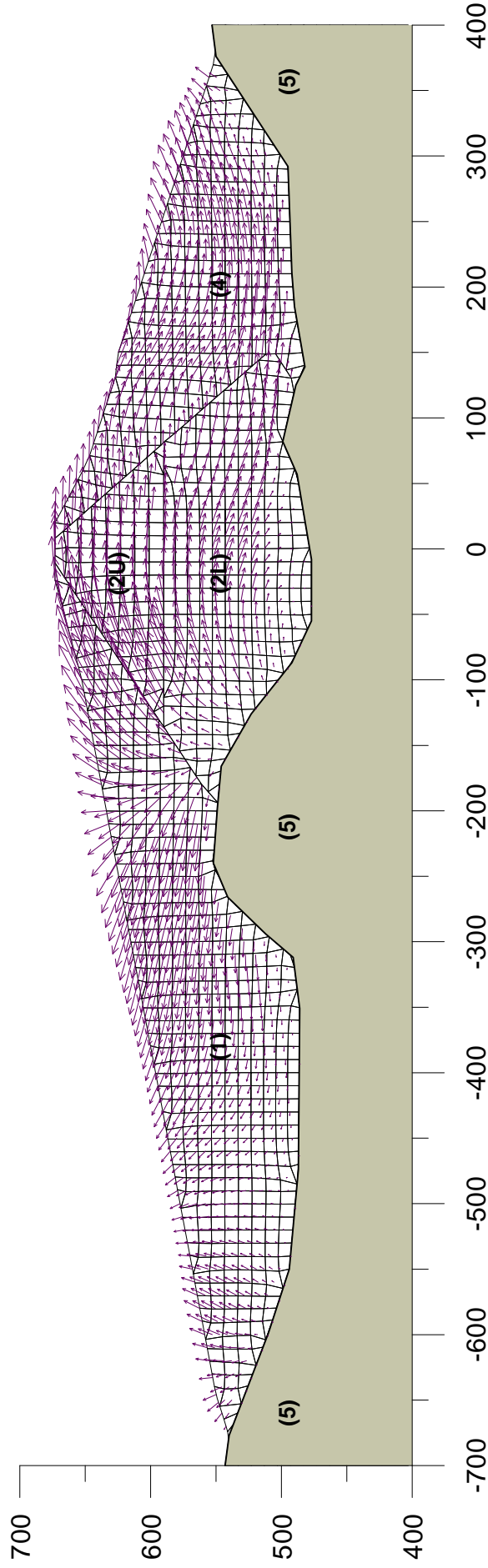


CASE 1 COMPUTED DISPLACEMENT  
CONTOURS - LENIHAN DAM  
SEISMIC STABILITY EVALUATIONS (SSE2)

Figure  
6-12A



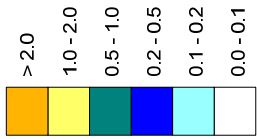
### CASE 1 - Undrained Strength Below & Effective Strength Above WT



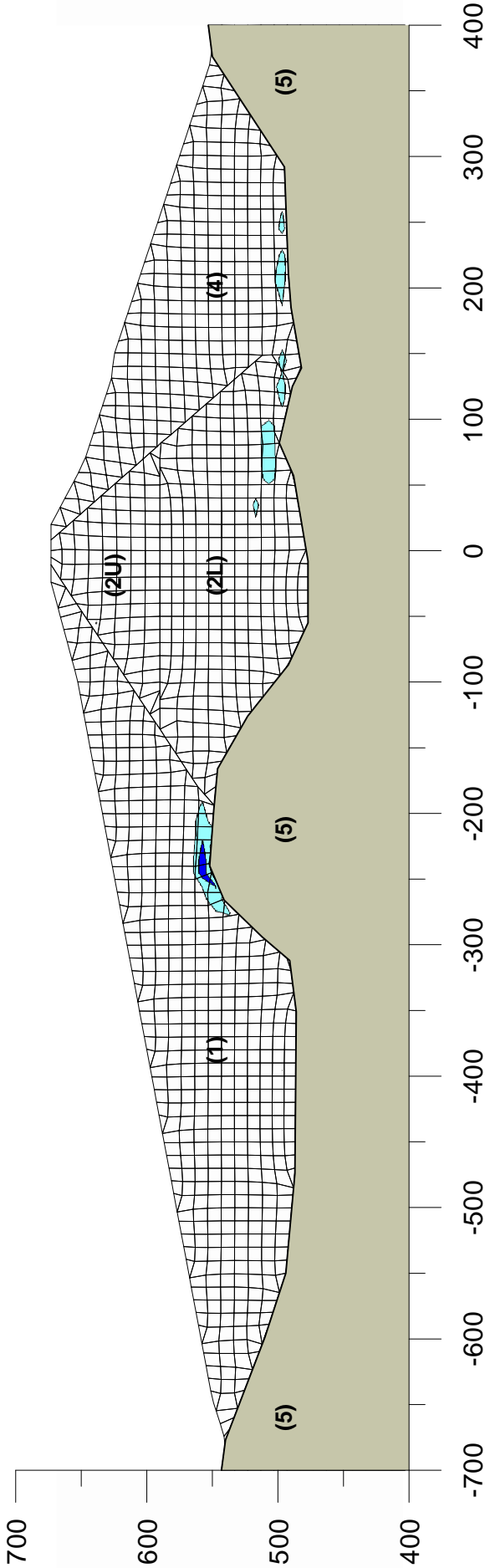
CASE 1 COMPUTED DISPLACEMENT  
VECTORS - LENIHAN DAM  
SEISMIC STABILITY EVALUATIONS (SSE2)

Figure  
6-12B

Shear Strain  
Scale:  
(%)



**CASE 1 - Undrained Strength Below & Effective Strength Above WT**





**TERRA / GeoPentech**  
a Joint Venture

CASE 1 COMPUTED SHEAR STRAIN  
CONTOURS - LENIHAN DAM  
SEISMIC STABILITY EVALUATIONS (SSE2)

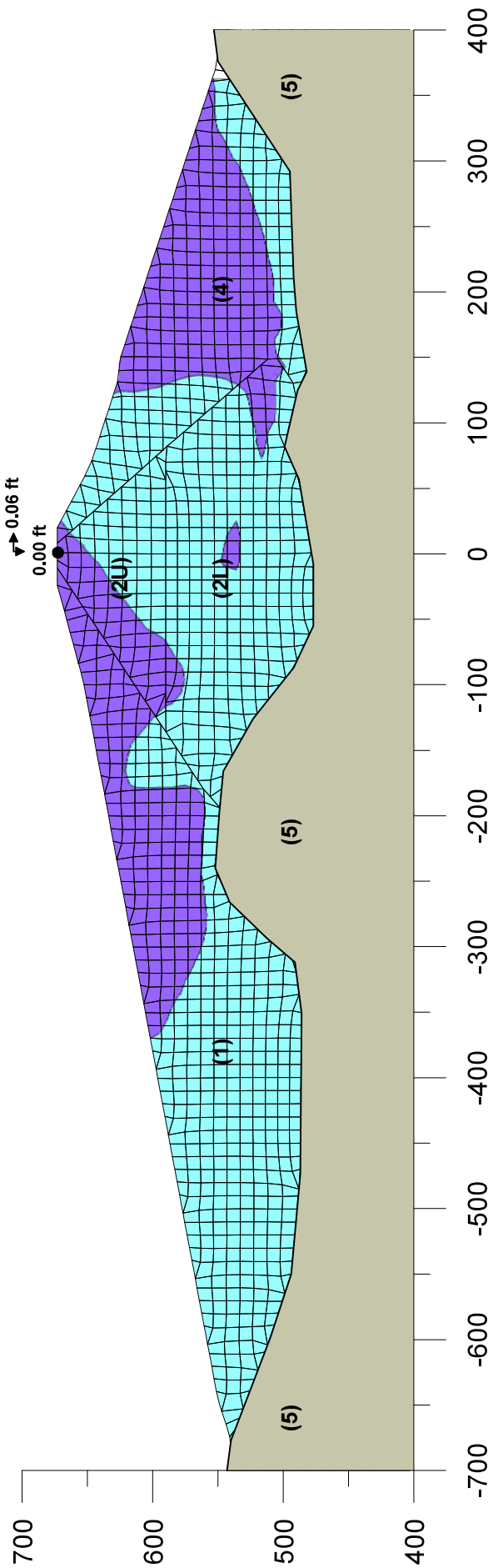
Figure  
6-12C



Displacement  
Scale:  
(ft)

> 0.7
0.6-0.7
0.5-0.6
0.4-0.5
0.3-0.4
0.2-0.3
0.15-0.2
0.10-0.15
0.005-0.10
0.00-0.005

CASE 2 - Undrained Strength Throughout



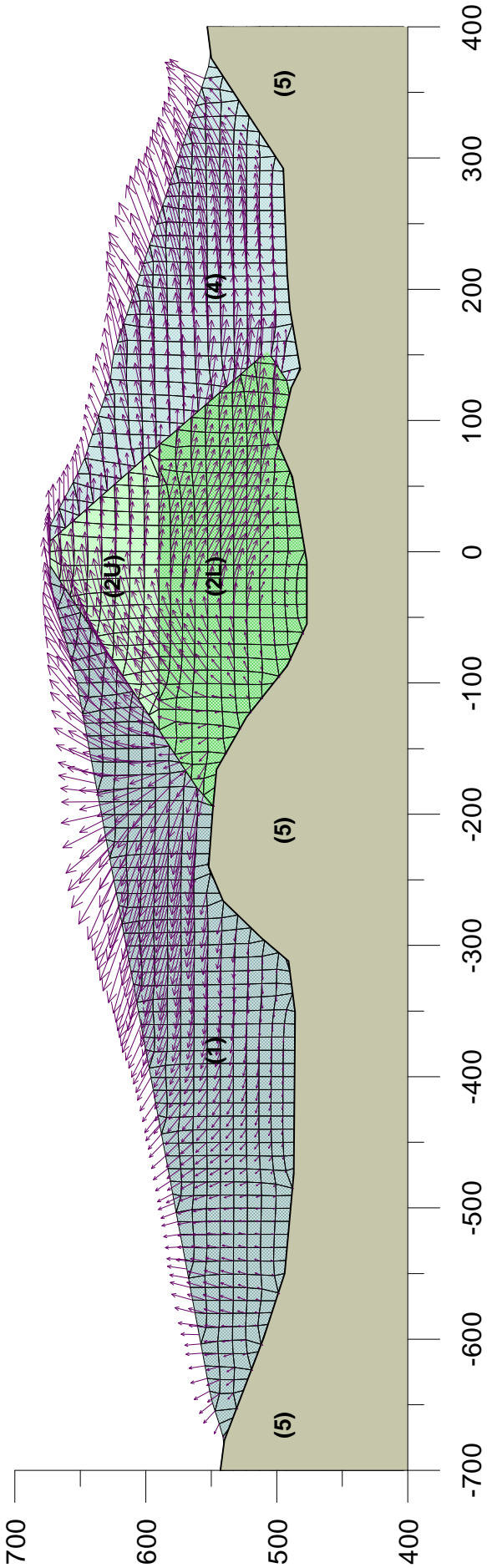
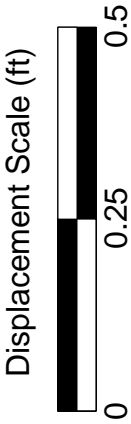


TERRA / Geopentech  
a Joint Venture

CASE 2 COMPUTED DISPLACEMENT  
CONTOURS - LENIHAN DAM  
SEISMIC STABILITY EVALUATIONS (SSE2)

Figure  
6-13A

CASE 2 - Undrained Strength Throughout



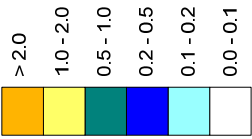


TERRA / GeoPentech  
a Joint Venture

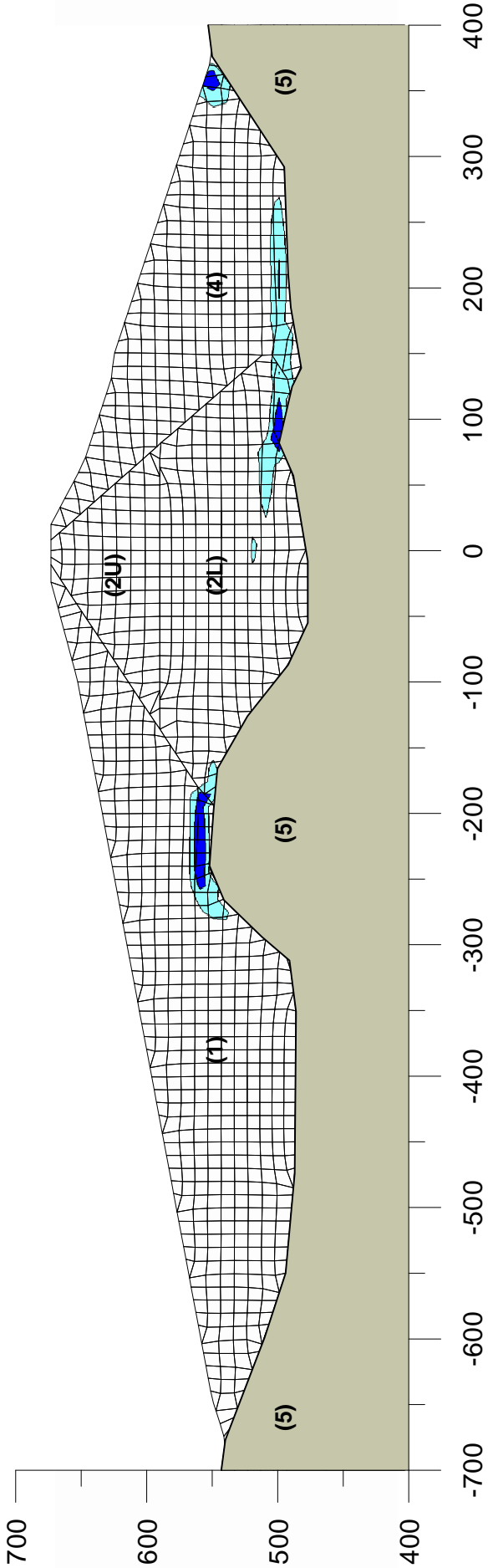
CASE 2 COMPUTED DISPLACEMENT  
VECTORS - LENIHAN DAM  
SEISMIC STABILITY EVALUATIONS (SSE2)

Figure  
6-13B

Shear Strain  
Scale:  
(%)



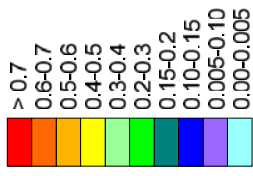
CASE 2 - Undrained Strength Throughout



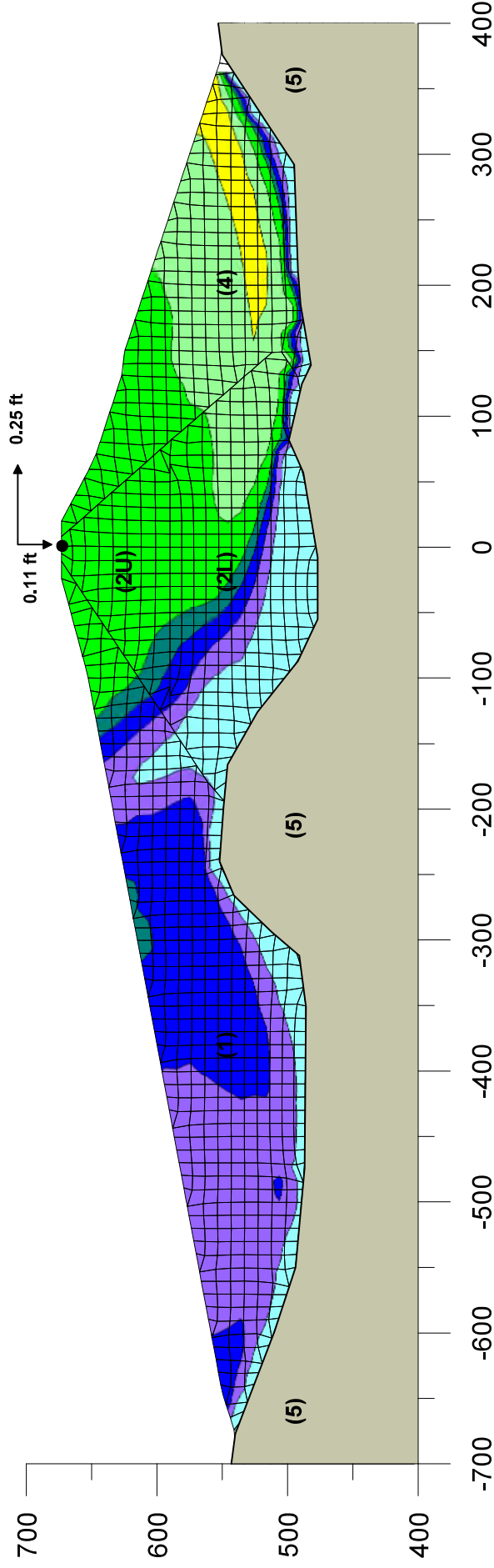
CASE 2 COMPUTED SHEAR STRAIN  
CONTOURS - LENIHAN DAM  
SEISMIC STABILITY EVALUATIONS (SSE2)

Figure  
6-13C

Displacement  
Scale:  
(ft)



## CASE 3 - Undrained Strength Throughout with 30% Reduction

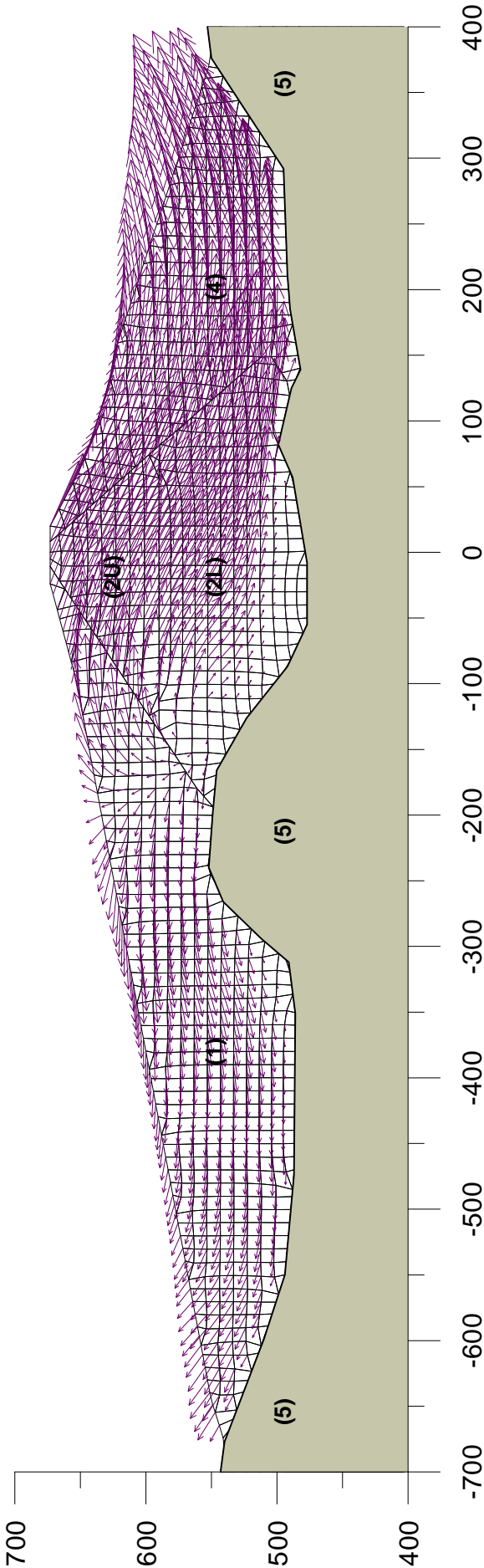
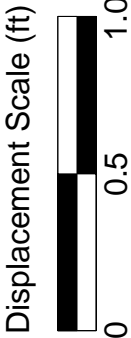


CASE 3 COMPUTED DISPLACEMENT  
CONTOURS - LENIHAN DAM  
SEISMIC STABILITY EVALUATIONS (SSE2)

Figure  
6-14A



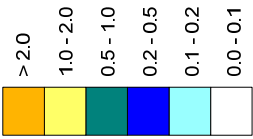
CASE 3 - Undrained Strength Throughout with 30% Reduction



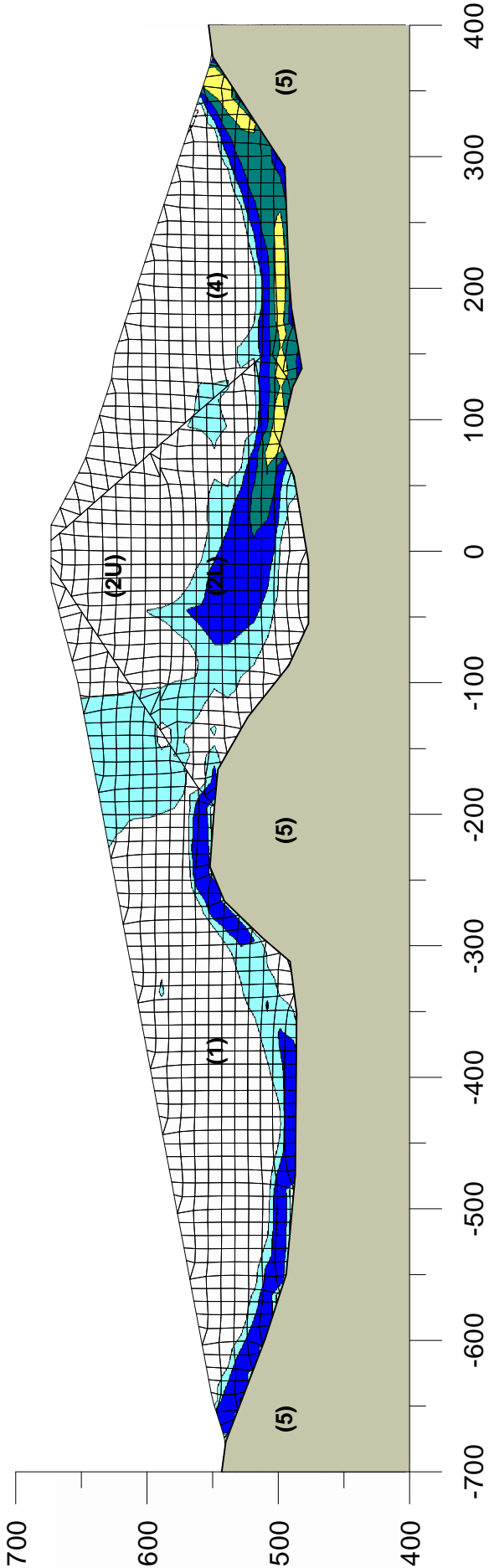
CASE 3 COMPUTED DISPLACEMENT  
VECTORS - LENIHAN DAM  
SEISMIC STABILITY EVALUATIONS (SSE2)

Figure  
6-14B

Shear Strain  
Scale:  
(%)



CASE 3 - Undrained Strength Throughout with 30% Reduction



CASE 3 COMPUTED SHEAR STRAIN  
CONTOURS - LENIHAN DAM  
SEISMIC STABILITY EVALUATIONS (SSE2)

Figure  
6-14C

